THE ROLE OF ABERRANT AKT ACTIVATION IN MELANOMA GROWTH AND METASTASIS

by

Joseph Hyosang Cho

A dissertation submitted to the faculty of
The University of Utah
in partial fulfillment of the requirements for the degree of

Doctor of Philosophy

Department of Oncological Sciences

The University of Utah

May 2016

The University of Utah Graduate School

STATEMENT OF DISSERTATION APPROVAL

The dissertation of **Joseph Hyosang Cho**

has been approved by the following supervisory committee members:

Sheri L. Holmen	, Chair	**5-28-15** Date Approved
Rodney A. Stewart	, Member	**5-28-15** Date Approved
Alana L. Welm	, Member	Date Approved
Stephen L. Lessnick	, Member	**5-28-15** Date Approved
Matthew W. VanBrocklin	, Member	**5-28-15** Date Approved

and by **Bradley R. Cairns** , Chair of

the Department of **Oncological Sciences**

and by David B. Kieda, Dean of The Graduate School.

ABSTRACT

Melanoma is the most deadly skin malignancy and one of the most rapidly increasing cancers. Like other cancers, melanoma is known to exploit specific signaling pathways for growth and disease progression. The AKT pathway is aberrantly activated in upwards of 70% of melanomas and several lines of clinical evidence suggest that increased AKT signaling plays a role in melanomagenesis. However, *in vivo* experimental data directly testing the role of aberrant AKT activation in melanoma has been lacking.

This dissertation addresses the role of aberrant AKT signaling in melanoma by expressing AKT isoforms and mutant protein in an established non-metastatic mouse model of melanoma. We report that expression of activated AKT1 in the context of $BRAF^{V600E}$; $INK4A/ARF^{Null}$ melanomas result in highly metastatic disease with lung and brain metastasis. Interestingly, loss of *Pten* in this same context does not yield significant metastasis but in combination with activated AKT1 results in a significant increase in brain metastasis compared to AKT1 expressing melanomas with wild-type PTEN. Upregulation of mTOR pathway components is observed in AKT1 expressing melanomas compared to PTEN silenced counterparts. Expression of activated AKT3 in the context of $BRAF^{V600E}$; $INK4A/ARF^{Null}$ melanomas results in significant metastatic disease to the brain while activated AKT2 expression in this same context does not result in observable brain lesions. Lastly, we investigated the role of $AKT3^{E17K}$ in

melanoma growth and metastasis. We report no observable brain metastases and instead found that *in vivo* expression of $AKT3^{E17K}$ in $BRAF^{V600E}$; $INK4A/ARF^{Null}$ melanomas yields highly aggressive lung lesions.

In summary, this dissertation furthers our knowledge of melanoma by providing experimental evidence for the role of aberrant AKT signaling in melanoma metastasis to the lungs and brain. Mechanistically, our data reveal that PTEN silencing and AKT1 activation differs in terms of promoting melanoma metastasis, that preferential organ-specific metastasis appears to be mediated through specific AKT isoforms, and that the melanoma relevant mutant protein, $AKT3^{E17K}$, may play a role in promoting lung metastasis. These findings advance our knowledge of melanoma and provide valuable insights for the clinical management of this disease.

Hallelujah and thank you Jesus!

Dedicated to my loving parents, Han Chun & Mi-young Cho

TABLE OF CONTENTS

LIST OF TABLES

LIST OF FIGURES

ACKNOWLEDGMENTS

Graduate school has been an experience of growth – in all aspects of my life. Mentally, I've honed my skills in thinking skeptically like a scientist. Physically, I've sprouted more white hairs and developed crease lines along my brow. Emotionally, I've weathered some of the darkest hours of my sheltered life and emerged stronger. Spiritually, I've come to faith in God and salvation through Jesus Christ. I am ever so thankful for the opportunities I've had in graduate school and to the many people who have made my training possible.

I would like to start by thanking my mentor, Dr. Sheri Holmen. It seems inadequate to just say "thanks" to a person who has so positively impacted my view of science and has guided me back to a place where it is a joy to do research. Dr. Holmen, you have been an incredible mentor and I am always in your debt for all you've done on my behalf. Your keen scientific insights, your strong leadership skills, and your unselfish dedication to the people in your charge are just a few of your many excellent qualities I hope to emulate. Thank you so very much for your mentorship.

I would like express my thanks to the members of my committee: Drs. Matthew VanBrocklin, Rodney Stewart, Stephen Lessnick, and Alana Welm. I thank each one of you for investing so much of your time and energy into my graduate school training. I've met with each one of you on several occasions and have received invaluable advice, both in matters of science and career. Thank you again.

I would like to also thank my previous mentor, Dr. Dave Jones, for allowing me to work in his lab and for teaching me fundamentals of a well-controlled experiment. I'd like to thank a former committee member, Dr. Dean Tantin, for his time and efforts during his tenure on my committee.

I would like to thank the MD/PhD program for their continued support, advocacy, encouragement, and guidance. I especially would like to thank Drs. Dean Li and Jerry Kaplan for accepting me into the program and keeping me on track. I am deeply appreciative of this opportunity and humbled to be among such a fine cohort of colleagues. I'd like to thank Dr. Gabrielle Kardon and our most recent addition, Dr. Mary Hartnett, for their support and efforts on behalf of myself and the MD/PhD program.

Janet! You get your own paragraph. Thank you so much for being such a wonderful person, friend, advocate and MD/PhD mom. You believed in me through the hardest times of graduate school. I can't thank you enough for all your encouraging words and unwavering support.

I would also like to thank the Department of Oncological Sciences, especially Dee DalPonte and Jessica Askin, for all their work in keeping the department running and meeting the needs of us graduate students.

I also want to thank all the students, post-docs, and faculty in the Department who have contributed to my education. I'd especially like to thank the former members of the Jones Lab and the members of the Holmen Lab. My education would not have been possible without their support, comradery, and instruction. I'd like to acknowledge and thank Drs. Angela Andersen, Sue Hammoud, and James Robinson. Much of the research presented in this dissertation was initiated by James Robinson and it was he who trained

me when I first started in the Holmen Lab. I would like to thank several other colleagues in the Holmen Lab with whom I've also had fruitful collaborations: Russell Green, David Kircher, Rowan Arave, and Joyce Tross. I would like to thank my two undergraduate interns, Sean Strain and Adam Welker, for their hard work and enthusiasm.

I'd like to thank and acknowledge several of my friends who have supported me along the path of graduate school. Gdubs and Mwade, thanks for being a part of my Core. Mike Gee and other Co-op members, it is a true privilege to live cooperatively together. Members of the Thursday night Bible study group, I am blessed to be connected with each one of you. To my house church in the Missio Dei Community and the Sunday night group at Hannah & Dave's, thanks for the warm friendship and continued prayers. To all my brothers from the Salt Lake Rescue Mission, your stories of redemption inspire me. I love you guys.

Lastly, I'd like to express my deep gratitude to my family. Mom and Dad, it would take too long to cite every sacrifice made to ensure the opportunities that have culminated in obtaining this PhD. Your love and prayers have support me throughout these years. I love you both and can't thank God enough for giving me such wonderful, loving parents. Hannah, Dave, Mia, and Ethan, it is awesome having you guys nearby. Thanks for all your love and encouragement. Miriam, Bob, Allie, and Michael, thanks for always being there when needed to provide love and support. I love y'all and thank God for the privilege of walking this life together as family.

"To be grateful is to recognize the Love of God in everything He has given us - and He has given us everything. Every breath we draw is a gift of His love, every moment of existence is a grace, for it brings with it immense graces from Him."

-Thomas Merton

CHAPTER 1

INTRODUCTION

1.1 Melanoma Statistics

Melanoma is a very aggressive cancer that accounts for less than 2% of all skin cancers yet causes the majority of skin cancer-related deaths (American Cancer Society, 2015). It is one of the most rapidly increasing cancers in the United States with 73,870 new cases of melanoma projected in 2015 (Siegel et al., 2015). The 5-year survival for localized (Stage I and II) melanoma is quite favorable at 98%, but the survival rates decline sharply to 63% and 16% for regional (Stage III) and distant metastatic (Stage IV) diseases, respectively (U.S. Cancer Statistics Working Group, 2014). These statistical data portray the gravity of melanoma and urgently call our attention to better understand the biology of this disease.

1.2 Melanocyte Origin of Melanoma

Melanoma is a cancer arising from melanin-producing cells known as melanocytes. During development, melanocytes emerge from highly migratory embryonic cells known as the neural crest and eventually occupy terminal niches such as the basal epidermis and hair follicles (Mayer, 1973). Melanocytes are not restricted to the

integumentary system and are known to also reside in anatomic locations such as the uvea, the inner ear, the heart, and the leptomeninges (Cichorek et al., 2013; Goldgeier et al., 1984; Plonka et al., 2009). The location of a melanocyte within the body appears to dictate its morphology, gene expression, and function (Whiteman et al., 2011). The migratory behavior of melanocyte precursors and the nonuniformity among melanocyte lineages correlate well with fundamental characteristics of melanoma such as metastatic propensity and disease heterogeneity.

1.3 Melanoma Classification

Melanoma is a heterogeneous disease comprised of several subtypes. Originally, the classification of melanomas into subtypes was based on gross clinical and pathological features (Arrington et al., 1977; Clark, 1967; McGovern, 1970). Four main subtypes were identified by the mid-1970s – superficial spreading melanoma, nodular melanoma, lentigo maligna melanoma, and acral lentiginous melanoma (Arrington et al., 1977; Clark et al., 1969). Additional subtypes such as desmoplastic melanoma and nevoid melanoma were later added and currently at least ten melanoma subtypes are recognized by the World Health Organization (LeBoit et al., 2006). It was thought that each subtype of melanoma was associated with different prognoses and clinical behaviors; however, these notions were largely unfounded (Clark et al., 1969; Gershenwald et al., 2010; McGovern et al., 1979; Soong et al., 2010). Instead, clinical features such as tumor thickness, mitotic index, presence of ulceration, and other patient characteristics correlate with primary melanoma prognosis, regardless of subtype (Azzola et al., 2003; Francken et al., 2004; Scolyer et al., 2003). Moreover, melanoma subtyping based on World Health Organization criteria has not played a significant role in

determining clinical management (Scolyer and Prieto, 2011). The overall lack of utility significantly undermined the importance of melanoma classification until the recent acquisition of large genomic data sets and the emergence of targeted therapies based on genetic mutations made molecular classification clinically relevant (Bauer et al., 2011; Curtin et al., 2005; Hodis et al., 2012; Krauthammer et al., 2012). Although the current criteria for melanoma classification remains an ever-evolving concept, it is now universally recognized that melanoma encompasses several different types and should be addressed accordingly (Broekaert et al., 2010; Fecher et al., 2007; Scolyer and Prieto, 2011; Whiteman et al., 2011).

1.4 Melanomagenesis

During the mid-1980s, Clark and colleagues proposed a stepwise model of melanomagenesis beginning with benign melanocytes and ending with metastatic melanoma (Clark et al., 1984). They proposed that melanoma begins as a benign nevus (mole), an aggregated proliferation of melanocytes usually located at the epidermal-dermal junction or within the dermis. Clark *et al.* hypothesized that a benign nevus then progressively acquires characteristics such as cytological atypia and altered growth patterns eventually becoming a dysplatic nevus. From the pre-cancerous stage of a dysplastic nevus, the model speculated that melanomas arise, initially as *in situ* lesions within the epidermal-dermal junction and subsequently transform into invasive melanomas. Upon breaching the dermis, it was then surmised that melanoma cells co-opt the circulatory and lymphatic systems to metastasize both regionally and to distant sites.

The simplistic Clark *et al*. model, while full of limitations and exceptions,

provided a much-needed framework for thinking about the process of melanomagenesis. Two notable shortcomings were not addressed by this model: 70-80% of melanomas arise independent of a nevus precursor and 4-12% of melanomas have no identifiable primary lesion (Bevona et al., 2003; Gruber et al., 1989; Marks et al., 1990). However, in support of the Clark *et al.* model was the observation that 80% of human melanocytic nevi harbor an activating mutation in the *v-Raf murine sarcoma viral oncogene homolog B* (*BRAF*) gene, a mutation also observed in 40-60% of cutaneous melanomas (Hocker and Tsao, 2007; Pollock et al., 2003; Poynter et al., 2006). In mice, melanocyte-specific expression of mutant BRAF promotes formation of benign nevi and only in combination with additional genetic modification gives rise to metastatic melanoma (Dankort et al., 2009). These data support the theory of a step-wise transformation process whereby successive accumulation of genetic and/or epigenetic changes propel oncogenic transformation from melanocyte to melanoma (Miller and Mihm, 2006).

1.5 Clinical Metastasis of Melanoma

The aggressive nature of melanoma is defined by the disease's propensity to metastasize, often early in the course of the disease. This is exemplified by the fact that while only 4% of all melanomas are diagnosed as stage IV, up to a third of all melanoma patients experience recurrent disease, mostly from unidentified metastases (Howlader et al., 2014; Soong et al., 1998). Melanoma metastasizes by a lymphatic, circulatory, or even para-vascular route (Bald et al., 2014; Zbytek et al., 2008). Clinically, the spread of melanoma manifests as one of the following: satellite/in-transit metastasis, regional lymph node metastasis, and distant metastasis (Mervic, 2012). The initial site of metastatic disease progression varies. About half of all

melanoma patients initially develop regional lymph node metastasis, a third initially develop distant metastasis, and the remainder present with satellite/in-transit skin metastases (Leiter et al., 2004; Meier et al., 2002). The presence of metastasis, like in other malignancies, poses an ominous sign for melanoma prognosis and is reflected by the successive decline in one-year survival rates for patients with one, two, or three different visceral metastases at 36%, 13%, and 1%, respectively (Balch et al., 2003). Thus, great vigilance is required in the clinical setting when monitoring melanoma metastasis and recurrence.

Several prognostic tools have been developed over the years to better predict melanoma outcomes. The single most useful factor for prognosticating melanoma metastasis is primary tumor thickness, also known as Breslow thickness (Breslow, 1970). Follow-up studies clearly demonstrate that Breslow thickness strongly correlates with metastatic potential and recurrence (Schultz et al., 1990). Interestingly, even small differences in thickness (1-2 mm) can substantially alter prognosis (Balch et al., 2001). Regional lymph nodes are frequently the first noncontiguous site of metastasis in melanoma (Nathanson, 2003). A biopsy of the proximal most draining lymph node to the primary tumor, also known as the sentinel lymph node, is recommended for melanomas with Breslow thickness of 1 mm or greater, changing both treatment and prognosis based on the presence of absence of tumor cells (Balch et al., 2001). Other factors found to correlate with an increased probability of melanoma metastasis are ulceration of the primary tumor, presence of mitotic figures, and absence of tumor-infiltrating lymphocytes (Gimotty et al., 2004).

1.6 Biology of Melanoma Metastasis

Melanoma-related deaths are universally due to complications from metastatic disease. This causal relationship holds true for the majority of cancers. An estimated 90% of all cancer-related deaths are attributed to metastasis and thus its study has elicited much attention (Mehlen and Puisieux, 2006). As early as the mid-1800s, the prominent physician-scientist, Rudolf Virchow, posited that sites of cancer metastasis were explainable by the circulatory migration of tumor cells (Virchow, 1989). This hypothesis seemed reasonable and in some malignancies, such as colon cancer, has found support (Hess et al., 2006). However, many tumors metastasize to specific organs in ways that cannot simply be explained by Virchow's hypothesis. By the late-1800s, Fuchs and Paget countered Virchow's hypothesis and proposed that tumor cells do not metastasize indiscriminately but instead have a predilection for colonizing specific organs (Paget, 1889; Piris and Mihm, 2007). Thus was born the "seed-and-soil" hypothesis, where the "seed" or metastasizing cancer cell is thought to have a preference for growing in certain "soil" or organ niches. Paget's initial finding from metastatic breast cancer patient autopsies strongly supported this alternative hypothesis and it continues to garner support to this day (Paget, 1889).

The pattern of melanoma metastasis lends some support for Virchow's hypothesis but is more often cited as strong evidence for the "seed and soil" theory. Melanoma spreads regionally in a fashion that Virchow would have predicted. The most common sites of melanoma metastasis are adjacent skin and regionally draining lymph nodes (Balch et al., 2003). Metastasis to the nearby skin is one of the first external indicators that hematogenous and/or lymphatic spread has occurred (Wolf et al., 2004). In contrast,

the metastatic patterns of stage IV melanoma strongly support the "seed-and-soil" hypothesis with distant organs such as the lung, brain, liver, bone, and intestine as common sites of metastatic spread regardless of the primary lesion's originating location (Patel et al., 1978). The lungs are often the first distant site melanoma colonizes while organs such as the intestines and bone usually represent areas of late metastasis (Balch et al., 2003). Brain and liver metastases exhibit an inverse correlation with the presence of one often excluding the other, implying a nonrandomness to melanoma dissemination. A subtype of melanoma involving the orbit known as uveal melanoma exclusively metastasizes to the liver in 55% of stage IV patients and involves the liver in 87-92% of all metastatic patients (Bakalian et al., 2008; Lorigan et al., 1991). Additional distant sites of melanoma metastasis are as follows: the heart, pancreas, adrenal glands, spleen, stomach, esophagus, thyroid gland, kidney, genitals, blood vessels, skeletal muscles, and other locations (Balch et al., 2003; Damsky et al., 2011b; Patel et al., 1978).

Beyond clinical findings, melanoma cells provide experimental evidence that supports the "seed and soil" hypothesis. Hart and Fidler reported that B16 melanoma cells implanted into syngeneic mice preferentially grow in the lungs and ovaries but fail to grow in the kidneys (Hart and Fidler, 1980). They further demonstrated, through radiolabeling B16 cells, that initial tumor seeding in each organ was not significantly different, strongly supporting the idea of an organ-specific preference by the tumor cells. As mentioned earlier, uveal melanoma has a strong predilection for liver metastasis and laboratory findings support this preference. Following injection into nude mice, fluorescently-labeled uveal melanoma cells specifically colonize the liver and remain dormant in the liver for weeks (Logan et al., 2008). When human melanoma cell lines

derived from either cutaneous lesions, lymph nodes, or brain metastases were injected into the subarachnoid space of nude mice, all produced growths in the leptomeninges, the innermost layers of tissue covering the central nervous system (Fujimaki et al., 1996). However, only melanoma cells derived from the brain metastases were capable of invasion and growth within the brain parenchyma, suggesting these cells retained attributes that allowed site-specific growth. In line with this study, it was also demonstrated that human and mouse melanoma cells injected into the internal carotid artery of nude mice produce different patterns of cerebral metastases reminiscent of where the cells were derived from; cells from brain metastases colonized the brain parenchyma while cells originating from lymph node metastases took up residence in the meninges (Schackert et al., 1990). The clinical and experimental evidence for distinct patterns of distant melanoma spread has created much interest around the subject of why certain organs are targeted by melanoma. These answers are likely to be found deep within the genetics of melanoma.

1.7 Genetics of Melanoma Metastasis

Among all cancer types, melanoma has the highest average somatic mutation burden (Alexandrov et al., 2013). The mutations harbored by melanoma are not entirely random and hold many clues about this disease. Our current understanding of melanoma biology stems largely from deciphering its genetic mutational landscape and identifying signaling pathways exploited by melanoma (Daniotti et al., 2004; Davies and Samuels, 2010; Hodis et al., 2012). This section highlights a few of the important genetic alterations observed in melanoma and the functional relevance of these mutations in

melanoma metastasis.

The importance of Mitogen-activated protein kinases (MAPK) in melanomagenesis was first recognized through observations of *Neuroblastoma RAS viral oncogene homolog* (*NRAS*) mutations, which occur at a frequency of about 15%-20% of all melanomas (Albino et al., 1984; Albino et al., 1989; Padua et al., 1985). BRAF is a direct downstream effector of NRAS and *BRAF* mutations are found in ~50% of malignant melanomas (Davies et al., 2002; Pollock and Meltzer, 2002). Over 90% of the BRAF mutations in melanoma occur at codon 600, with the vast majority of these mutations rendering the substitution of glutamic acid for valine at the 600 amino acid position (Ascierto et al., 2012). Successful pharmaceutical interventions for metastatic melanomas harboring *BRAF* mutations further demonstrate the importance of MAPK signaling in this disease.

Aberrant activation of the Phosphoinositide 3-kinase/Protein kinase B (PI3K/AKT) pathway in melanoma is accomplished via several genetic alterations including deletions, inactivation, and epigenetic silencing of negative regulators and activating mutations and/or copy number amplification of positive regulators including the AKT isoforms. Phosphatase and tensin homolog, also known as PTEN, is well known for its role in negatively regulating AKT pathway activity and deletions/inactivating mutations of this tumor-suppressor are observed in up to 43% of melanomas (Hodis et al., 2012; Mikhail et al., 2005). PH domain and leucine rich repeat protein phosphatase 1 (PHLPP1) selectively reduces AKT activation and its gene expression was recently shown to be suppressed in melanomas through a mechanism involving DNA methylation (Dong et al., 2014). Phosphatidylinositol-4,5-bisphosphate

3-kinase, catalytic subunit alpha (PIK3CA) is the kinase subunit of PI3K and activating mutations in *PIK3CA* are observed in 1-5% of melanomas (Curtin et al., 2006; Omholt et al., 2006). *AKT* isoforms acquire activating mutations in 1-2% of melanomas (Davies et al., 2008), but more frequently genomic amplification or increased expression of *AKT* is observed in melanoma (Bastian et al., 1998; Stahl et al., 2004).

Disruption of the *Cyclin dependent kinase inhibitor 2A* (*CDKN2A* or *INK4A/ARF*) locus, which encodes two proteins, INK4a and ARF, is associated with familial melanomas and targeted in 55-70% of melanomas (Hodis et al., 2012). INK4a is a negative regulator of the retinoblastoma protein (pRB) pathway, which is critically involved in controlling the cell cycle (Sharpless and DePinho, 1999). The *Alternate open reading frame* (*ARF*) gene product regulates an equally important cellular pathway – the p53 pathway (Sharpless and DePinho, 1999). ARF is a negative regulator of Mouse double minute 2 (MDM2), the canonical negative regulator of p53, and functionally ARF acts as a positive regulator of p53 by promoting apoptosis in response to aberrant mitogenic stimuli. Thus, ARF mutations result in dysfunctional p53. Indeed, the importance of p53 loss is reiterated by the observance of mutations at this gene locus in about 20% of melanomas (Albino et al., 1994; Hodis et al., 2012).

Experimental evidence from transgenic mouse models confirm the importance of the genetic alterations observed clinically and also establish the existence of cooperation between mutations in promoting melanoma progression. It had been noted that *NRAS* and *BRAF* mutations occur in a near mutually exclusive fashion (Colombino et al., 2012; Hodis et al., 2012). Activating mutations in *BRAF* frequently co-occur with *PTEN* mutations but are less frequently observed in NRAS mutant melanomas (Tsao et al.,

2004). Since NRAS regulates both the MAPK pathway and the PI3K/AKT pathway, it is thought that combined activation of BRAF and PTEN silencing functionally mimics mutant NRAS and demonstrates that the two pathways cooperate in melanoma development. Interestingly, mice harboring a *Braf*^{V600E} mutation in their melanocytes do not develop melanomas but in combination with *Pten* loss, their melanocytes transform into metastatic melanomas that spread to the lymph nodes and lung (Dankort et al., 2009). Mice with global deletion of *Ink4a/Arf* develop a wide spectrum of tumors, but melanomas are not observed (Serrano et al., 1996). However, when deletion of *Ink4a/Arf* occurs in melanocytes in conjunction with MAPK pathway activity (via NRAS or HRAS activation), non-metastatic melanomas arise (Chin et al., 1997; VanBrocklin et al., 2010). Increasing the metastatic potential of melanomas in genetically engineered mouse models has been accomplished by further manipulating other cellular pathways via mutations to genes such as *β-catenin* and *Liver kinase B1* (*Lkb1*) (Damsky et al., 2015; Damsky et al., 2011a; Liu et al., 2012). These examples demonstrate how melanoma co-opts various cellular pathways to promote disease progression and lend a platform to further study organ-specific metastasis.

1.8 Melanoma Brain Metastasis

Brain metastases are a major complication of metastatic melanoma and are responsible for up to half of all melanoma deaths (Budman et al., 1978; Davies et al., 2011; Yashin et al., 2013). Among all cancers that metastasize to the brain, melanoma has one of the highest propensity for colonizing this organ (Marchetti et al., 2003a). One out of eight melanoma patients presents with brain metastasis at stage IV diagnosis (Tas,

2012). This fraction increases to three out of four metastatic melanoma patients at autopsy (Amer et al., 1978; Patel et al., 1978). Brain metastasis bodes very unfavorably for prognosis in melanoma and overall survival time ranges between 4-9 months after diagnosis (Davies et al., 2011; Fife et al., 2004).

The morbidity and mortality associated with melanoma brain metastasis are most often attributed to hemorrhage and increased intracranial pressure. Among all brain malignancies, melanoma brain metastases have the highest risk of hemorrhage with 27-40% of all intracranial lesions showing active hemorrhage on neuroimaging and up to 71% of patients with melanoma brain metastases showing evidence of prior hemorrhage by histopathology (Ewend et al., 1996; Marek and Ehud, 2000). In addition to the hemorrhage, brain metastases are associated with other complications such as hydrocephalous from obstructed flow of cerebrospinal fluid and local mass effect by tumor expansion (Chaichana and Chaichana, 2011). These complications place the patient at risk for increased intracranial pressure and commonly manifest as headaches, nausea, mental status change, vomiting, cranial nerve palsies, visual deficits, hemiparesis, and sensory loss (Ewend et al., 1996). Focal and generalized seizures are also common sequelae of brain metastases and further add to the morbidity of this complication.

Current clinical therapy for melanoma brain metastasis can be divided into three broad categories: palliative, definitive, and investigational (Chaichana and Chaichana, 2011; Gorantla et al., 2013). Palliative care includes steroids to reduce inflammation caused by hemorrhage and edema, anticonvulsants to combat seizures secondary to the metastatic lesion, and anticoagulants to prevent postoperative thromboembolic disease. Definitive therapy includes radiation, either whole brain radiation therapy or stereotactic

radiosurgery, surgical resection, and chemotherapy (Eichler and Loeffler, 2007). Investigational therapies encompasses the recently approved targeted and immune therapies, which show great promise (Flanigan et al., 2011).

General recommendations for a particular definitive therapy are based on several criteria including the size of the brain metastasis, the location of the brain metastasis, and the presence of other brain metastases (Chaichana and Chaichana, 2011; Goulart et al., 2011). Other important factors include the presence and/or extent of extra-cranial metastases and the overall health of the patient. The median overall survival of brain metastasis patients opting out of definitive therapy is approximately 1-2 months (Sampson et al., 1998). Melanoma is notoriously radio-resistant and thus, surgical resection is recommended if the metastasis is solitary or limited in number and located in a surgically accessible area (Barranco et al., 1971). Immediate tumor de-bulking, definitive targeting of the lesion, and histological analysis of resected tissues are all advantages of surgical resection. Melanoma brain metastasis patients who are candidates for surgical resection and initially receive this treatment have a median overall survival of 9.83 months (Davies et al., 2011). Patients with multiple melanoma brain metastases or disseminated carcinomatous cell spreading in the brain also known as “military metastases” are not surgical candidates and are recommended alternative therapies such as radiation and chemotherapy. Radiation for melanoma brain metastases can be administered in a targeted and nontargeted fashion. Stereotactic radiosurgery is a targeted approach that involves the administration of a single fraction of ionizing radiation via several converging beams of radiation onto a targeted site. The use of multiple beams of radiation from various sources all targeting the same area has been demonstrated to

minimize extraneous exposure and mitigate the undesired side-effects of radiotherapy (Nieder et al., 2014). Melanoma patients recommended to receive stereotactic radiosurgery and initially treated with this modality have a median overall survival of 7.69 months (Davies et al., 2011). Whole brain radiation therapy is untargeted over the entire brain and is particularly useful for treating undetectable micro-metastases or when the number of brain metastases is such that it precludes a targeted approach (Khan and Dicker, 2013). Despite the many possible side-effects including cognitive dysfunction, whole brain radiation improves clinical outcomes and melanoma brain metastasis patients receiving this therapy have a median survival of 3.86 months (Davies et al., 2011). Standard chemotherapy for metastatic melanoma in the brain has not proven very effective. Temozolamide, fotemustine, and thalidomides are used clinically in combination or alone but have very low response rates ranging between 7-10% and patients receiving chemotherapy alone to treat melanoma brain metastases have a median overall survival of 4.64 months (Agarwala et al., 2004; Avril et al., 2004; Chaichana and Chaichana, 2011; Davies et al., 2011).

Targeted therapies are not standard of care for treatment of melanoma brain metastasis, but anecdotal evidence suggests these therapies could have clinical utility and should be considered for further investigation (Flanigan et al., 2011). A pilot study investigating BRAF inhibition and melanoma brain metastasis reported a response rate of 90% (9/10 patients) in terms of reduced size of brain lesions prompting follow-up studies (Falchook et al., 2012). Additional study with a larger patient cohort reported a response rate of 39% in melanoma brain metastasis patients with the $BRAF^{V600E}$ mutation treated with dabrafenib, a BRAF inhibitor, and median progression free survival and overall

survival of 16 months and 33 months, respectively (Long et al., 2012). However, a different study found 19% of melanoma patients without brain metastases given the BRAF inhibitor vemurafenib actually develop brain metastases as the only site of metastasis while on this targeted therapy (Kim et al., 2011). These contradictory outcomes underlie the need for additional clinical studies on the use of targeted therapies for melanoma brain metastases.

Immune-based therapies have yielded very promising results in melanoma and these therapies are currently under investigation for melanoma brain metastases. A retrospective study found that two out of seven melanoma patients with untreated brain metastases had a complete response to IL-2 treatment (Guirguis et al., 2002). Another retrospective review reported that two out of fifteen melanoma patients with brain metastases showed a complete response to IL-2 (Powell and Dudek, 2009). Adoptive cell transfer (ACT) of tumor-infiltrating lymphocytes has generated significant interest in melanoma therapy and has been demonstrated to have efficacy against brain metastases (Hong et al., 2010; Vonderheide and June, 2014). In brief, T cells from a melanoma patient are harvested from their tumor tissue, selectively expanded with or without further genetic manipulation and after patient lympho/myelo-depletion are re-introduced into the patient. This form of therapy has generated encouraging results reporting complete responses in seven patients and partial responses in six patients out of a total of seventeen melanoma patients with brain metastases that received ACT therapy (Hong et al., 2010). Check-point inhibitors represent a new class of immune-based therapies comprised of antibodies against specific immune-modulating molecules that regulate the amplitude and duration of T cell responses (Pardoll, 2012). Currently, there are two molecules targeted

by clinically available check-point inhibitors: Cytotoxic T-lymphocyte protein 4 (CTLA-4) and Programmed cell death protein 1 (PD-1) (Ott et al., 2013; Webster, 2014). Check-point inhibitors have demonstrated significant clinical benefit in the treatment of metastatic melanoma (Brahmer et al., 2012; Hamid et al., 2013; Hodi et al., 2010; Topalian et al., 2012). Anti-PD-1 therapies (pembrolizumab and nivolumab) are a more recent development and data on the effectiveness of PD-1 inhibition against melanoma brain metastases is currently pending. However, anti-CTLA-4 therapy (ipilimumab) was shown through retrospective analysis of phase II data to have some efficacy against brain metastases (Schartz et al., 2010; Weber et al., 2011). More impressive have been reports of CTLA-4 blockade combined with other therapies such as fotemustine and stereotactic radiosurgery yielding disease control in 50% of patients and extending median survival from 4.9 months to 21.3 months with these combinations, respectively (Di Giacomo et al., 2012; Knisely et al., 2012).

Although the benefits of recent therapeutic breakthroughs have trickled down and improved clinical outcomes for melanoma brain metastasis (Flanigan et al., 2011), large advances in this field remain elusive (Gorantla et al., 2013). This reflects the fact that brain metastasis is one of the least understood aspects of melanoma (Filder et al., 1999; Yashin et al., 2013). One of the key unanswered questions in melanoma brain metastasis is “How does melanoma colonize the brain?” The molecular mechanisms that facilitate the establishment of melanoma in the brain are not well understood. A significant focus of this dissertation is to explore the role of aberrant AKT signaling in promoting melanoma brain metastasis.

1.9 Mechanisms of Melanoma Brain Metastasis

Recent imaging work by the Winkler lab described *in vivo* melanoma brain metastasis formation over the course of several sequential steps and shed light on necessary processes during brain colonization (Kienast et al., 2010). Using a mouse with a chronic cranial window, a multiphoton laser scanning microscope, and fluorescently labeled melanoma cells, they identified four steps a mobile, would-be metastatic cell follows in order to establish itself as a bona fide brain metastasis: arrest at vascular branch point, early extravasation, persistent close contact to microvessels and perivascular growth by vessel co-option. Using these steps as a frame work for brain metastasis, we will discuss mechanisms implicated in melanoma's colonization of the brain.

Arresting at intracranial vascular branch points implies that a mobile cell could be directed in its migration to the brain by external cues like chemokines or brain-specific ligands. Interestingly, expression of the chemokine receptor CCR4 is significantly greater in a brain-metastasizing melanoma cell line compared with a non-brain metastasizing counterpart (Izraely et al., 2010). Follow up studies revealed that brain-derived soluble factors upregulate CCR4 in melanoma cells and specifically enhance cell migration in brain-metastasizing melanoma cells (Klein et al., 2012). Endothelin receptor B (EDBRB) is another molecule that could drive melanoma's preferential colonization of the brain. Cruz-Munoz *et al.* demonstrated using a xenograft mouse model of melanoma brain metastasis that EDNRB overexpression enhanced the metastatic potential of the implanted tumor cells and resulted in more brain metastases compared with control tumor cells (Cruz-Munoz et al., 2012). Specifically blocking the EDNRB receptor negated the

enhanced metastatic phenotype and resulted in an increased overall survival in the mice. The fact that EDNRB ligand is highly expressed in the brain (Firth and Ratcliffe, 1992), supports the idea that EDNRB-mediated signaling could drive preferential metastasis to the brain. In the mid-1970s, researchers noted that melanoma cells had a very high density of receptors for and strong affinity towards nerve growth factor (NGF), opening up the idea that a ligand receptor interaction could be the basis for melanoma's predilection for brain metastasis (Fabricant et al., 1977). Subsequent studies determined that $p75^{NTR}$, a receptor for NGF is highly upregulated in melanoma cells and associated with brain metastasis (Herlyn et al., 1985; Herrmann et al., 1993). Other receptors such as TrkC, the putative receptor for neurotrophin-3 (NT-3) is also highly expressed on melanoma cells, providing more evidence that neurotrophins may play a homing role in melanoma brain metastasis (Marchetti et al., 2003b). Interestingly, astrocytes found at the stromal-tumor interface of melanoma brain metastases display increased expression of neurotrophins like NGF and NT-3, further supporting the hypothesis that these ligands originate from the brain and attract melanoma cells (Marchetti et al., 1995; Yoshida and Gage, 1992).

The blood-brain barrier (BBB) presents a formidable border that tumor cells must cross in order to establish residence in the brain. The BBB is composed of cerebral endothelial cells connected together by tight junction proteins and reinforced by a relatively thick basement membrane plus an underlying layer of astrocytes (Abbott et al., 2010). One of the main functions of the BBB is to strictly regulate the flow of ions, nutrients, and cells into the brain parenchyma. Several mechanisms have been implicated in promoting extravasation through the BBB in melanoma brain metastasis. Stoletov *et*

al. recently demonstrated that melanoma cells utilize the gap junction protein Connexin-26 (Cx26) to associate with cerebral vasculature during the initiation of brain metastasis (Stoletov et al., 2013). Silencing of Cx26 in melanoma cells inhibits extravasation and *in vivo* brain colonization (Stoletov et al., 2013). Heparanase (HPSE) is an enzyme that degrades heparan sulfate chains of proteoglycans enriched in endothelial cell layers and several lines of evidence suggest HPSE may act in a brain-specific manner allowing penetration of the blood-brain barrier by metastatic melanoma cells (Marchetti, 2002; Marchetti et al., 2000; Murry et al., 2006). The presence of HPSE increases invasion of melanoma cells into brain tissues in brain slice models (Murry et al., 2006). Furthermore, co-incubation of brain metastatic melanoma cells with astrocytes results in elevated HPSE activity and increased invasive phenotype *in vitro* (Marchetti et al., 2000). The role of HPSE in brain-specific metastasis is further supported by the fact that neurotrophins such as NGF enhance HPSE activity (Marchetti et al., 1993). Pleckstrin homology domain-containing family A member 5 (PLEKHA5) is a recently described candidate to emerge from integrated comparisons of clinical melanoma samples and cell lines with a brain homing phenotype (Jilaveanu et al., 2014). PLEKHA5 expression in melanoma patients was associated with decreased brain metastasis free survival, defined as the elapsed time from diagnosis of first distant metastasis to diagnosis of brain metastasis. *In vitro* studies revealed that PLEKHA5 silencing decreased melanoma cell survival and inhibited transmigration through an artificial BBB, suggesting that PLEKHA5 plays a role in viability and extravasation into the brain parenchyma.

Securing access to the blood supply is a critical process for melanoma to establish residence in the brain and is carried out in two steps - persistent close contact to

microvessels and perivascular growth by vessel co-option (Kienast et al., 2010). Mentioned previously for being involved in extravasation, Cx26 is also implicated in vessel co-option during melanoma metastasis to the brain (Stoletov et al., 2013). Stat3 activation has been implicated in promoting brain metastasis by stimulating vascular remodeling through increased expression of basic fibroblast growth factor (bFGF), vascular endothelial growth factor (VEGF), and matrix metalloproteinase-2 (MMP-2) (Xie et al, 2006, Huang et al 2008). Interestingly, the PI3K-AKT pathway, discussed in more detail in the following section, is connected to vascular co-option and angiogenesis via its role in regulating VEGF, HIF1α, and ANG2 (Ju et al., 2014; Karar and Maity, 2011; Phung et al., 2015; Phung et al., 2006).

1.10 AKT Signaling and Melanoma Metastasis

Aberrant AKT signaling is observed in up to 70% of melanomas and is associated with disease progression (Dai et al., 2005; Davies et al., 2009; Smalley, 2009). Phosphorylation at Ser473 and Thr308 induces AKT activation and phosphorylated AKT is known to progressively accumulate in lesions undergoing melanomagenesis, with especially high levels in metastatic tissues (Dai et al., 2005; Stahl et al., 2004). Furthermore, over-expression of AKT in a radially growing melanoma cell line conferred an invasive, vertical growth phenotype when subcutaneously implanted in mice (Govindarajan et al., 2007). Clinical data strongly suggest that AKT signaling is involved in melanoma metastasis to the brain (Dai et al., 2005; Davies et al., 2009). A comparison between lung, liver, and brain metastases from human melanoma samples found significantly higher levels of phosphorylated-AKT and a downstream target,

phosphorylated-GSK3β, in brain metastases compared to lung and liver metastases (Davies et al., 2009). In line with increased AKT activity, PTEN levels were significantly lower in brain metastases compared with lung and liver metastases. Follow-up studies comparing patient-matched brain versus extracranial melanoma metastases yielded additional evidence supporting increased AKT activity as a defining feature of brain metastasis (Chen et al., 2014; Niessner et al., 2013). In addition, the loss of PTEN protein expression in melanoma patient lymph node metastases is associated with significantly shorter time to brain metastasis but not with other organ metastases (Bucheit et al., 2014). Although these lines of evidence strongly implicate the involvement of AKT signaling in melanoma brain metastasis, the role of aberrant AKT activation in this capacity has not been directly tested *in vivo*.

1.11 Animal Models of Melanoma Brain Metastasis

A major obstacle in studying melanoma brain metastasis has been the lack of an animal model that mimics the metastatic patterns observed in the human disease. Cruz-Munoz *et al.* described a model engineered by sub-dermal injection of severe-combined immune-deficient (SCID) mice with metastatic human melanoma cells (Cruz-Munoz et al., 2008). Other models have employed intra-carotid or intra-cardiac injection of melanoma cells into similar immune-compromised mice (Fujimaki et al., 1993; Morsi et al., 2013). Drews and coworkers injected chick embryos with melanoma cells in the rhombencephalic brain vesicles to investigate their invasive growth in this environment (Busch et al., 2012). While these models have provided valuable information regarding specific steps in melanoma metastasis, none described to date arise spontaneously in

immunocompetent animals and proceed through every step of the metastatic cascade.

1.12 Conclusions

Melanoma is a very aggressive cancer that arises from melanocytes. While melanoma is a disease of several subtypes defined by distinct clinical presentations and genetic mutations, a universal characteristic of melanoma is its inherent capacity to metastasize. Genetic insights have led to new targeted therapies and recent therapeutic breakthroughs with immune therapies have shifted the treatment paradigm of metastatic melanoma. However, despite the clinical progress, melanoma brain metastasis remains a serious concern due to the high mortality and morbidity associated with this complication. The mechanisms driving melanoma to the brain are not well understood and animal models recapitulating the steps of melanoma brain metastasis are lacking. Therefore, to develop breakthrough therapeutics for melanoma brain metastasis, we must investigate the molecular pathways promoting disease progression and develop better animal models that faithfully mimic the spread of melanoma to the brain similar to the human disease.

1.13 Preview

The work presented in this dissertation investigates the role of aberrant AKT activation in melanoma development and progression. Based on several studies implicating elevated AKT signaling in melanoma metastasis to the brain, we examine the *in vivo* role of activated and wild-type AKT1, AKT2, and AKT3 as well as mutant $AKT3^{E17K}$ in promoting melanoma spread in a non-metastatic $BRAF^{V600E}$/INK4A-ARF^{Null} mouse model of melanoma. We report highly penetrant melanomas with

development of spontaneous lung and brain metastases after a relatively short latency. To our knowledge, this is the first *in vivo* melanoma model described that develops spontaneous brain metastases. Our findings also demonstrate unexpected differences in metastatic potential between melanomas with PTEN silencing versus AKT1 activation, and between melanomas expressing different activated AKT isoforms and $AKT3^{E17K}$. Upregulation of mTOR signaling downstream of AKT activation is implicated in promoting melanoma brain metastasis. In addition to the molecular mechanisms examined, our *in vivo* model provides a valuable tool to further understand the biology of melanoma brain metastasis and to evaluate therapeutic strategies aimed at preventing and treating these deleterious lesions.

1.14 References

Abbott, N.J., Patabendige, A.A.K., Dolman, D.E.M., Yusof, S.R., and Begley, D.J. (2010). Structure and function of the blood–brain barrier. Neurobiology of Disease *37*, 13-25.

Agarwala, S.S., Kirkwood, J.M., Gore, M., Dreno, B., Thatcher, N., Czarnetski, B., Atkins, M., Buzaid, A., Skarlos, D., and Rankin, E.M. (2004). Temozolomide for the treatment of brain metastases associated with metastatic melanoma: A phase II study. Journal of Clinical Oncology *22*, 2101-2107.

Albino, A.P., Le Strange, R., Oliff, A.I., Furth, M.E., and Old, L.J. (1984). Transforming ras genes from human melanoma: A manifestation of tumour heterogeneity? Nature *308*, 69-72.

Albino, A.P., Nanus, D.M., Mentle, I.R., Cordon-Cardo, C., McNutt, N.S., Bressler, J., and Andreeff, M. (1989). Analysis of ras oncogenes in malignant melanoma and precursor lesions: Correlation of point mutations with differentiation phenotype. Oncogene *4*, 1363-1374.

Albino, A.P., Vidal, M.J., McNutt, N.S., Shea, C.R., Prieto, V.G., Nanus, D.M., Palmer, J.M., and Hayward, N.K. (1994). Mutation and expression of the p53 gene in human malignant melanoma. Melanoma Research *4*, 35-45.

Alexandrov, L.B., Nik-Zainal, S., Wedge, D.C., Aparicio, S.A.J.R., Behjati, S., Biankin, A.V., Bignell, G.R., Bolli, N., Borg, A., Borresen-Dale, A.-L.*, et al.* (2013). Signatures of mutational processes in human cancer. Nature *500*, 415-421.

Amer, M.H., Al-Sarraf, M., Baker, L.H., and Vaitkevicius, V.K. (1978). Malignant melanoma and central nervous system metastases. Incidence, diagnosis, treatment and survival. Cancer *42*, 660-668.

American Cancer Society. Cancer Facts & Figures 2015. Atlanta: American Cancer Society; 2015.

Arrington, J.H.r., Reed, R.J., Ichinose, H., and Krementz, E.T. (1977). Plantar lentiginous melanoma: A distinctive variant of human cutaneous malignant. American Journal of Surgical Pathology *1*, 131-143.

Ascierto, P., Kirkwood, J., Grob, J.-J., Simeone, E., Grimaldi, A., Maio, M., Palmieri, G., Testori, A., Marincola, F., and Mozzillo, N. (2012). The role of BRAF V600 mutation in melanoma. Journal of Translational Medicine *10*, 85.

Avril, M.F., Aamdal, S., Grob, J.J., Hauschild, A., Mohr, P., Bonerandi, J.J., Weichenthal, M., Neuber, K., Bieber, T., Gilde, K.*, et al.* (2004). Fotemustine compared with dacarbazine in patients with disseminated malignant melanoma: A phase III study. Journal of Clinical Oncology *22*, 1118-1125.

Azzola, M.F., Shaw, H.M., Thompson, J.F., Soong, S.-j., Scolyer, R.A., Watson, G.F., Colman, M.H., and Zhang, Y. (2003). Tumor mitotic rate is a more powerful prognostic indicator than ulceration in patients with primary cutaneous melanoma. Cancer *97*, 1488-1498.

Bakalian, S., Marshall, J.-C., Logan, P., Faingold, D., Maloney, S., Di Cesare, S., Martins, C., Fernandes, B.F., and Burnier, M.N. (2008). Molecular pathways mediating liver metastasis in patients with uveal melanoma. Clinical Cancer Research *14*, 951-956.

Balch, C.M., Houghton, A.N., Sober, A.J., and Soong, S.J. (2003). Cutaneous Melanoma, 4th edition (St. Louis, MO, USA: Quality Medical Publishing).

Balch, C.M., Soong, S.-J., Gershenwald, J.E., Thompson, J.F., Reintgen, D.S., Cascinelli, N., Urist, M., McMasters, K.M., Ross, M.I., Kirkwood, J.M.*, et al.* (2001). Prognostic factors analysis of 17,600 melanoma patients: Validation of the American Joint Committee on cancer melanoma staging system. Journal of Clinical Oncology *19*, 3622-3634.

Bald, T., Quast, T., Landsberg, J., Rogava, M., Glodde, N., Lopez-Ramos, D., Kohlmeyer, J., Riesenberg, S., van den Boorn-Konijnenberg, D., Homig-Holzel, C.*, et al.* (2014). Ultraviolet-radiation-induced inflammation promotes angiotropism and metastasis in melanoma. Nature *507*, 109-113.

Barranco, S.C., Romsdahl, M.M., and Humphrey, R.M. (1971). The radiation response of human malignant melanoma cells grown in vitro. Cancer Research *31*, 830-833.

Bastian, B.C., LeBoit, P.E., Hamm, H., Bröcker, E.-B., and Pinkel, D. (1998). Chromosomal gains and losses in primary cutaneous melanomas detected by comparative Genomic hybridization. Cancer Research *58*, 2170-2175.

Bauer, J., Büttner, P., Murali, R., Okamoto, I., Kolaitis, N.A., Landi, M.T., Scolyer, R.A., and Bastian, B.C. (2011). BRAF mutations in cutaneous melanoma are independently associated with age, anatomic site of the primary tumor, and the degree of solar elastosis at the primary tumor site. Pigment Cell & Melanoma Research *24*, 345-351.

Bevona, C., Goggins, W., Quinn, T., Fullerton, J., and Tsao, H. (2003). Cutaneous melanomas associated with nevi. Archives of Dermatology *139*, 1620-1624.

Brahmer, J.R., Tykodi, S.S., Chow, L.Q.M., Hwu, W.-J., Topalian, S.L., Hwu, P., Drake, C.G., Camacho, L.H., Kauh, J., Odunsi, K.*, et al.* (2012). Safety and activity of anti–PD-L1 antibody in patients with advanced cancer. New England Journal of Medicine *366*, 2455-2465.

Breslow, A. (1970). Thickness, cross-sectional areas and depth of invasion in the prognosis of cutaneous melanoma. Annals of Surgery *172*, 902-908.

Broekaert, S.M.C., Roy, R., Okamoto, I., van den Oord, J., Bauer, J., Garbe, C., Barnhill, R.L., Busam, K.J., Cochran, A.J., Cook, M.G.*, et al.* (2010). Genetic and morphologic features for melanoma classification. Pigment Cell & Melanoma Research *23*, 763-770.

Bucheit, A.D., Chen, G., Siroy, A., Tetzlaff, M., Broaddus, R., Milton, D., Fox, P., Bassett, R., Hwu, P., Gershenwald, J.E.*, et al.* (2014). Complete loss of PTEN protein expression correlates with shorter time to brain metastasis and survival in stage IIIB/C melanoma patients with BRAFV600 mutations. Clinical Cancer Research *20*, 5527-5536.

Budman, D.R., Camacho, E., and Wittes, R.E. (1978). The current causes of death in patients with malignant melanoma. European Journal of Cancer (1965) *14*, 327-330.

Busch, C., Krochmann, J., and Drews, U. (2012). Human melanoma cells in the rhombencephalon of the chick embryo: A novel model for brain metastasis. Experimental Dermatology *21*, 944-947.

Chaichana, K.K., and Chaichana, K.L. (2011). Diagnosis and treatment options for brain metastasis of melanoma, Treatment of Metastatic Melanoma, Ms Rachael Morton (Ed.), INTECH Open Access Publisher. Available from: http://www.intechopen.com/books/treatment-of-metastatic-melanoma/diagnosis-and-treatment-options-for-brain-metastasis-of-melanona

Chen, G., Chakravarti, N., Aardalen, K., Lazar, A.J., Tetzlaff, M.T., Wubbenhorst, B., Kim, S.-B., Kopetz, S., Ledoux, A.A., Gopal, Y.N.V.*, et al.* (2014). Molecular profiling

of patient-matched brain and extracranial melanoma metastases implicates the PI3K pathway as a therapeutic target. Clinical Cancer Research *20*, 5537-5546.

Chin, L., Pomerantz, J., Polsky, D., Jacobson, M., Cohen, C., Cordon-Cardo, C., Horner, J.W., and DePinho, R.A. (1997). Cooperative effects of INK4a and ras in melanoma susceptibility in vivo. Genes & Development *11*, 2822-2834.

Cichorek, M., Wachulska, M., Stasiewicz, A., and Tymińska, A. (2013). Skin melanocytes: Biology and development. Advances in Dermatology and Allergology/Postępy Dermatologii I Alergologii *30*, 30-41.

Clark, J., Wallace H., From, L., Bernardino, E.A., and Mihm, M. (1969). The histogenesis and biological behavior of primary human malignant melanomas of the skin. Cancer Research *29*, 705-726.

Clark, W.H., Jr., ed. (1967). A classification of malignant melanoma in man correlated with histogenesis and biological behaviour, 1st edition (London: Pergamon Press Ltd.).

Clark, W.H., Jr., Elder, D.E., Guerry, D., 4th, Epstein, M.N., Greene, M.H., and Van Horn, M. (1984). A study of tumor progression: The precursor lesions of superficial spreading and nodular melanoma. Human Pathology *15*, 1147-1165.

Colombino, M., Capone, M., Lissia, A., Cossu, A., Rubino, C., De Giorgi, V., Massi, D., Fonsatti, E., Staibano, S., Nappi, O.*, et al.* (2012). BRAF/NRAS mutation frequencies among primary tumors and metastases in patients with melanoma. Journal of Clinical Oncology *30*, 2522-2529.

Cruz-Munoz, W., Jaramillo, M.L., Man, S., Xu, P., Banville, M., Collins, C., Nantel, A., Francia, G., Morgan, S.S., Cranmer, L.D.*, et al.* (2012). Roles for endothelin receptor B and BCL2A1 in spontaneous CNS metastasis of melanoma. Cancer Research *72*, 4909-4919.

Cruz-Munoz, W., Man, S., Xu, P., and Kerbel, R.S. (2008). Development of a preclinical model of spontaneous human melanoma central nervous system metastasis. Cancer Research *68*, 4500-4505.

Curtin, J.A., Fridlyand, J., Kageshita, T., Patel, H.N., Busam, K.J., Kutzner, H., Cho, K.-H., Aiba, S., Bröcker, E.-B., LeBoit, P.E.*, et al.* (2005). Distinct sets of genetic alterations in melanoma. New England Journal of Medicine *353*, 2135-2147.

Curtin, J.A., Stark, M.S., Pinkel, D., Hayward, N.K., and Bastian, B.C. (2006). PI3-kinase subunits are infrequent somatic targets in melanoma. Journal of Investigative Dermatology *126*, 1660-1663.

Dai, D.L., Martinka, M., and Li, G. (2005). Prognostic significance of activated Akt expression in melanoma: A clinicopathologic study of 292 cases. Journal of Clinical Oncology *23*, 1473-1482.

Damsky, W., Micevic, G., Meeth, K., Muthusamy, V., Curley, D.P., Santhanakrishnan, M., Erdelyi, I., Platt, J.T., Huang, L., Theodosakis, N.*, et al.* (2015). mTORC1 activation blocks BrafV600E-induced growth arrest but is insufficient for melanoma formation. Cancer Cell *27*, 41-56.

Damsky, W.E., Curley, D.P., Santhanakrishnan, M., Rosenbaum, L.E., Platt, J.T., Gould-Rothberg, B.E., Taketo, M.M., Dankort, D., Rimm, D.L., McMahon, M.*, et al.* (2011a). Beta-catenin signaling controls metastasis in Braf-activated Pten-deficient melanomas. Cancer Cell *20*, 741-754.

Damsky, W.E., Rosenbaum, L.E., and Bosenberg, M. (2011b). Decoding melanoma metastasis. Cancers *3*, 126-163.

Daniotti, M., Oggionni, M., Ranzani, T., Vallacchi, V., Campi, V., Di Stasi, D., Torre, G.D., Perrone, F., Luoni, C., Suardi, S.*, et al.* (2004). BRAF alterations are associated with complex mutational profiles in malignant melanoma. Oncogene *23*, 5968-5977.

Dankort, D., Curley, D.P., Cartlidge, R.A., Nelson, B., Karnezis, A.N., Damsky Jr, W.E., You, M.J., DePinho, R.A., McMahon, M., and Bosenberg, M. (2009). BrafV600E cooperates with Pten loss to induce metastatic melanoma. Nature Genetics *41*, 544-552.

Davies, H., Bignell, G.R., Cox, C., Stephens, P., Edkins, S., Clegg, S., Teague, J., Woffendin, H., Garnett, M.J., Bottomley, W.*, et al.* (2002). Mutations of the BRAF gene in human cancer. Nature *417*, 949-954.

Davies, M.A., Liu, P., McIntyre, S., Kim, K.B., Papadopoulos, N., Hwu, W.-J., Hwu, P., and Bedikian, A. (2011). Prognostic factors for survival in melanoma patients with brain metastases. Cancer *117*, 1687-1696.

Davies, M.A., and Samuels, Y. (2010). Analysis of the genome to personalize therapy for melanoma. Oncogene *29*, 5545-5555.

Davies, M.A., Stemke-Hale, K., Lin, E., Tellez, C., Deng, W., Gopal, Y.N., Woodman, S.E., Calderone, T.C., Ju, Z., Lazar, A.J.*, et al.* (2009). Integrated molecular and clinical analysis of AKT activation in metastatic melanoma. Clinical Cancer Research *15*, 7538-7546.

Davies, M.A., Stemke-Hale, K., Tellez, C., Calderone, T.L., Deng, W., Prieto, V.G., Lazar, A.J.F., Gershenwald, J.E., and Mills, G.B. (2008). A novel AKT3 mutation in melanoma tumours and cell lines. British Journal of Cancer *99*, 1265-1268.

Di Giacomo, A.M., Ascierto, P.A., Pilla, L., Santinami, M., Ferrucci, P.F., Giannarelli, D., Marasco, A., Rivoltini, L., Simeone, E., Nicoletti, S.V.L.*, et al.* (2012). Ipilimumab and fotemustine in patients with advanced melanoma (NIBIT-M1): An open-label, single-arm phase 2 trial. The Lancet Oncology *13*, 879-886.

Dong, L., Jin, L., Tseng, H.Y., Wang, C.Y., Wilmott, J.S., Yosufi, B., Yan, X.G., Jiang, C.C., Scolyer, R.A., Zhang, X.D.*, et al.* (2014). Oncogenic suppression of PHLPP1 in human melanoma. Oncogene *33*, 4756-4766.

Eichler, A.F., and Loeffler, J.S. (2007). Multidisciplinary management of brain metastases. The Oncologist *12*, 884-898.

Ewend, M.G., Carey, L.A., and Brem, H. (1996). Treatment of melanoma metastases in the brain. Seminars in Surgical Oncology *12*, 429-435.

Fabricant, R.N., De Larco, J.E., and Todaro, G.J. (1977). Nerve growth factor receptors on human melanoma cells in culture. Proceedings of the National Academy of Sciences *74*, 565-569.

Falchook, G.S., Long, G.V., Kurzrock, R., Kim, K.B., Arkenau, T.H., Brown, M.P., Hamid, O., Infante, J.R., Millward, M., Pavlick, A.C.*, et al.* (2012). Dabrafenib in patients with melanoma, untreated brain metastases, and other solid tumours: A phase 1 dose-escalation trial. The Lancet *379*, 1893-1901.

Fecher, L.A., Cummings, S.D., Keefe, M.J., and Alani, R.M. (2007). Toward a molecular classification of melanoma. Journal of Clinical Oncology *25*, 1606-1620.

Fife, K.M., Colman, M.H., Stevens, G.N., Firth, I.C., Moon, D., Shannon, K.F., Harman, R., Petersen-Schaefer, K., Zacest, A.C., Besser, M.*, et al.* (2004). Determinants of outcome in melanoma patients with cerebral metastases. Journal of Clinical Oncology *22*, 1293-1300.

Filder, I.J., Schackert, G., Zhang, R.-d., Radinsky, R., and Fujimaki, T. (1999). The biology of melanoma brain metastasis. Cancer and Metastasis Reviews *18*, 387-400.

Firth, J.D., and Ratcliffe, P.J. (1992). Organ distribution of the three rat endothelin messenger RNAs and the effects of ischemia on renal gene expression. The Journal of Clinical Investigation *90*, 1023-1031.

Flanigan, J.C., Jilaveanu, L.B., Faries, M., Sznol, M., Ariyan, S., Yu, J.B., Knisely, J.P.S., Chiang, V.L., and Kluger, H.M. (2011). Melanoma brain metastases: Is it time to reassess the bias? Current Problems in Cancer *35*, 200-210.

Francken, A.B., Shaw, H.M., Thompson, J.F., Soong, S.-j., Accortt, N.A., Azzola, M.F., Scolyer, R.A., Milton, G.W., McCarthy, W.H., Colman, M.H.*, et al.* (2004). The prognostic importance of tumor mitotic rate confirmed in 1317 patients with primary cutaneous melanoma and long follow-up. Annals of Surgical Oncology *11*, 426-433.

Fujimaki, T., Fan, D., Price, J.E., Staroselsky, A., Gohji, K., Bucana, C.D., and Fidler, I.J. (1993). Critical factors regulating site-specific brain metastasis of murine melanomas. International Journal of Oncology *3*, 789-799.

Fujimaki, T., Price, J.E., Fan, D., Bucana, C.D., Itoh, K., Kirino, T., and Fidler, I.J. (1996). Selective growth of human melanoma cells in the brain parenchyma of nude mice. Melanoma Research *6*, 363-371.

Gershenwald, J.E., Soong, S.J., and Balch, C.M. (2010). 2010 TNM staging system for cutaneous melanoma...and beyond. Annals of Surgical Oncology *17*, 1475-1477.

Gimotty, P.A., Guerry, D., Ming, M.E., Elenitsas, R., Xu, X., Czerniecki, B., Spitz, F., Schuchter, L., and Elder, D. (2004). Thin primary cutaneous malignant melanoma: A prognostic tree for 10-year metastasis is more accurate than American Joint Committee on cancer staging. Journal of Clinical Oncology *22*, 3668-3676.

Goldgeier, M.H., Klein, L.E., Klein-Angerer, S., Moellmann, G., and Nordlund, J.J. (1984). The distribution of melanocytes in the leptomeninges of the human brain. Journal of Investigative Dermatology *82*, 235-238.

Gorantla, V., Kirkwood, J., and Tawbi, H. (2013). Melanoma brain metastases: An unmet challenge in the era of active therapy. Current Oncology Reports *15*, 483-491.

Goulart, C.R., Mattei, T.A., and Ramina, R. (2011). Cerebral melanoma metastases: A critical review on diagnostic methods and therapeutic options. ISRN Surgery *2011*, 9.

Govindarajan, B., Sligh, J.E., Vincent, B.J., Li, M., Canter, J.A., Nickoloff, B.J., Rodenburg, R.J., Smeitink, J.A., Oberley, L., Zhang, Y.*, et al.* (2007). Overexpression of Akt converts radial growth melanoma to vertical growth melanoma. The Journal of Clinical Investigation *117*, 719-729.

Gruber, S.B., Barnhill, R.L., Stenn, K.S., and Roush, G.C. (1989). Nevomelanocytic proliferations in association with cutaneous malignant melanoma. Journal of the American Acadamy of Dermatology *21*, 773-780.

Guirguis, L.M., Yang, J.C., White, D.E., Steinberg, S.M., Liewehr, D.J., Rosenberg, S.A., and Schwartzentruber, D.J. (2002). Safety and efficacy of high-dose interleukin-2 therapy in patients with brain metastases. Journal of Immunotherapy (Hagerstown, Md : 1997) *25*, 82-87.

Hamid, O., Robert, C., Daud, A., Hodi, F.S., Hwu, W.-J., Kefford, R., Wolchok, J.D., Hersey, P., Joseph, R.W., Weber, J.S.*, et al.* (2013). Safety and tumor responses with Lambrolizumab (Anti–PD-1) in melanoma. New England Journal of Medicine *369*, 134-144.

Hart, I.R., and Fidler, I.J. (1980). Role of organ selectivity in the determination of metastatic patterns of B16 melanoma. Cancer Research *40*, 2281-2287.

Herlyn, M., Thurin, J., Balaban, G., Bennicelli, J.L., Herlyn, D., Elder, D.E., Bondi, E., Guerry, D., Nowell, P., Clark, W.H., et al. (1985). Characteristics of cultured human

melanocytes isolated from different stages of tumor progression. Cancer Research *45*, 5670-5676.

Herrmann, J.L., Menter, D.G., Hamada, J., Marchetti, D., Nakajima, M., and Nicolson, G.L. (1993). Mediation of NGF-stimulated extracellular matrix invasion by the human melanoma low-affinity p75 neurotrophin receptor: Melanoma p75 functions independently of trkA. Molecular Biology of the Cell *4*, 1205-1216.

Hess, K.R., Varadhachary, G.R., Taylor, S.H., Wei, W., Raber, M.N., Lenzi, R., and Abbruzzese, J.L. (2006). Metastatic patterns in adenocarcinoma. Cancer *106*, 1624-1633.

Hocker, T., and Tsao, H. (2007). Ultraviolet radiation and melanoma: A systematic review and analysis of reported sequence variants. Human Mutation *28*, 578-588.

Hodi, F.S., O'Day, S.J., McDermott, D.F., Weber, R.W., Sosman, J.A., Haanen, J.B., Gonzalez, R., Robert, C., Schadendorf, D., Hassel, J.C.*, et al.* (2010). Improved survival with Ipilimumab in patients with metastatic melanoma. New England Journal of Medicine *363*, 711-723.

Hodis, E., Watson, I.R., Kryukov, G.V., Arold, S.T., Imielinski, M., Theurillat, J.-P., Nickerson, E., Auclair, D., Li, L., Place, C.*, et al.* (2012). A landscape of driver mutations in melanoma. Cell *150*, 251-263.

Hong, J.J., Rosenberg, S.A., Dudley, M.E., Yang, J.C., White, D.E., Butman, J.A., and Sherry, R.M. (2010). Successful treatment of melanoma brain metastases with adoptive cell therapy. Clinical Cancer Research *16*, 4892-4898.

Howlader, N., Noone, A.M., Krapcho, M., Garshell, J., Miller, D., Altekruse, S.F., Kosary, C.L., Yu, M., Ruhl, J., Tatalovich, Z.*, et al.* (2014). SEER Cancer Statistics Review, 1975-2011 (Bethesda, MD: National Cancer Institute).

Izraely, S., Klein, A., Sagi-Assif, O., Meshel, T., Tsarfaty, G., Hoon, D.S.B., and Witz, I.P. (2010). Chemokine-chemokine receptor axes in melanoma brain metastasis. Immunology Letters *130*, 107-114.

Jilaveanu, L.B., Parisi, F., Barr, M.L., Zito, C.R., Cruz-Munoz, W., Kerbel, R.S., Rimm, D.L., Bosenberg, M.W., Halaban, R., Kluger, Y.*, et al.* (2014). PLEKHA5 as a biomarker and potential mediator of melanoma brain metastasis. Clinical Cancer Research *21*, 2138-2147.

Ju, R., Zhuang, Z.W., Zhang, J., Lanahan, A.A., Kyriakides, T., Sessa, W.C., and Simons, M. (2014). Angiopoietin-2 secretion by endothelial cell exosomes: Regulation by the phosphatidylinositol 3-kinase (PI3K)/Akt/endothelial nitric oxide synthase (eNOS) and syndecan-4/synthenin pathways. Journal of Biological Chemistry *289*, 510-519.

Karar, J., and Maity, A. (2011). PI3K/AKT/mTOR pathway in angiogenesis. Frontiers in Molecular Neuroscience *4*.

Khan, A.J., and Dicker, A.P. (2013). On the merits and limitations of whole-brain radiation therapy. Journal of Clinical Oncology *31*, 11-13.

Kienast, Y., von Baumgarten, L., Fuhrmann, M., Klinkert, W.E.F., Goldbrunner, R., Herms, J., and Winkler, F. (2010). Real-time imaging reveals the single steps of brain metastasis formation. Nature Medicine *16*, 116.

Kim, K., Flaherty, K., Chapman, P., Sosman, J., Ribas, A., McArthur, G., Amaravadi, R., Lee, R., Nolop, K., and Puzanov, I. (2011). Pattern and outcome of disease progression in phase I study of vemurafenib in patients with metastatic melanoma (MM). Journal of Clinical Oncology *29*, 530s.

Klein, A., Sagi-Assif, O., Izraely, S., Meshel, T., Pasmanik-Chor, M., Nahmias, C., Couraud, P.-O., Erez, N., Hoon, D.S.B., and Witz, I.P. (2012). The metastatic microenvironment: Brain-derived soluble factors alter the malignant phenotype of cutaneous and brain-metastasizing melanoma cells. International Journal of Cancer *131*, 2509-2518.

Knisely, J.P., Yu, J.B., Flanigan, J.C., Sznol, M., Kluger, H.M., and Chiang, V.L. (2012). Radiosurgery for melanoma brain metastases in the ipilimumab era and the possibility of longer survival. Journal of Neurosurgery *117*, 227-233.

Krauthammer, M., Kong, Y., Ha, B.H., Evans, P., Bacchiocchi, A., McCusker, J.P., Cheng, E., Davis, M.J., Goh, G., Choi, M*., et al.* (2012). Exome sequencing identifies recurrent somatic RAC1 mutations in melanoma. Nature Genetics *44*, 1006-1014.

LeBoit, P.E., Burg, G., Weedon, D., and Sarasain, A. (2006). World Health Organization Classification of Tumours (Lyon: IARC Press).

Leiter, U., Meier, F., Schittek, B., and Garbe, C. (2004). The natural course of cutaneous melanoma. Journal of Surgical Oncology *86*, 172-178.

Liu, W., Monahan, K.B., Pfefferle, A.D., Shimamura, T., Sorrentino, J., Chan, K.T., Roadcap, D.W., Ollila, D.W., Thomas, N.E., Castrillon, D.H*., et al.* (2012). LKB1/STK11 inactivation leads to expansion of a prometastatic tumor subpopulation in melanoma. Cancer Cell *21*, 751-764.

Logan, P.T., Fernandes, B.F., Di Cesare, S., Marshall, J.-C.A., Maloney, S.C., and Burnier, M.N., Jr. (2008). Single-cell tumor dormancy model of uveal melanoma. Clinical & Experimental Metastasis *25*, 509-516.

Long, G.V., Trefzer, U., Davies, M.A., Kefford, R.F., Ascierto, P.A., Chapman, P.B.,Puzanov, I., Hauschild, A., Robert, C., Algazi, A., et al. (2012). Dabrafenib in patients with Val600Glu or Val600Lys BRAF-mutant melanoma metastatic to the brain (BREAK-MB): A multicentre, open-label, phase 2 trial. The Lancet Oncology *13*, 1087-1095.

Lorigan, J.G., Wallace, S., and Mavligit, G.M. (1991). The prevalence and location of metastases from ocular melanoma: Imaging study in 110 patients. American Journal of Roentgenology *157*, 1279-1281.

Marchetti, D. (2002). Heparanase: A target for therapy of brain invasive tumors? Expert Review of Neurotherapeutics *2*, 459-463.

Marchetti, D., Denkins, Y., Reiland, J., Greiter-Wilke, A., Galjour, J., Murry, B., Blust, J., and Roy, M. (2003a). Brain-metastatic melanoma: A neurotrophic perspective. Pathology Oncology Research *9*, 147-158.

Marchetti, D., Li, J., and Shen, R. (2000). Astrocytes contribute to the metastatic brain specificity of melanoma cells by producing heparanase. Society for Neuroscience Abstracts *26*, Abstract No.-189.117.

Marchetti, D., McCutcheon, I., Ross, M., and Nicolson, G. (1995). Inverse expression of neurotrophins and neurotrophin receptros at the invasion front of human-melanoma brain metastases. International Journal of Oncology *7*, 87-94.

Marchetti, D., Menter, D., Jin, L., Nakajima, M., and Nicolson, G.L. (1993). Nerve growth factor effects on human and mouse melanoma cell invasion and heparanase production. International Journal of Cancer *55*, 692-699.

Marchetti, D., Murry, B., Galjour, J., and Wilke-Greiter, A. (2003b). Human melanoma TrkC: Its association with a purine-analog-sensitive kinase activity. Journal of Cellular Biochemistry *88*, 865-872.

Marek, W., and Ehud, A. (2000). Surgical treatment of brain metastases from melanoma: A retrospective study of 91 patients. Journal of Neurosurgery *93*, 9-18.

Marks, R., Dorevitch, A.P., and Mason, G. (1990). Do all melanomas come from "moles"? A study of the histological association. Australasian Journal of Dermatology *31*, 77-80.

Mayer, T.C. (1973). The migratory pathway of neural crest cells into the skin of mouse embryos. Developmental Biology *34*, 39-46.

McGovern, V.J. (1970). The classification of melanoma and its relationship with prognosis. Pathology *2*, 85-98.

McGovern, V.J., Shaw, H.M., Milton, G.W., and Farago, G.A. (1979). Prognostic significance of the histological features of malignant melanoma. Histopathology *3*, 385-393.

Mehlen, P., and Puisieux, A. (2006). Metastasis: A question of life or death. Nature Reviews of Cancer *6*, 449-458.

Meier, F., Will, S., Ellwanger, U., Schlagenhauff, B., Schittek, B., Rassner, G., and Garbe, C. (2002). Metastatic pathways and time courses in the orderly progression of cutaneous melanoma. British Journal of Dermatology *147*, 62-70.

Mervic, L. (2012). Time course and pattern of metastasis of cutaneous melanoma differ between men and women. PLoS ONE *7*, e32955.

Mikhail, M., Velazquez, E., Shapiro, R., Berman, R., Pavlick, A., Sorhaindo, L., Spira, J., Mir, C., Panageas, K.S., Polsky, D.*, et al.* (2005). PTEN expression in melanoma: Relationship with patient survival, Bcl-2 expression, and proliferation. Clinical Cancer Research *11*, 5153-5157.

Miller, A.J., and Mihm, M.C. (2006). Melanoma. New England Journal of Medicine *355*, 51-65.

Morsi, A., Gaziel-Sovran, A., Cruz-Munoz, W., Kerbel, R.S., Golfinos, J.G., Hernando, E., and Wadghiri, Y.Z. (2013). Development and characterization of a clinically relevant mouse model of melanoma brain metastasis. Pigment Cell & Melanoma Research *26*, 743-745.

Murry, B.P., Blust, B.E., Singh, A., Foster, T.P., and Marchetti, D. (2006). Heparanase brain: Mechanisms of melanoma metastasis to the development and use of a brain slice model. Journal of Cellular Biochemistry *97*, 217-225.

Nathanson, S.D. (2003). Insights into the mechanisms of lymph node metastasis. Cancer *98*, 413-423.

Nieder, C., Grosu, A., and Gaspar, L. (2014). Stereotactic radiosurgery (SRS) for brain metastases: A systematic review. Radiation Oncology *9*, 155.

Niessner, H., Forschner, A., Klumpp, B., Honegger, J.B., Witte, M., Bornemann, A., Dummer, R., Adam, A., Bauer, J., Tabatabai, G.*, et al.* (2013). Targeting hyperactivation of the AKT survival pathway to overcome therapy resistance of melanoma brain metastases. Cancer Medicine *2*, 76-85.

Omholt, K., Kröckel, D., Ringborg, U., and Hansson, J. (2006). Mutations of PIK3CA are rare in cutaneous melanoma. Melanoma Research *16*, 197-200.

Ott, P.A., Hodi, F.S., and Robert, C. (2013). CTLA-4 and PD-1/PD-L1 blockade: New immunotherapeutic modalities with durable clinical benefit in melanoma patients. Clinical Cancer Research *19*, 5300-5309.

Padua, R.A., Barrass, N.C., and Currie, G.A. (1985). Activation of N-ras in a human melanoma cell line. Molecular and Cellular Biology *5*, 582-585.

Paget, S. (1889). The distribution of secondary growths in cancer of the breast. The Lancet *133*, 571-573.

Pardoll, D.M. (2012). The blockade of immune checkpoints in cancer immunotherapy. Nature Reviews of Cancer *12*, 252-264.

Patel, J.K., Didolkar, M.S., Pickren, J.W., and Moore, R.H. (1978). Metastatic pattern of malignant melanoma: A study of 216 autopsy cases. The American Journal of Surgery *135*, 807-810.

Phung, T.L., Du, W., Xue, Q., Ayyaswamy, S., Gerald, D., Antonello, Z., Nhek, S., Perruzzi, C.A., Acevedo, I., Ramanna-Valmiki, R.*, et al.* (2015). Akt1 and Akt3 exert opposing roles in the regulation of vascular tumor growth. Cancer Research *75*, 40-50.

Phung, T.L., Ziv, K., Dabydeen, D., Eyiah-Mensah, G., Riveros, M., Perruzzi, C., Sun, J., Monahan-Earley, R.A., Shiojima, I., Nagy, J.A.*, et al.* (2006). Pathological angiogenesis is induced by sustained Akt signaling and inhibited by rapamycin. Cancer Cell *10*, 159-170.

Piris, A., and Mihm, M. (2007). Mechanisms of metastasis: Seed and soil. In cancer metastasis and the lymphovascular system: Basis for rational therapy, S.L. Leong, ed. (Springer US), pp. 119-127.

Plonka, P.M., Passeron, T., Brenner, M., Tobin, D.J., Shibahara, S., Thomas, A., Slominski, A., Kadekaro, A.L., Hershkovitz, D., Peters, E.*, et al.* (2009). What are melanocytes really doing all day long…? Experimental Dermatology *18*, 799-819.

Pollock, P.M., Harper, U.L., Hansen, K.S., Yudt, L.M., Stark, M., Robbins, C.M., Moses, T.Y., Hostetter, G., Wagner, U., Kakareka, J.*, et al.* (2003). High frequency of BRAF mutations in nevi. Nature Genetics *33*, 19-20.

Pollock, P.M., and Meltzer, P.S. (2002). A genome-based strategy uncovers frequent BRAF mutations in melanoma. Cancer Cell *2*, 5-7.

Powell, S., and Dudek, A.Z. (2009). Single-institution outcome of high-dose interleukin-2 (HD IL-2) therapy for metastatic melanoma and analysis of favorable response in brain metastases. Anticancer Research *29*, 4189-4193.

Poynter, J.N., Elder, J.T., Fullen, D.R., Nair, R.P., Soengas, M.S., Johnson, T.M., Redman, B., Thomas, N.E., and Gruber, S.B. (2006). BRAF and NRAS mutations in melanoma and melanocytic nevi. Melanoma Research *16*, 267-273.

Sampson, J.H., Carter, J.H., Jr., Friedman, A.H., and Seigler, H.F. (1998). Demographics, prognosis, and therapy in 702 patients with brain metastases from malignant melanoma. Journal of Neurosurgery *88*, 11-20.

Schackert, G., Price, J.E., Zhang, R.D., Bucana, C.D., Itoh, K., and Fidler, I.J. (1990). Regional growth of different human melanomas as metastases in the brain of nude mice. The American Journal of Pathology *136*, 95-102.

Schartz, N.E.C., Farges, C., Madelaine, I., Bruzzoni, H., Calvo, F., Hoos, A., and Lebbe, C. (2010). Complete regression of a previously untreated melanoma brain metastasis with ipilimumab. Melanoma Research *20*, 247-250.

Schultz, S., Kane, M., Roush, R., Miller, V., Berd, D., Goldman, L., and Mastrangelo, M. (1990). Time to recurrence varies inversely with thickness in clinical stage 1 cutaneous. Surgery, Gynecology & Obstetrics *171*, 393-397.

Scolyer, R.A., and Prieto, V.G. (2011). Melanoma pathology: Important issues for cliniciansinvolved in the multidisciplinary care of melanoma patients. Surgical Oncology Clinics of North America *20*, 19-37.

Scolyer, R.A., Shaw, H.M., Thompson, J.F., Li, L.X., Colman, M.H., Lo, S.K., McCarthy, S.W., Palmer, A.A., Nicoll, K.D., Dutta, B.*, et al.* (2003). Interobserver reproducibility of histopathologic prognostic variables in primary. The American Journal of Surgical Pathology 2003 Dec;27(12):1571-6 *27*, 1571-1576.

Serrano, M., Lee, H.-W., Chin, L., Cordon-Cardo, C., Beach, D., and DePinho, R.A. (1996). Role of the INK4a locus in tumor suppression and cell mortality. Cell *85*, 27-37.

Sharpless, N.E., and DePinho, R.A. (1999). The INK4A/ARF locus and its two gene products. Current Opinion in Genetics & Development *9*, 22-30.

Siegel, R.L., Miller, K.D., and Jemal, A. (2015). Cancer statistics, 2015. CA: A Cancer Journal for Clinicians *65*, 5-29.

Smalley, K.S.M. (2009). Understanding melanoma signaling networks as the basis for molecular targeted therapy. Journal of Investigative Dermatology *130*, 28-37.

Soong, S.-j., Ding, S., Coit, D., Balch, C., Gershenwald, J., Thompson, J., and Gimotty, P. (2010). Predicting survival outcome of localized melanoma: An electronic prediction tool based on the AJCC melanoma database. Annals of Surgical Oncology *17*, 2006-2014.

Soong, S.-J., Harrison, R.A., McCarthy, W.H., Urist, M.M., and Balch, C.M. (1998). Factors affecting survival following local, regional, or distant recurrence from localized melanoma. Journal of Surgical Oncology *67*, 228-233.

Stahl, J.M., Sharma, A., Cheung, M., Zimmerman, M., Cheng, J.Q., Bosenberg, M.W., Kester, M., Sandirasegarane, L., and Robertson, G.P. (2004). Deregulated Akt3 activity promotes development of malignant melanoma. Cancer Research *64*, 7002-7010.

Stoletov, K., Strnadel, J., Zardouzian, E., Momiyama, M., Park, F.D., Kelber, J.A., Pizzo, D.P., Hoffman, R., VandenBerg, S.R., and Klemke, R.L. (2013). Role of connexins in metastatic breast cancer and melanoma brain colonization. Journal of Cell Science *126*, 904-913.

Tas, F. (2012). Metastatic behavior in melanoma: Timing, pattern, survival, and influencing factors. Journal of Oncology 2012, 9.

Topalian, S.L., Hodi, F.S., Brahmer, J.R., Gettinger, S.N., Smith, D.C., McDermott, D.F., Powderly, J.D., Carvajal, R.D., Sosman, J.A., Atkins, M.B.*, et al.* (2012). Safety, activity, and immune correlates of anti–PD-1 antibody in cancer. New England Journal of Medicine *366*, 2443-2454.

Tsao, H., Goel, V., Wu, H., Yang, G., and Haluska, F.G. (2004). Genetic interaction between NRAS and BRAF mutations and PTEN/MMAC1 inactivation in melanoma. Journal of Investigative Dermatology *122*, 337-341.

VanBrocklin, M.W., Robinson, J.P., Lastwika, K.J., Khoury, J.D., and Holmen, S.L. (2010). Targeted delivery of NRASQ61R and Cre-recombinase to post-natal melanocytes induces melanoma in Ink4a/Arflox/lox mice. Pigment Cell & Melanoma Research *23*, 531-541.

Virchow, R. (1989). As based upon physiological and pathological histology. Nutrition Reviews *47*, 23-25.

Vonderheide, R.H., and June, C.H. (2014). Engineering T cells for cancer: Our synthetic future. Immunological Reviews *257*, 7-13.

Weber, J.S., Amin, A., Minor, D., Siegel, J., Berman, D., and O'Day, S.J. (2011). Safety and clinical activity of ipilimumab in melanoma patients with brain metastases: Retrospective analysis of data from a phase 2 trial. Melanoma Research *21*, 530-534.

Webster, R.M. (2014). The immune checkpoint inhibitors: Where are we now? Nature Reviews Drug Discovery *13*, 883-884.

Whiteman, D.C., Pavan, W.J., and Bastian, B.C. (2011). The melanomas: A synthesis of epidemiological, clinical, histopathological, genetic, and biological aspects, supporting distinct subtypes, causal pathways, and cells of origin. Pigment Cell & Melanoma Research *24*, 879-897.

Wolf, I.H., Richtig, E., Kopera, D., and Kerl, H. (2004). Locoregional cutaneousmetastases of malignant melanoma and their management. Dermatologic Surgery *30*, 244-247.

Yashin, A.I., Wu, D., Arbeev, K.G., Kulminski, A.M., Stallard, E., and Ukraintseva, S.V. (2013). Why does melanoma metastasize into the brain? Genes with pleiotropic effects might be the key. Frontiers in Genetics *4*, 75.

Yoshida, K., and Gage, F.H. (1992). Cooperative regulation of nerve growth factor synthesis and secretion in fibroblasts and astrocytes by fibroblast growth factor and other cytokines. Brain Research *569*, 14-25.

Zbytek, B., Carlson, J.A., Granese, J., Ross, J., Mihm, M., and Slominski, A. (2008). Current concepts of metastasis in melanoma. Expert Review of Dermatology *3*, 569-585.

CHAPTER 2

AKT1 ACTIVATION PROMOTES THE DEVELOPMENT OF BRAIN MELANOMA METASTASES

2.1 Preface

This chapter is a re-formatted version of a manuscript submitted to *Cell Reports* in April 2015. The work presented herein was completed with the following co-authors: James P. Robinson, Rowan A. Arave, Russell D. Green, David A. Kircher, Guo Chen, Michael A. Davies, Allie H. Grossmann, Matthew W. VanBrocklin, Martin McMahon, and Sheri L. Holmen.

2.2 Introduction

Recent approvals of more efficacious therapies have shifted the treatment paradigm for melanoma and have provided much needed breakthroughs in this disease (Girotti et al., 2014). However, the increasing incidence of melanoma and the mortality associated with advanced stages of the disease remain cause for concern. More than half of all melanoma deaths are due to brain metastases (Davies et al., 2011), which are one of the most common and devastating complications of melanoma. Up to 75% of patients with stage IV melanoma will develop brain metastases and the prognosis for these patients is extremely poor (Chaichana and Chaichana, 2011). Despite recent therapeutic

advances, melanoma brain metastasis continues to pose a significant clinical challenge and demands further investigation into the molecular mechanisms driving distant dissemination of this disease.

Clinical data provides compelling correlative evidence that AKT signaling is involved in melanoma metastasis, especially to the brain (Dai et al., 2005; Davies et al., 2009). A comparison between lung, liver, and brain metastases from human melanoma samples noted significantly higher levels of phosphorylated AKT and a downstream target, phosphorylated GSK3β, in brain metastases compared to lung and liver metastases. In line with increased AKT activity, PTEN protein levels were significantly lower in brain metastases compared with lung and liver metastases (Davies et al., 2009; Niessner et al., 2013). Follow-up studies comparing patient-matched brain versus extracranial melanoma metastases found additional evidence of increased AKT activity as a feature of brain metastases but PTEN protein levels were similar between the matched metastases (Chen et al., 2014). Furthermore, PTEN silencing combined with expression of $BRAF^{V600E}$ in mouse melanocytes *in vivo* resulted in melanoma formation and development of lymph node and lung metastases but not brain metastases (Dankort et al., 2009).

PTEN is a phosphatase with activity against both lipid and protein substrates (Chalhoub and Baker, 2009). Its major substrate is phosphatidylinositol-3,4,5-triphosphate (PIP_3), which binds to AKT via its pleckstrin homology (PH) domain and acts to recruit AKT to the membrane where it is activated through phosphorylation by phosphoinositide-dependent kinase 1 (PDK1) and the mammalian target of rapamycin complex 2 (mTORC2). PTEN specifically dephosphorylates the 3′ position of PIP_3 to create phosphatidylinositol-4,5-bisphosphate (PIP_2) and thereby suppresses membrane

recruitment and downstream signaling of AKT. Loss of PTEN results in increased levels of PIP3 and subsequent AKT activation. However, several studies suggest that PTEN loss does not phenocopy AKT activation (Ackler et al., 2002; Li et al., 2002; Majumder et al., 2003; Marsh Durban et al., 2013; Wang et al., 2003). Furthermore, the effects of activated AKT in the context of aberrant mitogen-activated protein kinase (MAPK) signaling have not been directly assessed in a mouse model of spontaneous melanoma metastasis.

In this study we describe the first *in vivo* melanoma model that develops both spontaneous lung and brain metastases similar to the human disease. Using an established mouse model of melanoma that allows postnatal gene delivery to somatic cells, we assessed the ability of PTEN silencing or AKT1 activation, either alone or in combination, to promote melanomagenesis and metastasis in the context of mutant $BRAF^{V600E}$ and silencing of INK4A and ARF. While both PTEN silencing or expression of activated AKT1 promoted melanoma formation in this context, only melanomas with activated AKT1 developed spontaneous brain metastases. Additionally, PTEN silencing cooperated with active AKT1 to accelerate both tumor formation and metastasis. Further analysis of the differences between these tumors revealed activation of mTORC signaling in tumors driven by activated AKT, further supporting a role for this pathway in melanoma metastasis (Damsky et al., 2015; Liu et al., 2012). This model provides a valuable tool to further define the mechanisms that promote melanoma metastases to the brain and a powerful platform to advance the development of anti-melanoma therapies. Our findings demonstrate distinct differences in the metastatic potential of melanomas with AKT1 activation versus PTEN silencing and may provide valuable insights for

assessing risk for the development of melanoma brain metastases and for guiding clinical treatment.

2.3 Results

2.3.1 $BRAF^{V600E}$/INK4A-ARF^{Null} melanomas are not metastatic. To evaluate melanoma metastasis in the context of specific genetic alterations, we utilized an established melanoma mouse model based on the RCAS/TVA system that allows for targeted delivery of specific genes to post-natal melanocytes (VanBrocklin et al., 2010). This system utilizes a viral vector, RCASBP(A), hereafter referred to as RCAS, and its receptor TVA. Transgenic mice that express TVA under the control of the dopachrome tautomerase (DCT) promoter allow targeting of the virus, and expression of the genes it contains, specifically to melanocytes. To assess metastasis using this model in the context of mutationally activated $BRAF^{V600E}$, we compound generated *Dct::TVA*;$BRaf^{CA}$;$Cdkn2a^{lox/lox}$ mice (VanBrocklin et al., 2010) carrying a conditional Cre-activated allele of *Braf*. The $Braf^{CA}$ allele expresses wild-type BRAF prior to Cre-mediated recombination after which $BRAF^{V600E}$ is expressed from the normal chromosomal locus (Dankort et al., 2007). The $Cdkn2a^{lox}$ allele expresses normal INK4A and ARF prior to Cre-mediated recombination after which expression of both $p16^{INK4A}$ and $p19^{ARF}$ is extinguished. (Aguirre et al., 2003).

Newborn *Dct::TVA;Braf* ^{CA};$Cdkn2a^{lox/lox}$ mice were injected subcutaneously with a RCAS virus encoding *Cre* to induce $BRAF^{V600E}$ expression with concomitant silencing of INK4A and ARF in melanocytes. While $Braf^{CA}$; $Cdkn2a^{lox/lox}$ mice lacking Dct::TVA injected with RCAS:*Cre* remained tumor free for the duration of the study (150 days, *n* =

40), 47% (16/34) of the *Dct::TVA;Braf* ^{CA}; *Cdkn2a*$^{lox/lox}$ mice infected with the RCAS:*Cre* virus developed tumors at the site of injection (Table 2.1). The mean survival for tumor-bearing mice in this cohort was 88.9 ± 8.6 days (Figure 2.1). All major organs were examined at euthanasia but no melanoma metastases were observed in any of the tumor-bearing mice.

2.3.2 PTEN silencing increases tumor incidence and reduces tumor latency but does not enhance metastasis. Because BRAF^{V600E} cooperates with PTEN silencing to induce metastatic melanoma (Dankort et al., 2009), we generated *Dct::TVA*;*Braf*^{CA};*Cdkn2a*$^{lox/lox}$;*Pten*$^{lox/lox}$ (*Pten*$^{lox/lox}$) mice. The *Pten*^{lox} allele used here expresses normal PTEN prior to Cre-mediated recombination after which deletion of the exon 5 sequence generates a *Pten* null allele (Zheng et al., 2008). Newborn *Dct::TVA;Braf*^{CA};*Cdkn2a*$^{lox/lox}$;*Pten*$^{lox/lox}$ mice were injected subcutaneously with RCAS:*Cre* to induce BRAF^{V600E} with concomitant silencing of INK4A, ARF and PTEN in melanocytes. Importantly, control mice, *Braf*^{CA};*Cdkn2a*$^{lox/lox}$;*Pten*$^{lox/lox}$ lacking *Dct::TVA* infected with RCAS:*Cre* remained tumor free for the duration of the study (150 days, *n = 40*). Tumors developed at the site of injection in all of the *Dct::TVA*-positive *Braf*^{CA};*Cdkn2a*$^{lox/lox}$;*Pten*$^{lox/lox}$ mice infected with RCAS:*Cre* viruses (24/24; Figure 2.1 and Table 2.1). The mean survival was 57.8 ± 3.4 days in this cohort (Figure 2.1). Expression of Cre was assessed by RT-PCR (Figure 2.2A) and recombination of *Pten*^{lox} was confirmed by PCR in all of the tumors that developed (Figure 2.2B). In these mice, lung metastases were detected in 8.3 % (2/24) of the mice whose melanomas had PTEN silencing. However, using a Fisher's exact test we determined that this difference was not significant when compared with mice whose tumors expressed PTEN (*P = 0.5)*.

2.3.3 Expression of activated AKT1 promotes melanoma formation and metastasis. Several studies have shown that PTEN silencing confers a different phenotype than AKT activation (Majumder et al., 2003; Wang et al., 2003). Therefore, we evaluated the effect of mutationally activated AKT1 on melanoma formation and progression *in vivo*. Newborn *Dct::TVA;Braf*^{CA};*Cdkn2a*$^{lox/lox}$ (*Pten*^{WT}) mice were injected subcutaneously with RCAS viruses encoding myristoylated (myr) *Akt1* alone or in combination with viruses encoding *Cre*. While *Dct::TVA;Braf*^{CA};*Cdkn2a*$^{lox/lox}$ mice injected with viruses encoding myr*Akt1* alone remained tumor free for the duration of the study (150 days, *n = 21*), 88% (24/27) of the mice injected with both myr*Akt1* and *Cre* encoding viruses developed tumors at the site of injection (Figure 2.1 and Table 2.1). The mean survival of the tumor-bearing mice in this cohort was 65.3 ± 4.7 days (Figure 2.1). It is important to note that AKT1 expression is not required for tumor formation in the context of BRAF^{V600E}/INK4A-ARF silencing; tumors develop in nearly half of *Dct::TVA;Braf* ^{CA};*Cdkn2a*$^{lox/lox}$ mice infected with viruses encoding *Cre* only (Figure 2.1). Of the 24 mice that developed tumors when injected with myr*Akt1* and *Cre* viruses, AKT1 expression was detected in 18 of the tumors by IHC for the HA epitope tag on myrAKT1 (Figure 2.3). The mean survival was 58.9 ± 3.5 in this myrAKT1-confirmed cohort (Figure 2.4 and Table 2.1). A significant difference in survival was observed between mice whose tumors expressed myrAKT1 and those without myrAKT1 (P = 2.3 x 10^{-9}). A significant difference in survival was also observed between the *Pten*$^{lox/lox}$ cohort injected with viruses encoding *Cre* only when compared with all of the mice in the *Pten*^{WT} cohort injected with two separate viruses encoding *Cre* and myr*Akt1* (P = 0.045) (Figure 2.1 and Table 2.1). However, comparison between the mice whose tumors were found to express myrAKT1 by IHC

(18/24) and mice whose tumors lacked PTEN revealed no significant difference in survival (P = 0.994; Figure 2.4). All major organs were examined in tumor-bearing mice. Interestingly, lung metastases were observed in 67% (12/18) and brain metastases were observed in 17% (3/18) of the mice whose tumors expressed myrAKT1. This difference was statistically significant when compared with both the $Pten^{WT}$ and the $Pten^{lox/lox}$ cohorts injected with RCAS:*Cre* viruses ($P < 0.0001$).

2.3.4 PTEN silencing cooperates with activated AKT1 to accelerate melanomagenesis and to promote metastasis. Our data revealed differences in the development of metastases between cohorts of mice whose tumors lacked PTEN compared with mice whose tumors expressed myrAKT1. Therefore, we assessed whether PTEN silencing could cooperate with myrAKT1 activation to promote melanoma formation and progression. To test this, newborn *Dct::TVA;* $Braf^{CA}$;$Cdkn2a^{lox/lox}$;$Pten^{lox/lox}$ mice were injected subcutaneously with viruses encoding myr*Akt1* and *Cre*. Tumors developed at the site of injection in all of the mice in this cohort (14/14) and myrAKT1 expression was detected in all of these tumors by anti-HA IHC (Figure 2.5). Expression of Cre was assessed by RT-PCR (Figure 2.6A) and recombination of *Pten* was confirmed by PCR in all of the tumors that developed (Figure 2.6B). Interestingly, melanomas with concomitant PTEN silencing and myrAKT1 expression had significantly reduced survival compared with mice whose tumors only had PTEN silencing (P = 0.0009) or expressed myrAKT1 in the presence of PTEN (P = 0.0002). The mean survival in this cohort was 42.1 ± 2.8 days (Figure 2.4 and Table 2.1). All major organs were examined and lung and brain metastases were observed in 71% (10/14) and 79% (11/14) of the mice, respectively. A comparison of the sites of metastases revealed no significant difference in lung metastases (P = 1.0) but there was a statistically significant difference

in brain metastases between tumors driven by myrAKT1 in the presence or absence of PTEN ($P = 0.0009$).

2.3.5 Histological characterization of the mouse melanomas reveals features similar to the human disease. Melanomas arising in *Dct::TVA;Braf*^{CA};*Cdkn2a*$^{lox/lox}$ mice infected with both RCAS:*Cre* and RCAS:myr*Akt1* encoding viruses consisted primarily of short spindle cells, occasional epithelioid cells, and with high grade nuclear features prominent nucleoli. Intratumoral hemorrhage, coagulative tumor necrosis, and non-brisk inflammation (tumor infiltrating lymphocytes) were variably noted (Figure 2.7A). Mitotic figures were abundant and the majority of the cells expressed the Ki67 proliferation marker (Figure 2.7B). The activity of BRAF^{V600E} was assessed by IHC for pERK as a surrogate (Figure 2.7C). The melanocytic origin of these tumors was established by their immunoreactivity for a pan-melanoma cocktail consisting of antibodies to HMB-45, a pre-melanosomal glycoprotein gp100, and melanoma antigen recognized by T-cells-1 (MART-1) (Figure 2.7D). The combination of positivity for both HMB-45 and MART-1 is highly supportive of a melanoma diagnosis (Ohsie et al., 2008). Upon gross examination, lesions were visible on the surface of the lungs (Figure 2.7E) and microscopic examination confirmed the morphologic features of malignancy (Figure 2.7F-G). AKT1 expression was detected in the metastases by IHC for the HA epitope tag on myrAKT1 (Figure 2.7H). Brain metastases were also observed in *Dct::TVA;Braf*^{CA}*;Cdkn2a*$^{lox/lox}$ mice infected with both *Cre* and myr*Akt1* containing viruses (Figure 2.7I). Expression of myrAKT1 was confirmed in the brain metastases by IHC for the HA tag on virally delivered myrAKT1 (Figure 2.7J).

Primary tumors from each of the cohorts described above were assessed for the presence of phosphorylated AKT (pS473) by IHC and compared with

$BRAF^{V600E}$/INK4A-ARF^{Null} melanomas (Figure 2.8A-B). As expected, active pS473-AKT was detected in tumors lacking PTEN, expressing myrAKT1, or both (Figure 2.8C-H). The levels of pS473-AKT were also assessed by immunoblot analysis of lysates generated from fragments of tumors lacking PTEN, expressing myrAKT1, or both (Figure 2.9). In agreement with the IHC data, $PTEN^{Null}$ melanomas displayed higher levels of pS473-AKT (Figure 2.10). Expression of myrAKT1 was confirmed by immunoblotting for the HA epitope tag on myrAKT1. Cre-mediated expression of mutationally activated BRAF was assessed using an antibody specific for $BRAF^{V600E}$. Activity of the MAPK pathway was assessed by analysis of phosphorylated ERK expression. Total levels of ERK were similar between the samples. As expected, the level of total AKT was higher in the melanomas engineered to express myrAKT1 and a wider band representing the larger molecular mass of myrAKT1 was detected on the total AKT blot (Figure 2.9).

2.3.6 Reverse-phase protein array analysis revealed increased mTOR signaling in tumors expressing myrAKT1. To define differences in signaling between the melanomas lacking PTEN and those expressing myrAKT1 in a high-throughput manner we used a reverse-phase protein array (RPPA) approach. RPPA allows quantitative analysis of protein levels and activation using small amounts of protein (Liotta et al., 2003). Tumor-enriched protein isolates from five $PTEN^{Null}$ and four myrAKT1-expressing melanomas were analyzed by RPPA. The heat-map in Figure 2.11 shows the results of unsupervised hierarchical clustering of the results of this analysis, which showed a significant difference in protein modification/expression levels ($n=11$; $P < 0.05$ by unpaired t-testing) between the five PTENNull tumor samples and the

four myrAKT1-expressing melanoma samples. A list of all 131 epitopes assessed with their respective P-values is presented in Table 2.2. As expected, lower levels of PTEN expression were detected in the melanoma samples from *Pten*$^{lox/lox}$ mice. In agreement with both the IHC and immunoblot analyses, a higher level of pS473-AKT was observed in the PTEN^{Null} tumor samples. Interestingly, components of the mammalian target of rapamycin (mTOR) signaling pathway (e.g., RAPTOR, RICTOR, NF2 and MYH11) were significantly different between the two groups (Figure 2.11 and Figure 2.12).

2.4 Discussion

In this study we describe the first *in vivo* melanoma model that develops both spontaneous lung and brain metastases similar to human melanoma. A major obstacle in studying melanoma brain metastasis has been the lack of an animal model that mimics the metastatic patterns observed in the human disease. Cruz-Munoz *et al.* described a model engineered by sub-dermal injection of severe combined immunodeficiency (SCID) mice with metastatic human melanoma cells (Cruz-Munoz et al., 2008). Other models have employed intra-carotid or intra-cardiac injection of melanoma cells into immunocompromised mice (Fujimaki et al., 1993; Morsi et al., 2013). Drews and coworkers injected chick embryos with melanoma cells in the rhombencephalic brain vesicles to investigate their invasive growth in that environment (Busch et al., 2012). While these models have provided valuable information regarding specific steps in melanoma metastasis, none represent spontaneous brain metastasis in an animal with an intact immune system. Through combined PTEN silencing and mutational activation of AKT1 in the context of the BRAF^{V600E} oncoprotein kinase and INK4A-ARF silencing,

we have established a model of spontaneous lung and brain metastases that displays high penetrance and short latency. Furthermore, we provide compelling evidence that AKT1 activation plays a critical role in promoting melanoma brain metastasis *in vivo* via a mechanism that is independent of, yet augmented by, PTEN silencing.

We observed dramatically increased metastasis in mice bearing tumors driven by activated AKT1 compared with *Pten* loss. Moreover, AKT1 activation cooperated with *Pten* loss to accelerate tumor formation and further increase metastasis. Taken together, these results strongly suggest that *Pten* loss renders a phenotypically distinct pattern of melanoma development and progression from AKT1 activation. Studies in other cancers support the findings that PTEN silencing/mutation is not synonymous with AKT activation. Mice with prostate-specific PTEN silencing develop invasive prostate cancer with a frequency of 40-90%, whereas mice with prostate-specific constitutive activation of AKT only develop localized pre-neoplastic lesions (Majumder et al., 2003; Wang et al., 2003). In addition, mammary gland-specific PTEN silencing elicits excessive branching, accelerated ductal extension and mammary tumors with metastatic potential. By contrast, ectopic expression of activated AKT1 in the same context resulted in no major differences in ductal growth or epithelial differentiation compared to controls (Ackler et al., 2002; Li et al., 2002). Furthermore, the pharmacological inhibition of AKT was reported to have little effect on the growth of *Pten*-deficient melanomas driven by $BRAF^{V600E}$ (Marsh Durban et al., 2013).

Aberrant AKT signaling is implicated in several steps of melanoma pathogenesis including metastasis (Robertson, 2005). Phosphorylation at Ser473 and Thr308 induces AKT activation and phosphorylated AKT levels increase as tumors progress from benign nevi to metastases (Chen et al., 2014; Dai et al., 2005; Davies et al., 2009; Stahl et al.,

2004). Activation of the PI3K→AKT pathway in melanoma occurs via several mechanisms including deletion or inactivation of the negative regulator PTEN, which is observed in up to 43% of melanomas, through genomic amplification or increased gene expression of *AKT* (Bastian et al., 1998; Stahl et al., 2004), and activating mutations in *PIK3CA* and *AKT* isoforms, which occurs in 1-5% and 1-2% of melanomas, respectively (Curtin et al., 2006; Davies et al., 2008; Mikhail et al., 2005; Omholt et al., 2006). This is consistent with what has been observed in larger studies (Cerami et al., 2012; Hodis et al., 2012). Moreover, novel mutations in AKT1 confer a survival advantage for melanoma and are often found in the setting of drug-resistant, metastatic disease (Shi et al., 2014).

Interestingly, PTEN deficient melanomas had significantly higher levels of phosphorylated AKT (Figure 2.8D, Figure 2.9, and Figure 2.11) compared with tumors expressing myrAKT1 (Figure 2.8F, H, Figure 2.9, Figure 2.11) yet significantly fewer metastases. In mammals there are three isoforms of AKT, namely AKT1, AKT2 and AKT3. While the AKT isoforms share ~80% amino acid sequence identity, *in vivo* studies demonstrate that they have both redundant and non-overlapping functions (Gonzalez and McGraw, 2009). There have been conflicting reports regarding which isoforms of AKT are phosphorylated following PTEN loss in melanoma cells (Nogueira et al., 2010; Stahl et al., 2004). It is possible that signaling from AKT1 differs from the signaling that results from the activation of AKT isoforms with PTEN silencing. Some studies suggest that AKT isoforms have opposing functions with regards to tumorigenesis (Linnerth-Petrik et al., 2014; Maroulakou et al., 2007). Maroulakou et al. found that Akt1 ablation inhibited, whereas Akt2 ablation accelerated, development of mammary adenocarcinomas in two different

mouse models of breast cancer (Maroulakou et al., 2007). Wootton and coworkers recently reported similar findings that deletion of *Akt1* delayed tumor initiation in a murine lung cancer model, while loss of *Akt2* and *Akt3* significantly accelerated tumorigenesis (Linnerth-Petrik et al., 2014). It is possible that specific isoforms of AKT differentially contribute to tumor growth and/or metastatic potential in melanoma and that activation of AKT2 or AKT3 following PTEN loss may oppose the activity of AKT1 resulting in the different phenotypes we observed.

In this study we observed significant differences in mTORC pathway components between our PTEN deficient versus myrAKT1 expresssing melanomas suggesting a disrupted elevation of this signaling pathway. Several lines of evidence provide strong support that enhanced mTORC signaling promotes melanoma metastasis. mTOR is a kinase that assembles with accessory proteins to form mTOR complex 1 (mTORC1) or mTOR complex 2 (mTORC2) (Laplante and Sabatini, 2012). Specific functions differ depending on which mTOR complex forms, however both complexes function toward integrating growth factor stimulation and nutrient availability with protein synthesis and cell growth. Interestingly, mTORC1 and mTORC2 are functionally connected to one another through the PI3K→AKT pathway. Activated AKT turns on mTORC1 by directly inhibiting two of its negative regulators, PRAS40 and TSC2 (Inoki et al., 2002; Manning et al., 2002; Vander Haar et al., 2007). AKT is also known to inhibit AMP-activated protein kinase (AMPK)-mediated positive regulation of TSC2 (Hahn-Windgassen et al.,2005). Through a feedback inhibitory mechanism that involves S6K1, a major downstream effector of mTORC1, activated mTORC1 turns off AKT signaling by inhibiting IRS1, an activator of PI3K (Harrington et al., 2005; Manning, 2004). Conversely, mTORC2 acts as a positive regulator of AKT by phosphorylating the

activating AKT residue, Ser473 (Sarbassov et al., 2005).

Hyperactive mTORC signaling is disproportionately observed in melanomas (73%; 78/107) compared to benign nevi (4%; 3/67) (Karbowniczek et al., 2008). Deletion of *Lkb1*, a known negative regulator of mTORC signaling, in *KRas*-mutant mouse melanocytes results in the formation of highly metastatic melanomas *in vivo* (Liu et al., 2012). More recently, loss of *Lkb1* in the context of non-metastatic $BRAF^{V600E}$/INK4A-Arf^{Null} melanomas resulted in highly metastatic disease (Damsky et al., 2015). The pharmacological targeting of mTOR effectively blocks melanoma cell growth *in vitro* and in animal models (Dankort et al., 2009; Guba et al., 2002; Hidalgo and Rowinsky, 2000). Unfortunately, but not surprisingly, mTOR inhibitors have failed to demonstrate clinical efficacy against melanoma as mono-therapy and are currently being evaluated in combination with other therapies for this disease (Clinicaltrials.gov, 2015; Margolin et al., 2005). In line with increased mTORC signaling in melanoma metastasis we found that total protein and phospho-protein levels of Rictor, an exclusive mTORC2 component, were significantly higher in myrAKT1 expressing melanomas compared to PTEN deficient melanomas (Figure 2.11 and Figure 2.12). Taken together, our findings and those of others implicate increased mTORC signaling in promoting melanoma metastasis.

We report the first *in vivo*, autochthonous model of melanoma with spontaneous metastasis to the lungs and brain. Our data highlights the importance of AKT1 activationin promoting melanoma metastasis to the brain as well as differences between AKT1 activation and PTEN silencing. These data also revealed that PTEN silencing cooperates with activated AKT1 to promote melanoma brain metastases with shorter tumor latency. This model is likely to prove useful for further analysis of the biology of

melanoma metastasis as well as evaluation of specific therapies aimed at preventing or treating disseminated disease.

2.5 Materials and Methods

2.5.1 Vector constructs. The retroviral vectors in this study are replication-competent avian leukosis virus, Bryan polymerase-containing vectors of envelope subgroup A [designated RCASBP(A) and abbreviated RCAS]. RCAS-*Cre* and RCAS-myr*Akt1* have been described previously (Aoki et al., 1998; VanBrocklin et al., 2010).

2.5.2 Cell culture. DF-1 cells were grown in DMEM-high glucose media supplemented with 10% FBS (Invitrogen, Waltham, MA USA), 2.5mL Gentamicin (Invitrogen), and maintained at 39°C.

2.5.3 Virus propagation. Virus infection was initiated by calcium phosphate transfection of plasmid DNA into DF-1 cells. Viral spread was monitored by GFP positive control transfection and expression of the p27 viral capsid protein by Western blot.

2.5.4 Western blotting. Tumor samples were flash frozen in liquid nitrogen and pulverized using a mortar and pestle. The pulverized tumor samples were resuspended in RPPA buffer (Tibes et al., 2006) with protease and phosphatase inhibitors (Pierce Biotechnology, Rockford, IL, USA). Tumor samples in RPPA buffer were diluted in SDS-sample buffer and boiled for 10 minutes. The proteins were separated on a 4-20% Tris-glycine polyacrylamide gel, transferred to nitrocellulose, and incubated for 1 hour at room temperature in blocking solution (0.1% Tween-20 in 1× TBS with 5% nonfat dry milk, or 0.1% Tween-20 in 1× TBS with 5% BSA). Blots were immunostained with primary antibody at required dilution. All antibodies were diluted in TBS-T solution.

Western blots were incubated in the primary antibody for 1 hour at room temperature with constant shaking and then washed in TBS-T wash buffer (0.1% Tween-20 in 1× TBS). The blots were then incubated with an anti-mouse IgG-horseradish peroxidase secondary antibody diluted 1:1000 (Sigma-Aldrich Corp., St. Louis, MO, USA) for 1 hour at room temperature. The blots were washed in TBS-T wash buffer, incubated with enhanced chemiluminescence solutions according to the manufacturer's specifications (Amersham, Piscataway, NJ USA), and exposed to film. See Supplemental Information for a list of primary antibodies used.

2.5.5 Viral infections in vivo. Infected DF-1 cells from a confluent culture in a 10 cm dish were trypsinized, pelleted, resuspended in 50 μL PBS, and placed on ice. Newborn mice were injected subcutaneously behind the ear. Mice were monitored daily for tumor development. Mice received 50 μL of suspended myr*Akt1* cells and 50 μL of suspended *Cre* cells.

2.5.6 Histology and histochemical staining. Mice were euthanized at their experimental endpoints set according to the guidelines of the University of Utah Institutional Animal Care and Use Committee. Mouse tissues were fixed in formalin overnight, cut into three sections, and then dehydrated in 70% ethyl alcohol. Tissues were paraffin-embedded and 5μm sections were adhered to glass slides. Sections were stained with H&E or left unstained for immunohistochemistry.

2.5.7 Immunohistochemistry. Tissue sections were hydrated and deparaffinized and antigen retrieval was performed in 1× Rodent Decloaker buffer (Biocare Medical, Concord, CA USA) by boiling for 20 minutes in a Decloaking Chamber (Biocare Medical). Sections were treated with 3% hydrogen peroxide and blocked in Rodent Block (Biocare Medical) for 30 minutes. Primary antibodies were diluted in Renaissance

background reducing diluent (Biocare Medical). Sections were incubated overnight at 4°C and probed with Mouse on Mouse HRP polymer reagent (Biocare Medical). Visualization was carried out with DAB (Biocare Medical). Sections were counterstained with hematoxylin. See Supplemental Information for primary antibodies used.

2.5.8 Reverse-phase protein array (RPPA). Frozen tumor tissue was embedded in optimum cutting temperature (OCT) compound. H&E stained slides were reviewed by an experienced dermatopathologist (Alexander J. Lazar) to identify areas that contained >70% tumor cells. Regions with extensive necrosis, fibrosis, or hemorrhage within the tumor specimens were excluded. The H&E slides were used as a guide to macrodissect the OCT blocks and isolate tumor-enriched regions for further analysis. Ten to 20 μm tumor shears were generated by cryostat and were used for protein and total RNA extraction. Proteins were isolated from the tumor shears and RPPA was performed as previously described (Davies et al., 2009; Tibes et al., 2006).

2.5.9 Mice and genotyping. *Dct::TVA;Cdkn2a*$^{lox/lox}$ mice were crossed with *Braf*^{CA} mice to generate *Dct::TVA;Cdkn2a*$^{lox/lox}$*;Braf*^{CA} mice (designated as *Pten*^{WT}). Further breeding of *Pten*^{WT} mice with *Pten*$^{lox/lox}$ mice (a gift from Ronald DePinho) yielded *Dct::TVA;Cdkn2a*$^{lox/lox}$*;Braf*^{CA}; *Pten*$^{lox/lox}$ mice (referred to as *Pten*$^{lox/lox}$). DNA was prepared from tail biopsies and genotyped by PCR for the *Dct::TVA* transgene, *Cdkn2a*^{lox}*, Braf*^{CA}, *Pten*^{lox} and wild-type alleles as described (Dankort et al., 2007; VanBrocklin et al., 2010; Zheng et al., 2008).

2.5.10 Statistical analysis. Censored survival data was analyzed using a log-rank test of the Kaplan-Meier estimate of survival. Densitometry of the Western blot was performed using ImageJ (Schneider et al., 2012) and the data is represented as mean ±

S.E.M. Student's t test was used to compare protein expression levels between groups in the RPPA analysis. Protein-protein coefficients were determined by the Pearson correlation method and the significance of the interactions was determined by the t statistic using R software. Unsupervised hierarchical clustering of mean-centered protein expression values was done using Cluster 2.1 and Treeview software.

2.5.11 Study approval. All animal experimentation was performed in AAALAC approved facilities at the University of Utah. All animal protocols were reviewed and approved prior to experimentation by the Institutional Animal Care and Use Committee at the University of Utah.

2.6 Acknowledgments

J.H.C. and J.P.R. contributed to the experimental design and performed the majority of the experiments. G.C. and M.A.D. were responsible for the reverse-phase protein array experiments. R.A.A. performed immunohistochemistry. A.G. provided pathological analysis. J.H.C., J.P.R., R.D.G., D.A.K., M.W.V., M.M. and S.L.H. were responsible for mouse model establishment, tumor induction, and characterization. J.H.C., M.M., and S.L.H. prepared the manuscript.

2.7 References

Ackler, S., Ahmad, S., Tobias, C., Johnson, M.D., and Glazer, R.I. (2002). Delayed mammary gland involution in MMTV-AKT1 transgenic mice. Oncogene *21*, 198-206.

Aguirre, A.J., Bardeesy, N., Sinha, M., Lopez, L., Tuveson, D.A., Horner, J., Redston, M.S., and DePinho, R.A. (2003). Activated Kras and Ink4a/Arf deficiency cooperate to produce metastatic pancreatic ductal adenocarcinoma. Genes and Development *17*, 3112-3126.

Aoki, M., Batista, O., Bellacosa, A., Tsichlis, P., and Vogt, P.K. (1998). The akt kinase: Molecular determinants of oncogenicity. Proceedings of the National Academy of Sciences U S A *95*, 14950-14955.

Bastian, B.C., LeBoit, P.E., Hamm, H., Brocker, E.B., and Pinkel, D. (1998). Chromosomal gains and losses in primary cutaneous melanomas detected by comparative genomic hybridization. Cancer Research *58*, 2170-2175.

Busch, C., Krochmann, J., and Drews, U. (2012). Human melanoma cells in the rhombencephalon of the chick embryo: A novel model for brain metastasis. Experimental Dermatology *21*, 944-947.

Cerami, E., Gao, J., Dogrusoz, U., Gross, B.E., Sumer, S.O., Aksoy, B.A., Jacobsen, A., Byrne, C.J., Heuer, M.L., Larsson, E.*, et al.* (2012). The cBio cancer genomics portal: An open platform for exploring multidimensional cancer genomics data. Cancer Discovery *2*, 401-404.

Chaichana, K.K., and Chaichana, K.L. (2011). Diagnosis and treatment options for brain metastasis of melanoma. In treatment of metastatic melanoma, R. Morton, edition (Croatia: InTech), pp. 47-70.

Chalhoub, N., and Baker, S.J. (2009). PTEN and the PI3-kinase pathway in cancer. Annual Review of Pathology *4*, 127-150.

Chen, G., Chakravarti, N., Aardalen, K., Lazar, A.J., Tetzlaff, M., Wubberhorst, B., Kim, S.B., Kopetz, S., Ledoux, A., Vashisht Gopal, Y.N.*, et al.* (2014). Molecular profiling of patient-matched brain and extracranial melanoma metastases implicates the PI3K pathway as a therapeutic target. Clinical Cancer Research *20*, 5537-5546

Clinicaltrials.gov (2015).

Cruz-Munoz, W., Man, S., Xu, P., and Kerbel, R.S. (2008). Development of a preclinical model of spontaneous human melanoma central nervous system metastasis. Cancer Research *68*, 4500-4505.

Curtin, J.A., Busam, K., Pinkel, D., and Bastian, B.C. (2006). Somatic activation of KIT in distinct subtypes of melanoma. Journal of Clinical Oncology *24*, 4340-4346.

Dai, D.L., Martinka, M., and Li, G. (2005). Prognostic significance of activated Akt expression in melanoma: A clinicopathologic study of 292 cases. Journal of Clinical Oncology *23*, 1473-1482.

Damsky, W., Micevic, G., Meeth, K., Muthusamy, V., Curley, D.P., Santhanakrishnan, M., Erdelyi, I., Platt, J.T., Huang, L., Theodosakis, N., et al. (2015). mTORC1 activation blocks Braf(V600E)-induced growth arrest but is insufficient for melanoma formation. Cancer Cell *27*, 41-56.

Dankort, D., Curley, D.P., Cartlidge, R.A., Nelson, B., Karnezis, A.N., Damsky Jr, W.E., You, M.J., Depinho, R.A., McMahon, M., and Bosenberg, M. (2009). Braf(V600E) cooperates with Pten loss to induce metastatic melanoma. Nature Genetics *41*, 544-552.

Dankort, D., Filenova, E., Collado, M., Serrano, M., Jones, K., and McMahon, M. (2007). A new mouse model to explore the initiation, progression, and therapy of BRAFV600E-induced lung tumors. Genes & Development *21*, 379-384.

Davies, M.A., Liu, P., McIntyre, S., Kim, K.B., Papadopoulos, N., Hwu, W.J., Hwu, P., and Bedikian, A. (2011). Prognostic factors for survival in melanoma patients with brain metastases. Cancer *117*, 1687-1696.

Davies, M.A., Stemke-Hale, K., Lin, E., Tellez, C., Deng, W., Gopal, Y.N., Woodman, S.E., Calderone, T.C., Ju, Z., Lazar, A.J*., et al.* (2009). Integrated molecular and clinical analysis of AKT activation in metastatic melanoma. Clinical Cancer Research *15*, 7538-7546.

Davies, M.A., Stemke-Hale, K., Tellez, C., Calderone, T.L., Deng, W., Prieto, V.G., Lazar, A.J., Gershenwald, J.E., and Mills, G.B. (2008). A novel AKT3 mutation in melanoma tumours and cell lines. British Journal of Cancer *99*, 1265-1268.

Fujimaki, T., Fan, D., Staroselsky, A., Gohji, K., Bucana, C., and Fidler, I. (1993). Critical factors regulating site-specific brain metastasis of murine melanomas. International Journal of Oncology *3*, 789-799.

Girotti, M.R., Saturno, G., Lorigan, P., and Marais, R. (2014). No longer an untreatable disease: How targeted and immunotherapies have changed the management of melanoma patients. Molecular Oncology *8*, 1140-1158.

Gonzalez, E., and McGraw, T.E. (2009). The Akt kinases: Isoform specificity in metabolism and cancer. Cell Cycle *8*, 2502-2508.

Guba, M., von Breitenbuch, P., Steinbauer, M., Koehl, G., Flegel, S., Hornung, M., Bruns, C.J., Zuelke, C., Farkas, S., Anthuber, M., et al. (2002). Rapamycin inhibits primary and metastatic tumor growth by antiangiogenesis: Involvement of vascular endothelial growth factor. Nature Medicine *8*, 128-135.

Hahn-Windgassen, A., Nogueira, V., Chen, C.C., Skeen, J.E., Sonenberg, N., and Hay, N. (2005). Akt activates the mammalian target of rapamycin by regulating cellular ATP level and AMPK activity. The Journal of Biological Chemistry *280*, 32081-32089.

Harrington, L.S., Findlay, G.M., and Lamb, R.F. (2005). Restraining PI3K: mTOR signalling goes back to the membrane. Trends in Biochemical Science *30*, 35-42.

Hidalgo, M., and Rowinsky, E.K. (2000). The rapamycin-sensitive signal transduction pathway as a target for cancer therapy. Oncogene *19*, 6680-6686.

Hodis, E., Watson, I.R., Kryukov, G.V., Arold, S.T., Imielinski, M., Theurillat, J.P., Nickerson, E., Auclair, D., Li, L., Place, C.*, et al.* (2012). A landscape of driver mutations in melanoma. Cell *150*, 251-263.

Inoki, K., Li, Y., Zhu, T., Wu, J., and Guan, K.L. (2002). TSC2 is phosphorylated and inhibited by Akt and suppresses mTOR signalling. Nature Cell Biology *4*, 648-657.

Karbowniczek, M., Spittle, C.S., Morrison, T., Wu, H., and Henske, E.P. (2008). mTOR is activated in the majority of malignant melanomas. Journal of Investigative Dermatology *128*, 980-987.

Laplante, M., and Sabatini, D.M. (2012). mTOR signaling in growth control and disease. Cell *149*, 274-293.

Li, G., Robinson, G.W., Lesche, R., Martinez-Diaz, H., Jiang, Z., Rozengurt, N., Wagner, K.U., Wu, D.C., Lane, T.F., Liu, X.*, et al.* (2002). Conditional loss of PTEN leads to precocious development and neoplasia in the mammary gland. Development *129*, 4159-4170.

Linnerth-Petrik, N.M., Santry, L.A., Petrik, J.J., and Wootton, S.K. (2014). Opposing functions of Akt isoforms in lung tumor initiation and progression. PloS One *9*, e94595.

Liotta, L.A., Espina, V., Mehta, A.I., Calvert, V., Rosenblatt, K., Geho, D., Munson, P.J., Young, L., Wulfkuhle, J., and Petricoin, E.F., 3rd (2003). Protein microarrays: Meeting analytical challenges for clinical applications. Cancer Cell *3*, 317-325.

Liu, W., Monahan, K.B., Pfefferle, A.D., Shimamura, T., Sorrentino, J., Chan, K.T., Roadcap, D.W., Ollila, D.W., Thomas, N.E., Castrillon, D.H.*, et al.* (2012). LKB1/STK11 inactivation leads to expansion of a prometastatic tumor subpopulation in melanoma. Cancer Cell *21*, 751-764.

Majumder, P.K., Yeh, J.J., George, D.J., Febbo, P.G., Kum, J., Xue, Q., Bikoff, R., Ma, H., Kantoff, P.W., Golub, T.R., et al. (2003). Prostate intraepithelial neoplasia induced by prostate restricted Akt activation: The MPAKT model. Proceedings of the National Academy of Sciences U S A *100*, 7841-7846.

Manning, B.D. (2004). Balancing Akt with S6K: Implications for both metabolic diseases and tumorigenesis. The Journal of Cell Biology *167*, 399-403.

Manning, B.D., Tee, A.R., Logsdon, M.N., Blenis, J., and Cantley, L.C. (2002). Identification of the tuberous sclerosis complex-2 tumor suppressor gene product tuberin as a target of the phosphoinositide 3-kinase/akt pathway. Molecular Cell *10*, 151-162.

Margolin, K., Longmate, J., Baratta, T., Synold, T., Christensen, S., Weber, J., Gajewski, T., Quirt, I., and Doroshow, J.H. (2005). CCI-779 in metastatic melanoma: A phase II trial of the California Cancer Consortium. Cancer *104*, 1045-1048.

Maroulakou, I.G., Oemler, W., Naber, S.P., and Tsichlis, P.N. (2007). Akt1 ablation inhibits, whereas Akt2 ablation accelerates, the development of mammary adenocarcinomas in mouse mammary tumor virus (MMTV)-ErbB2/neu and MMTV-polyoma middle T transgenic mice. Cancer Research *67*, 167-177.

Marsh Durban, V., Deuker, M.M., Bosenberg, M.W., Phillips, W., and McMahon, M. (2013). Differential AKT dependency displayed by mouse models of BRAFV600E-initiated melanoma. Journal of Clinical Investigation *123*, 5104-5118.

Mikhail, M., Velazquez, E., Shapiro, R., Berman, R., Pavlick, A., Sorhaindo, L., Spira, J., Mir, C., Panageas, K.S., Polsky, D*., et al.* (2005). PTEN expression in melanoma: Relationship with patient survival, Bcl-2 expression, and proliferation. Clinical Cancer Research *11*, 5153-5157.

Morsi, A., Gaziel-Sovran, A., Cruz-Munoz, W., Kerbel, R.S., Golfinos, J.G., Hernando, E., and Wadghiri, Y.Z. (2013). Development and characterization of a clinically relevant mouse model of melanoma brain metastasis. Pigment Cell & Melanoma Research *26*, 743-745.

Niessner, H., Forschner, A., Klumpp, B., Honegger, J.B., Witte, M., Bornemann, A., Dummer, R., Adam, A., Bauer, J., Tabatabai, G*., et al.* (2013). Targeting hyperactivation of the AKT survival pathway to overcome therapy resistance of melanoma brain metastases. Cancer Medicine *2*, 76-85.

Nogueira, C., Kim, K.H., Sung, H., Paraiso, K.H., Dannenberg, J.H., Bosenberg, M., Chin, L., and Kim, M. (2010). Cooperative interactions of PTEN deficiency and RAS activation in melanoma metastasis. Oncogene *29*, 6222-6232.

Ohsie, S.J., Sarantopoulos, G.P., Cochran, A.J., and Binder, S.W. (2008). Immunohistochemical characteristics of melanoma. Journal of Cutaneous Pathology *35*, 433-444.

Omholt, K., Krockel, D., Ringborg, U., and Hansson, J. (2006). Mutations of PIK3CA are rare in cutaneous melanoma. Melanoma Research *16*, 197-200.

Robertson, G.P. (2005). Functional and therapeutic significance of Akt deregulation in malignant melanoma. Cancer and Metastasis Reviews *24*, 273-285.

Sarbassov, D.D., Guertin, D.A., Ali, S.M., and Sabatini, D.M. (2005). Phosphorylation and regulation of Akt/PKB by the rictor-mTOR complex. Science *307*, 1098-1101.

Schneider, C.A., Rasband, W.S., and Eliceiri, K.W. (2012). NIH Image to ImageJ: 25 years of image analysis. Nature Methods *9*, 671-675.

Shi, H., Hong, A., Kong, X., Koya, R.C., Song, C., Moriceau, G., Hugo, W., Yu, C.C., Ng, C., Chodon, T., et al. (2014). A novel AKT1 mutant amplifies an adaptive melanoma response to BRAF inhibition. Cancer Discovery *4*, 69-79.

Stahl, J.M., Sharma, A., Cheung, M., Zimmerman, M., Cheng, J.Q., Bosenberg, M.W., Kester, M., Sandirasegarane, L., and Robertson, G.P. (2004). Deregulated Akt3 activity promotes development of malignant melanoma. Cancer Research *64*, 7002-7010.

Tibes, R., Qiu, Y., Lu, Y., Hennessy, B., Andreeff, M., Mills, G.B., and Kornblau, S.M. (2006). Reverse phase protein array: Validation of a novel proteomic technology and utility for analysis of primary leukemia specimens and hematopoietic stem cells. Molecular Cancer Therapeutics *5*, 2512-2521.

VanBrocklin, M.W., Robinson, J.P., Lastwika, K.J., Khoury, J.D., and Holmen, S.L. (2010). Targeted delivery of NRASQ61R and Cre-recombinase to post-natal melanocytes induces melanoma in Ink4a/Arflox/lox mice. Pigment Cell & Melanoma Research *23*, 531-541.

Vander Haar, E., Lee, S.I., Bandhakavi, S., Griffin, T.J., and Kim, D.H. (2007). Insulin signalling to mTOR mediated by the Akt/PKB substrate PRAS40. Nature Cell Biology *9*, 316-323.

Wang, S., Gao, J., Lei, Q., Rozengurt, N., Pritchard, C., Jiao, J., Thomas, G.V., Li, G., Roy-Burman, P., Nelson, P.S*., et al.* (2003). Prostate-specific deletion of the murine Pten tumor suppressor gene leads to metastatic prostate cancer. Cancer Cell *4*, 209-221.

Zheng, H., Ying, H., Yan, H., Kimmelman, A.C., Hiller, D.J., Chen, A.J., Perry, S.R., Tonon, G., Chu, G.C., Ding, Z*., et al.* (2008). p53 and Pten control neural and glioma stem/progenitor cell renewal and differentiation. Nature *455*, 1129-1133.

Table 2.1 Summary of tumor formation. The mean survival (days) and tumor incidence (fraction of tumor-bearing mice per cohort) are listed for each mouse cohort according to genetic background and virally delivered genes.

Strain	Gene(s) delivered	Tumor Incidence	Mean survival (days)
Braf^{CA};Cdkn2a$^{lox/lox}$	*Cre*	0/40	N/A
Dct::TVA;Braf^{CA};Cdkn2a$^{lox/lox}$	*Cre*	16/34	88.9 ± 8.6
Braf^{CA};Cdkn2a$^{lox/lox}$;Pten$^{lox/lox}$	*Cre*	0/40	N/A
Dct::TVA;Braf^{CA};Cdkn2a$^{lox/lox}$;Pten$^{lox/lox}$	*Cre*	24/24	57.8 ± 3.4
Dct::TVA;Braf^{CA};Cdkn2a$^{lox/lox}$	myr*Akt1*	0/21	N/A
Dct::TVA;Braf^{CA};Cdkn2a$^{lox/lox}$	*Cre* + myr*Akt1*	24/27	65.3 ± 4.7
	myrAKT1 positive*	18/18	58.9 ± 3.5
Dct::TVA;Braf^{CA};Cdkn2a$^{lox/lox}$;Pten$^{lox/lox}$	*Cre* + myr*Akt1*	14/14	42.1 ± 2.8

*HA positive by IHC.

Table 2.2 Epitopes assessed by RPPA. The 131 epitopes assess by RPPA are listed with associated p-values for expression between for $PTEN^{Null}$ and myrAKT1-expressing melanomas.

Epitope name	P value (Pten-/- vs myrAKT1)
14-3-3_beta-R-V	0.986899929
14-3-3_zeta-R-V	0.107018017
4E-BP1-R-V	0.936245747
4E-BP1_pS65-R-V	0.070700747
4E-BP1_pT37_T46-R-V	0.99229202
53BP1-R-E	0.574164284
ACC_pS79-R-V	0.230415179
ACC1-R-E	0.194849917
ACVRL1-R-C	0.613499722
Akt-R-V	0.116263529
Akt_pS473-R-V	0.042699831
Akt_pT308-R-V	0.832904104
AMPK_alpha-R-C	0.804747501
AMPK_pT172-R-V	0.648308037
Annexin_I-R-E	0.816678879
AR-R-V	0.774308054
Bad_pS112-R-V	0.248710276
Bak-R-E	0.233740918
Bax-R-V	0.606409335
Bcl-xL-R-V	0.133610074
Beclin-G-C	0.782365968
beta-Catenin-R-V	0.337687651
Bid-R-C	0.380470389
Bim-R-V	0.666638882
c-Kit-R-V	0.09584474
c-Met_pY1235-R-V	0.179031136
c-Myc-R-C	0.174496331
C-Raf-R-V	0.093590223
C-Raf_pS338-R-E	0.140086355
Caspase-7_cleavedD198-R-C	0.914898043
Caveolin-1-R-V	0.132411194
CDK1-R-V	0.411494628
Chk1-R-E	0.613940163
Chk1_pS345-R-E	0.970126703
Chk2_pT68-R-E	0.539749452
cIAP-R-V	0.291991243
Claudin-7-R-V	0.180306755
Collagen_VI-R-V	0.271316434
Cyclin_B1-R-V	0.007704679
Cyclin_D1-R-V	0.555298373
DJ-1-R-E	0.483884585
Dvl3-R-V	0.456762712
E-Cadherin-R-V	0.11154638
eEF2-R-C	0.287981852
eEF2K-R-V	0.214172199
EGFR-R-V	0.221429256
EGFR_pY1068-R-C	0.332275723
EGFR_pY1173-R-V	0.702097331
eIF4E-R-V	0.111970978
eIF4G-R-C	0.8369896
ER-alpha-R-V	0.937165972
ER-alpha_pS118-R-V	0.077818823
FASN-R-V	0.527369196
Fibronectin-R-V	0.071035802
FOX03a-R-C	0.601223343
FoxM1-R-V	0.708119528
Gab2-R-V	0.683533567
GSK3-alpha-beta_pS21_S9-R-V	0.473012898
GSK3_pS9-R-V	0.465773117
HER2_pY1248-R-C	0.779326792
HER3-R-V	0.823319459
HER3_pY1298-R-C	0.239195226
IGFBP2-R-V	0.704959898
INPP4B-G-E	0.277609698
IRS1-R-V	0.076829417
JNK_pT183_pT185-R-V	0.40961812
JNK2-R-C	0.143253633
Lck-R-V	0.510284394
MAPK_pT202_Y204-R-V	0.040347328
MEK1-R-V	0.532053466
MEK1_pS217_S221-R-V	0.58581745
mTOR-R-V	0.17024293
mTOR_pS2448-R-C	0.051128166
MYH11-R-V	0.008008481
N-Cadherin-R-V	0.484162258
NDRG1_pT346-R-V	0.737156673
NF-kB-p65_pS536-R-C	0.681260761
NF2-R-C	0.005680786
Notch1-R-V	0.907635137
p27-R-V	0.943744838
p27_pT157-R-C	0.84505331
p27_pT198-R-V	0.12289665
p38_MAPK-R-E	0.327692275
p38_pT180_Y182-R-V	0.24863432
p53-R-E	0.424599929
p70S6K-R-V	0.600343069
p70S6K_pT389-R-V	0.935826407
p90RSK-R-C	0.4365333
p90RSK_pT359_S363-R-C	0.52225674
Paxillin-R-C	0.180331121
PDCD4-R-C	0.06552092
PDK1-R-V	0.192509816
PDK1_pS241-R-V	0.663867737
PEA15-R-V	0.350624594
PEA15_pS116-R-V	0.14612053
PI3K-p110-alpha-R-E	0.00164515
PI3K-p85-R-V	0.184651165
PKC-alpha_pS657-R-E	0.268995686
PKC-delta_pS664-R-V	0.890360155
PKC-pan_BetaII_pS660-R-V	0.236700005
PR-R-V	0.907888749
PRAS40_pT246-R-V	0.94253289
PTEN-R-V	0.012928935
Rab11-R-E	0.481445113
Rab25-R-E	0.427027919
Raptor-R-V	0.010958233
Rb_pS807_S811-R-V	0.431076702
RBM15-R-V	0.435704677
Rictor-R-C	0.01282843
Rictor_pT1135-R-V	0.013255368
S6_pS235_S236-R-V	0.787819865
S6_pS240_S244-R-V	0.192541095
Smad1-R-V	0.879881187
Smad3-R-V	0.257115147
Src_pY416-R-C	0.758488526
Src_pY527-R-V	0.160185242
STAT3_pY705-R-V	0.689276344
STAT5-alpha-R-V	0.364329377
Stathmin-R-V	0.34541852
TAZ-R-V	0.227110567
TIGAR-R-V	0.849650952
TRFC-R-V	0.868867142
TSC1-R-C	0.836626998
TTF1-R-V	0.090061686
Tuberin-R-E	0.405520087
VEGFR2-R-V	0.93708572
XRCC1-R-E	0.680321327
YAP-R-E	0.427038632
YAP_pS127-R-E	0.868654221
YB-1-R-V	0.044310894
YB-1_pS102-R-V	0.463380059

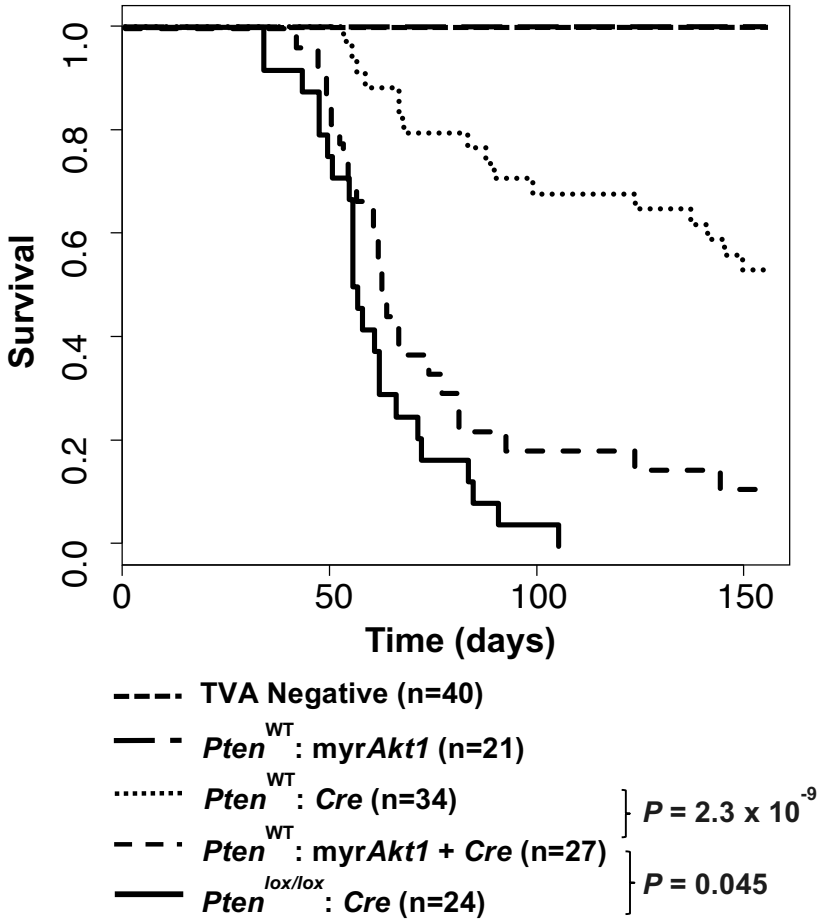

Figure 2.1 Kaplan-Meier percent survival curves for BRAF-induced tumors demonstrate that loss of *Pten* or expression of myrAKT1 significantly increases tumor incidence and reduces tumor latency. *Dct::TVA;Braf* ^{CA};*Cdkn2a*$^{lox/lox}$ mice (*Pten*^{WT}) were injected at birth with either *Cre* (small dashed line n = 34) or myr*Akt1* and *Cre* (wide dashed line n = 27) containing viruses as indicated. *Dct::TVA;Braf* ^{CA};*Cdkn2a*$^{lox/lox}$;*Pten*$^{lox/lox}$ mice (*Pten*$^{lox/lox}$) were injected with viruses encoding *Cre* (solid black line n = 24). TVA negative *Braf* ^{CA};*Cdkn2a*$^{lox/lox}$ and *Braf*^{CA};*Cdkn2a*$^{lox/lox}$;*Pten*$^{lox/lox}$ mice injected with *Cre* containing viruses (narrow dashed line n =40) and *Pten*^{WT} mice injected with myr*Akt1* containing viruses (off-width dashed line n=21) yielded no tumors and are shown as negative controls. A significant difference was observed between the survival of *Pten*^{WT} mice injected with *Cre* containing viruses and *Pten*^{WT} mice injected with myr*Akt1* and *Cre* containing viruses (P = 2.3 x 10^{-9}). A significant difference was also observed between the survival of *Pten*^{WT} mice injected with *Cre* and myr*Akt1* containing viruses and *Pten*$^{lox/lox}$ mice injected with *Cre* containing viruses (P = 0.045).

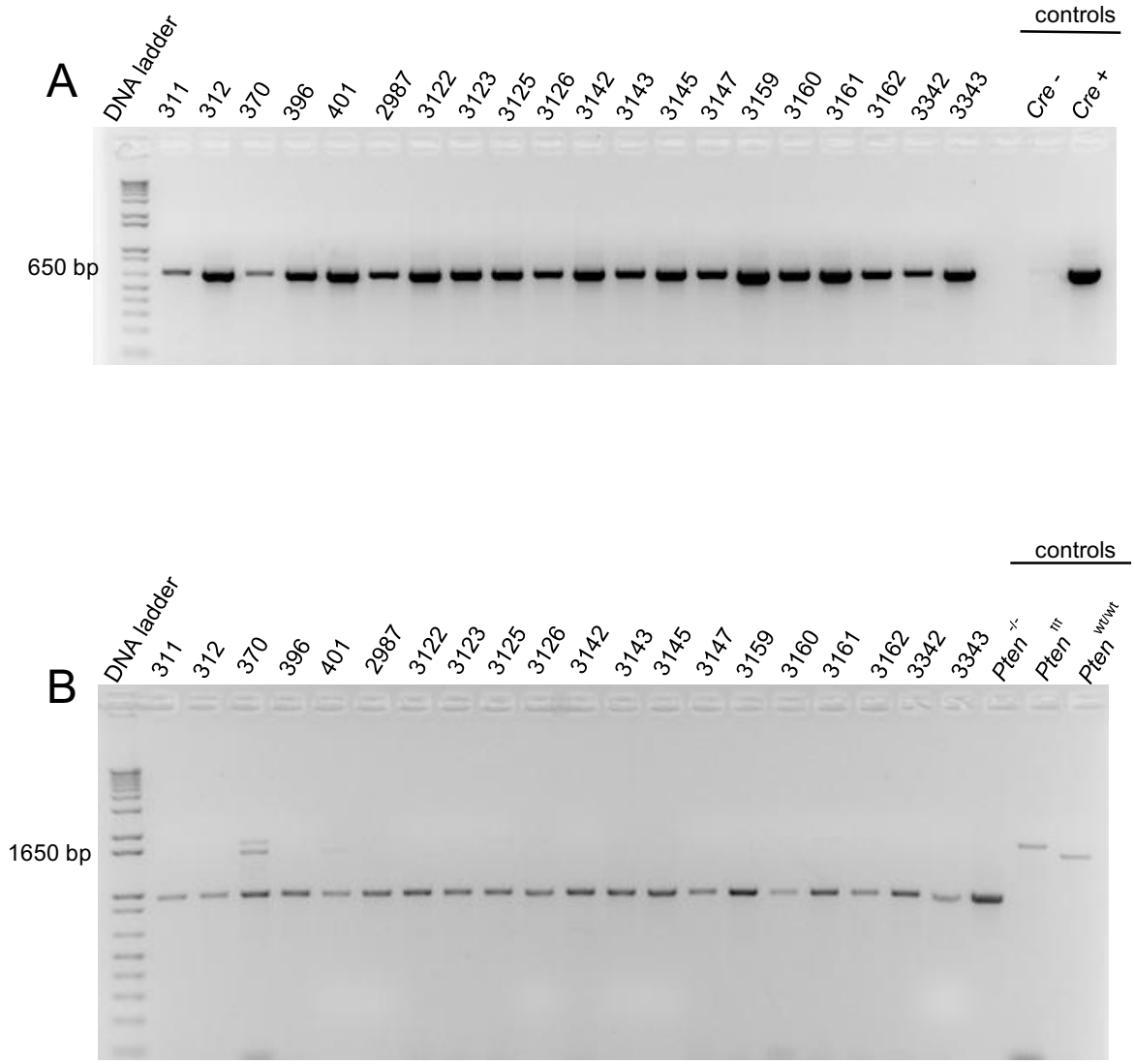

Figure 2.2 *Pten* loss in melanomas from *Dct::TVA;Braf*$^{CA/CA}$*;Cdkn2a*$^{lox/lox}$*;Pten*$^{lox/lox}$ mice injected with *Cre* containing viruses. A: Viral delivery and expression of Cre recombinase was confirmed by RT-PCR on mouse primary tumors. B: Deletion of *Pten* exon 5 was determined by PCR amplifying genomic DNA from mouse primary tumors.

Figure 2.3 Expression of myrAKT1 in melanomas from *Dct::TVA;Braf*$^{CA/CA}$*;Cdkn2a*$^{lox/lox}$ mice injected with myr*Akt1* and *Cre* containing viruses. Virally delivered myr*Akt1* expression was detected by IHC using an antibody to the HA epitope tag on myrAKT1. Tumors are shown by mouse ID number. Scale bar represents 200 μm.

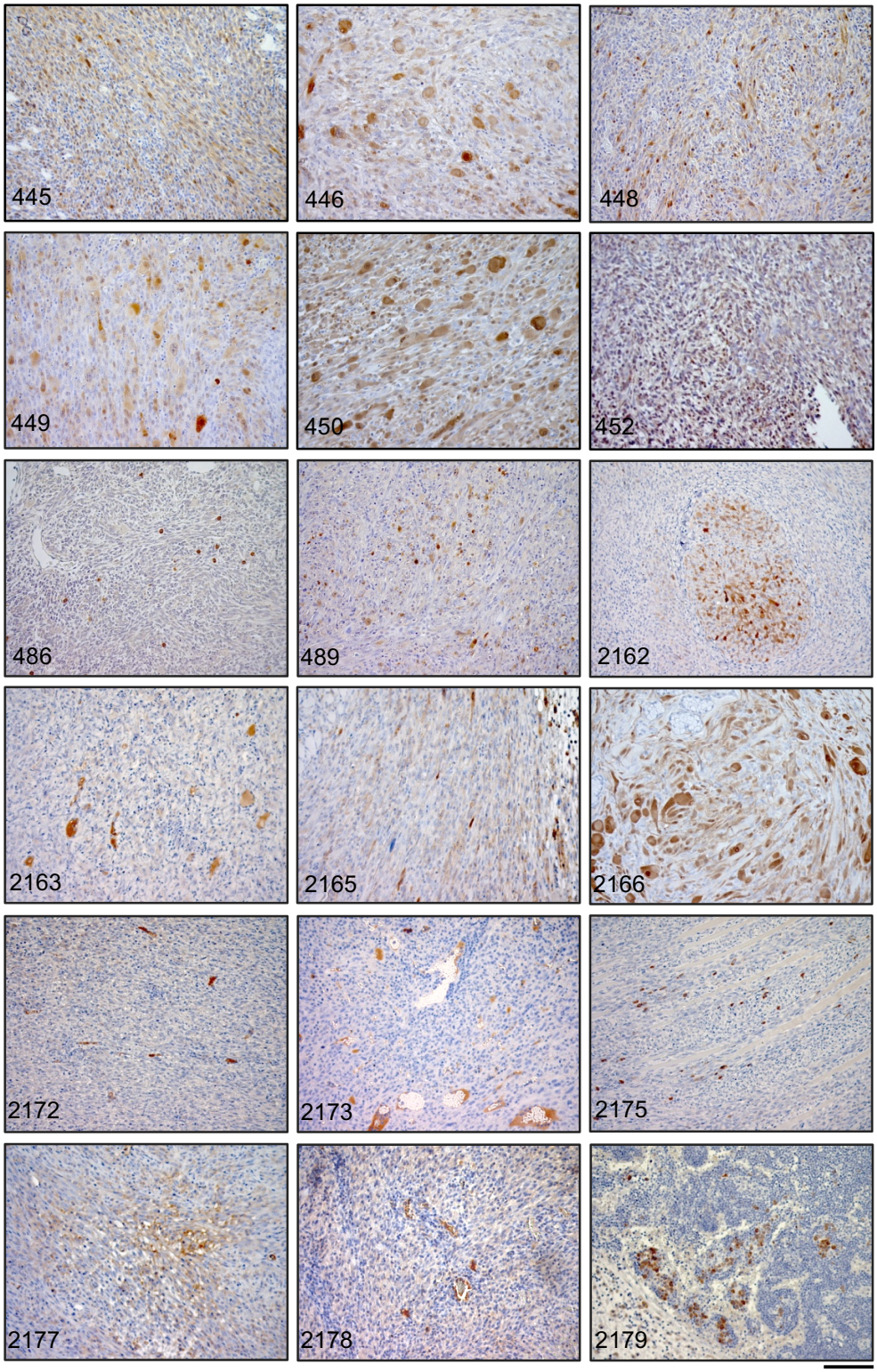
445
446
448
449
450
452
486
489
2162
2163
2165
2166
2172
2173
2175
2177
2178
2179

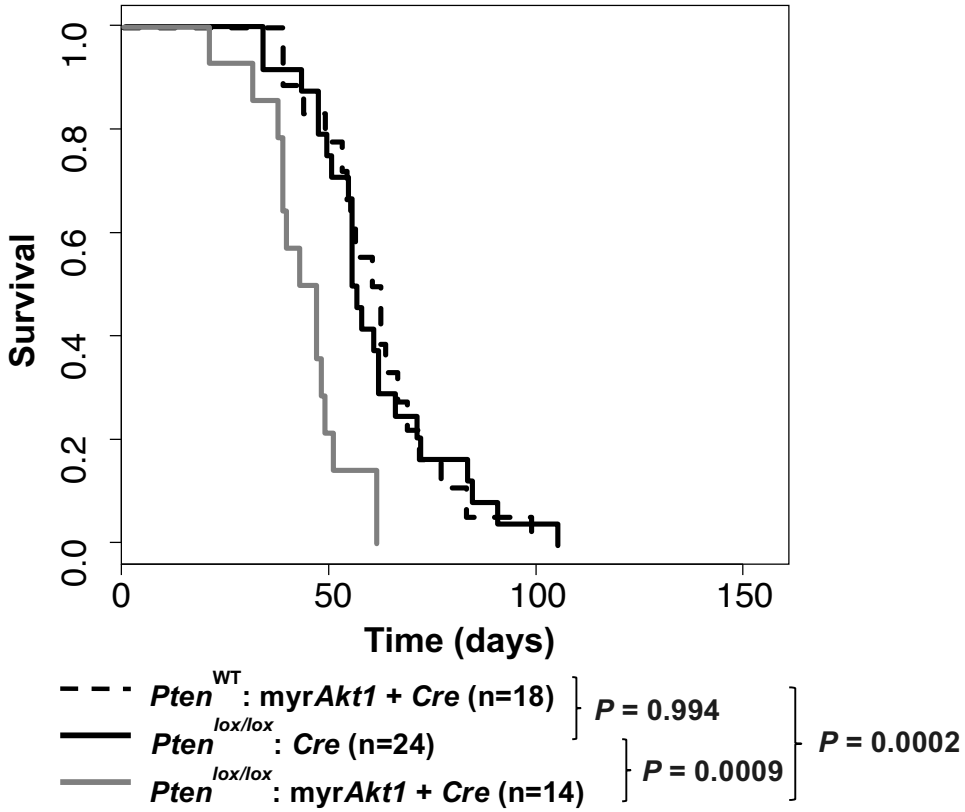

Figure 2.4 Kaplan-Meier percent survival curves for BRAF-induced tumors demonstrate loss of *Pten* cooperates with AKT1 activation to accelerate tumor formation. Comparison of the mice whose tumors were found to express myrAKT1 (wide dashed line n = 18) and mice whose tumors lacked *Pten* revealed no significant difference (P = 0.994) (solid black line n = 24). However, the survival of $Pten^{lox/lox}$ mice injected with myr*Akt1* and *Cre* containing viruses (solid gray line n = 14) differed significantly from the survival of $Pten^{lox/lox}$ mice injected with *Cre* containing viruses (P = 0.0009) and $Pten^{WT}$ mice injected with myr*Akt1* and *Cre* containing viruses (P = 0.0002).

Figure 2.5 Expression of myrAKT1 in melanomas from *Dct::TVA;Braf*$^{CA/CA}$*;Cdkn2a*$^{lox/lox}$*; Pten*$^{lox/lox}$ mice injected with myr*Akt1* and *Cre* containing viruses. Virally delivered myr*Akt1* expression was detected by IHC using an antibody to the HA epitope tag on myrAKT1. Tumors are shown by mouse ID number. Scale bar represents 200 μm.

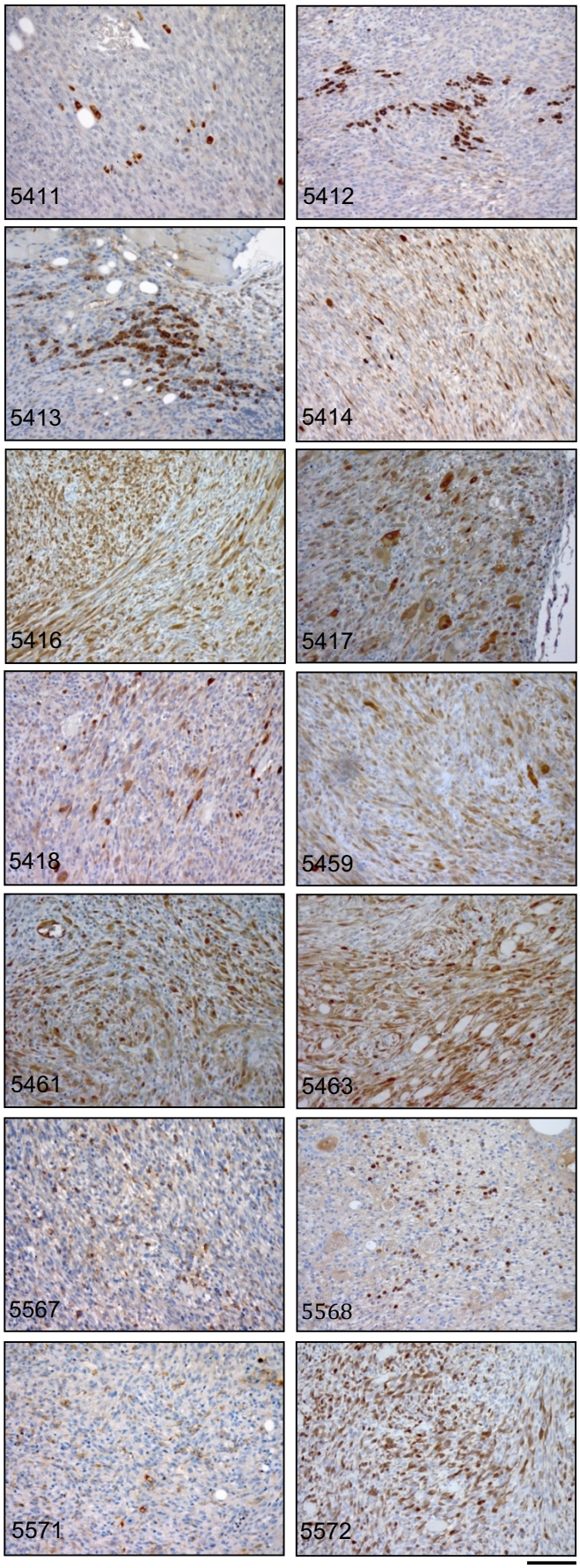
5411
5412
5413
5414
5416
5417
5418
5459
5461
5463
5567
5568
5571
5572

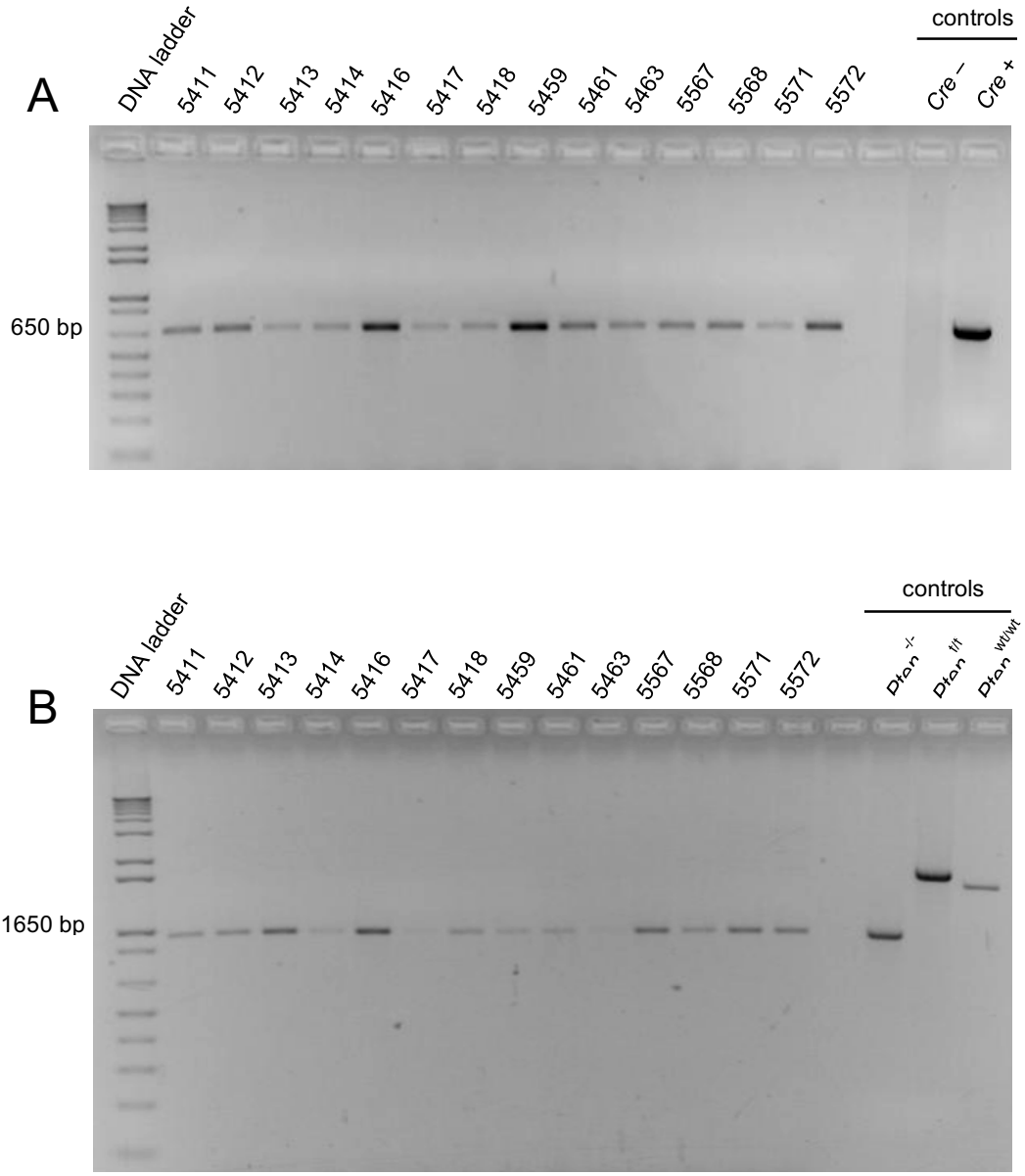

Figure 2.6 *Pten* loss in melanomas from *Dct::TVA;Braf*$^{CA/CA}$*;Cdkn2a*$^{lox/lox}$*;Pten*$^{lox/lox}$ mice injected with *Cre* and myr*Akt1* containing viruses. A: Viral delivery and expression of Cre recombinase was confirmed by RT-PCR on mouse primary tumors. B: Deletion of *Pten* exon 5 was determined by PCR amplifying genomic DNA from mouse primary tumors.

Figure 2.7 Histological analysis of BRAF^{V600E} and myrAKT1 induced tumors. A-D: Tumors were induced in *Dct::TVA;Braf* ^{CA};*Cdkn2a*$^{lox/lox}$ mice (*Pten*^{WT}) by subcutaneous injection of newborn mice with viruses containing myr*Akt1* and *Cre*. A: Representative tumor H&E; B: Ki67 IHC; C: P-ERK IHC; D: IHC for HMB-45, gp100 and MART-1 (pan-MEL). Scale bars represent 200 μm. E-H: Metastases to the lung were observed in *Pten*^{WT} mice injected with myr*Akt1* and *Cre* containing viruses. E: Representative gross lung with multiple metastatic lesions; F: Low magnification H&E of a lung with multiple melanoma metastases; G: Higher magnification H&E of a lung metastasis; H: HA IHC confirmed expression of myrAKT1. Scale bar represents 6 mm. I, J: Brain metastases were observed in *Pten*^{WT} mice injected with myr*Akt1* and *Cre* containing viruses. I: H&E of representative melanoma brain metastasis; J: HA IHC confirmed expression of myrAKT1. Scale bar represents 5 mm.

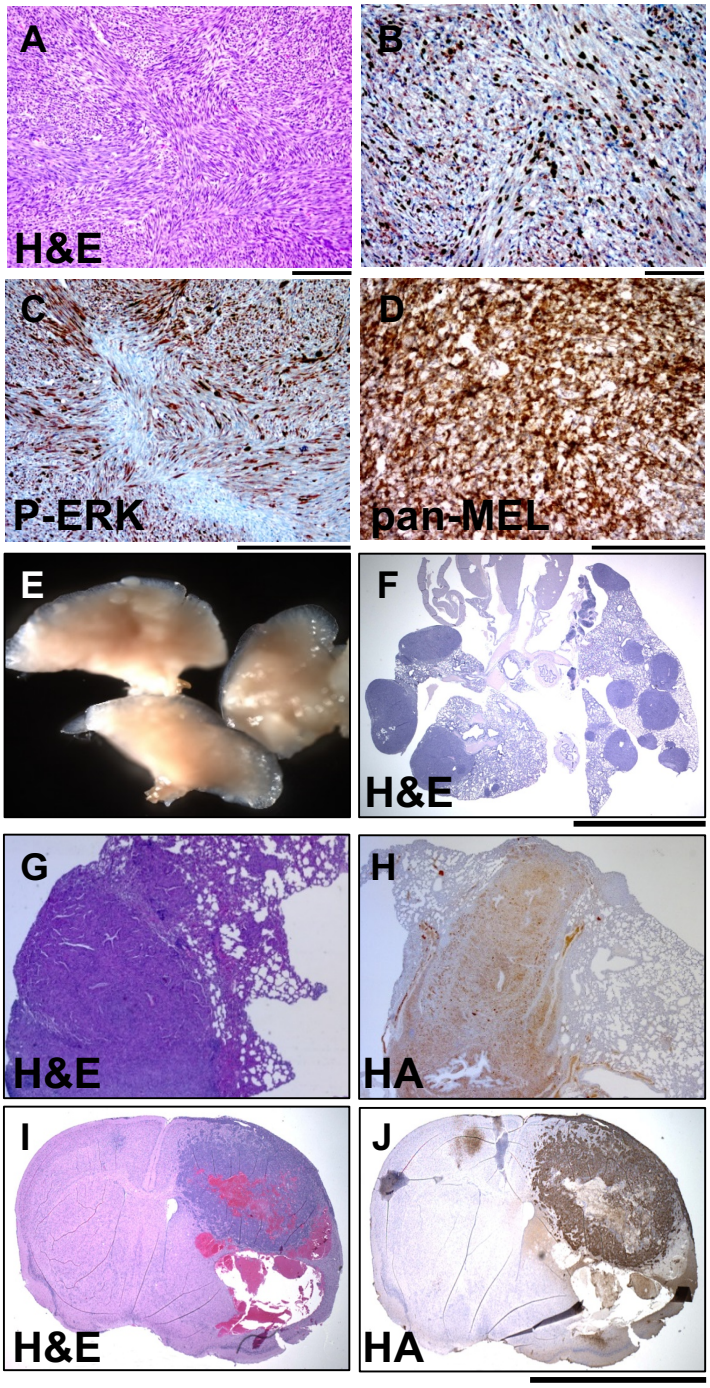
A
H&E
B
C
P-ERK
D
pan-MEL
E
F
H&E
G
H&E
H
HA
I
H&E
J
HA

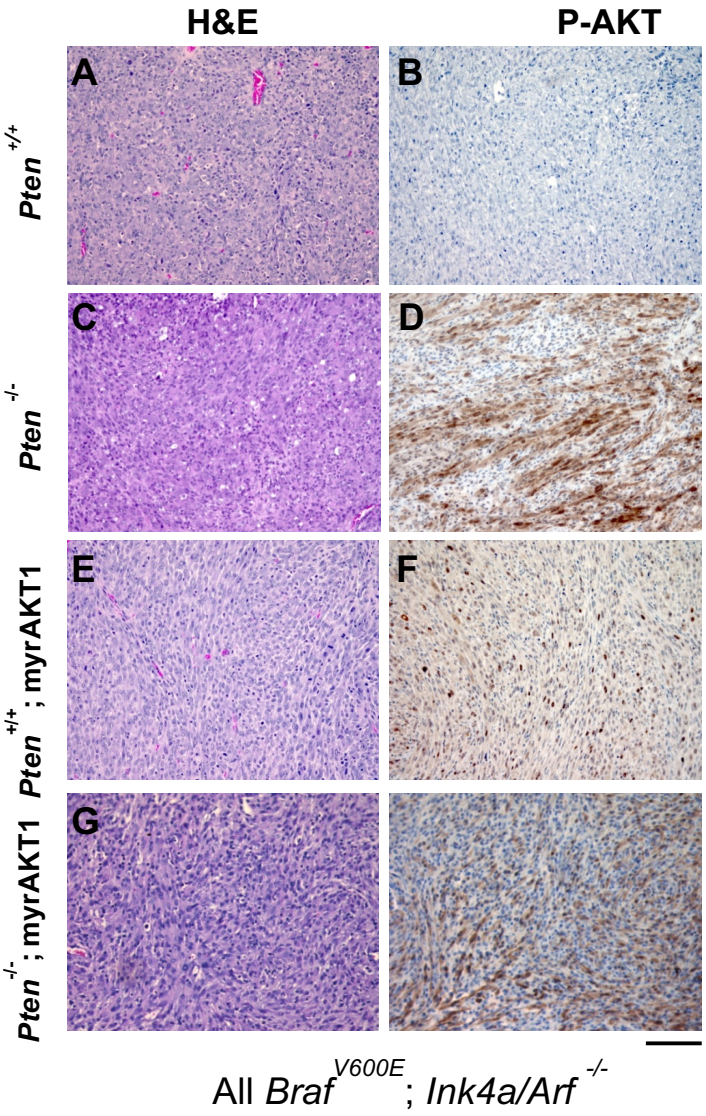

Figure 2.8 Comparison of AKT activity in mutant BRAF melanomas. The left panel (A, C, E, G) shows a representative H&E of the primary tumor and the right panel (B, D, F, H) shows P-AKT (pS473) IHC staining of an adjacent section. All tumors lack *Cdkn2a* expression and express mutant BRAF. *Pten* status and myrAKT1 expression are indicated on the left. Pertinent tumor genotypes are as follows: (A, B) $BRAF^{V600E}$*;*$Cdkn2a^{-/-}$; (C, D) $BRAF^{V600E}$*;*$Cdkn2a^{-/-}$*;*$Pten^{-/-}$; (E,F) $BRAF^{V600E}$ *;*$Cdkn2a^{-/-}$*;* myrAKT1 and (G,H) $BRAF^{V600E}$ *;*$Cdkn2a^{-/-}$*;*$Pten^{-/-}$ *;*myrAKT1. Scale bar represents 200 μm.

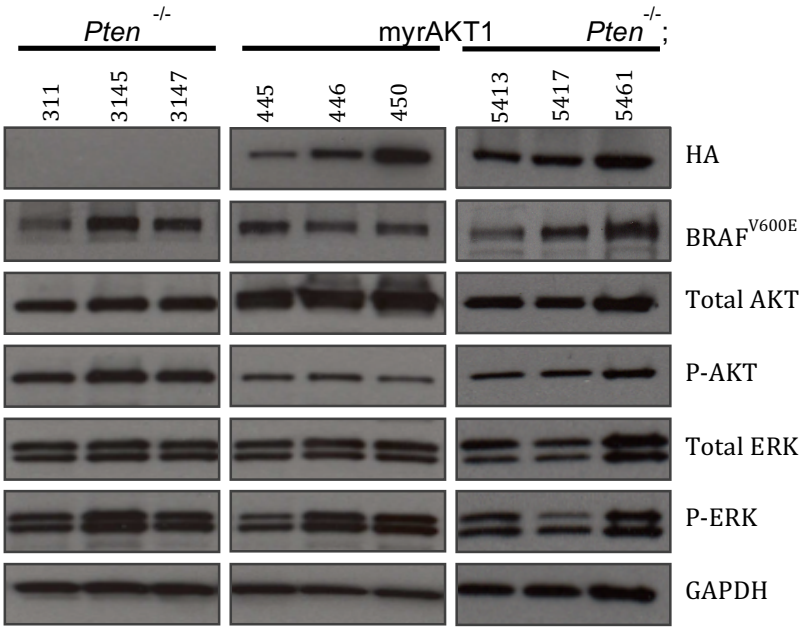

Figure 2.9 Protein expression in mutant BRAF melanomas. Expression of myrAKT1-HA was assessed in nine different tumor samples from three different genotypes: *Cdkn2a*$^{-/-}$;BRAF^{V600E}; *Pten*$^{-/-}$ (311, 3145, 3147), *Cdkn2a*$^{-/-}$;BRAF^{V600E};myrAKT1 (445, 446, 450) and *Cdkn2a*$^{-/-}$; BRAF^{V600E};*Pten*$^{-/-}$;myrAKT1 (5413, 5417, 5461). The cells were lysed in SDS lysis buffer and separated on 4–20% gradient polyacrylamide gels. Virally delivered myr*Akt1* expression was detected with an antibody to the HA epitope tag on myrAKT1. Activation of AKT was evaluated by blotting for phosphorylated AKT (p-AKT) and comparing the levels of total AKT expression. Mutant BRAF expression was confirmed and downstream activity was evaluated by blotting for phosphorylated ERK1/2 (p-ERK1/2) and comparing the levels of total ERK1/2 expression. GAPDH expression was used as a loading control.

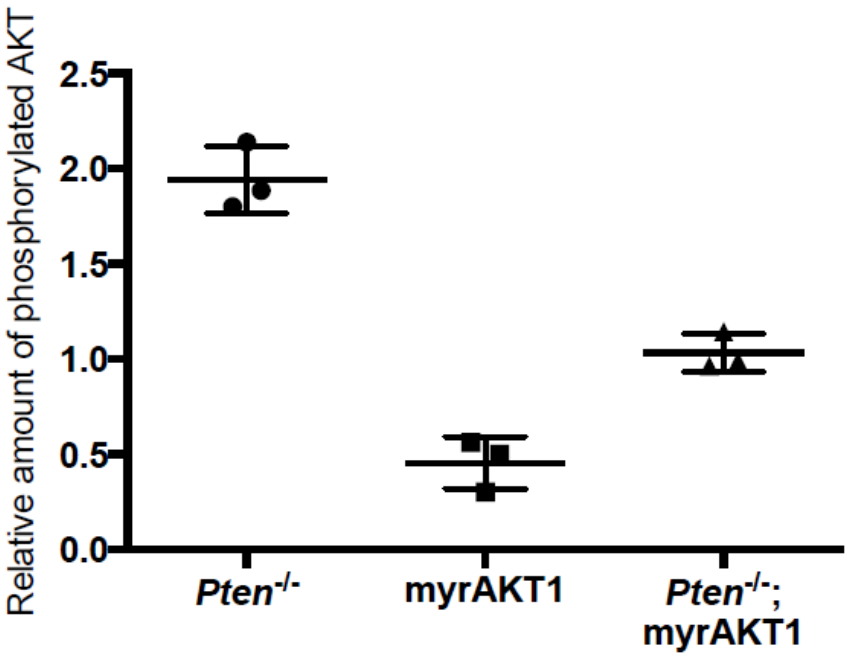

Figure 2.10 Levels of phosphorylated AKT are higher in tumors that have lost *Pten*. Scatter plot shows quantification of immunoblots. Data points equal individual tumors (n=3). Solid line within data points equals geometric mean. Error bars represent standard error of the mean.

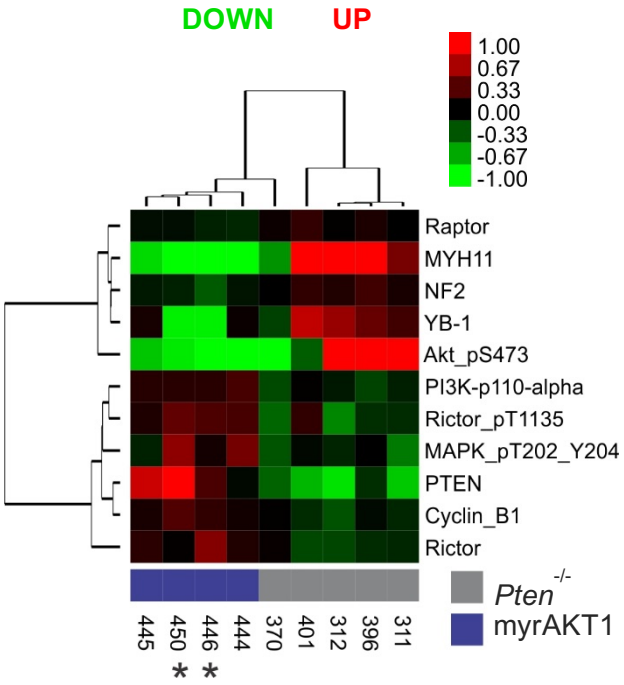

Figure 2.11 RPPA analysis of protein from *Pten*-null and myrAKT1 melanomas. Protein was isolated from *Cdkn2a*$^{-/-}$;BRAF^{V600E};*Pten*$^{-/-}$ (*Pten*$^{-/-}$) and *Cdkn2a*$^{-/-}$;BRAF^{V600E};myrAKT1 (myrAKT1) tumors; expression was assessed by RPPA. Log2 expression data was subjected to unsupervised clustering and the results are presented as a heat-map. Tumors were labeled *Pten*$^{-/-}$ (gray squares) or myrAKT1 (blue squares). The heat-map shown represents the proteins and phosphorylated proteins with a significant difference ($p < 0.05$ using unpaired t tests) between myrAKT1 and *Pten*$^{-/-}$ tumors. An asterisk (*) denotes a primary tumor from a mouse with brain metastasis.

Figure 2.12 Protein and phospho-protein levels from RPPA. Scatter plots show raw expression data from *Pten*$^{-/-}$ and myrAKT1 tumors according to targets that were significantly different ($p < 0.05$ using unpaired t tests) between the two tumor groups. Solid line within data points equals geometric mean. Error bars represent standard error of the mean.

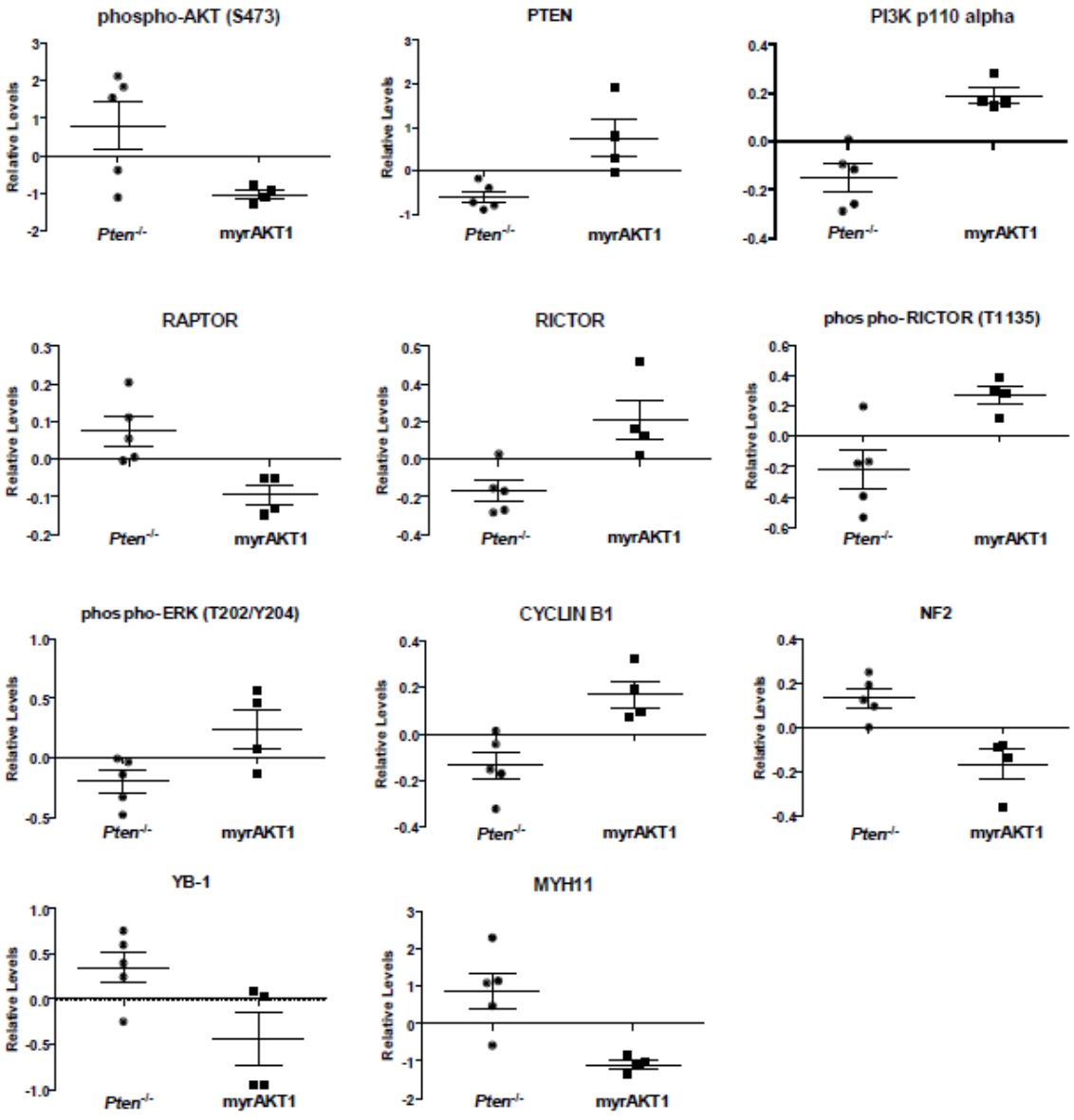
phospho-AKT (S473)
PTEN
PI3K p110 alpha
RAPTOR
RICTOR
phos pho-RICTOR (T1135)
phos pho-ERK (T202/Y204)
CYCLIN B1
NF2
YB-1
MYH11
Relative Levels
Pten-/-
myrAKT1

CHAPTER 3

DIFFERENTIAL METASTATIC POTENTIAL OF AKT ISOFORMS IN MELANOMA

3.1 Introduction

Brain metastases are a major concern for patients with malignant melanoma. Three out of four patients with stage IV disease will develop brain metastasis, making this one of the most common complications of metastatic melanoma (Chaichana and Chaichana, 2011). Consequently, an estimated half of all melanoma deaths are attributed to brain metastases (Davies et al., 2011). Therapeutic advances for brain metastasis have lagged behind the recent breakthroughs in treatment for extracranial metastatic melanoma (Flanigan et al., 2011; Girotti et al., 2014). Our limited understanding of the mechanisms driving melanoma to the brain make clinical management and prognosis of this complication extremely difficult. Further investigation into the molecular mechanisms of brain-specific tropism is warranted to counter the clinical demands of melanoma brain metastasis.

Clinical and experimental data strongly implicate aberrant AKT activation in promoting melanoma brain metastasis (Dai et al., 2005; Davies et al., 2009; Niessner et al., 2013; Chen et al., 2014). Two independent studies comparing patient-matched brain versus extracranial melanoma metastases found that increased AKT acitivty is a hallmark

of brain metastasis (Niessner et al., 2013; Chen et al., 2014). Another clinical study found that absence of detectable PTEN, a negative regulator of AKT activation, correlated with shorter time to brain metastasis among stage IIB/C melanoma patients with *BRAF*^{V600} mutations (Bucheit et al., 2014). Niessner *et al*. observed that melanoma cells grown in astrocyte-conditioned media have much stronger induction of AKT activity and markedly increased invasive potential compared with cells grown in fibroblast-conditioned media (Niessner et al., 2013). We recently reported that expression of activated AKT1 in a non-metastatic mouse model of melanoma results in highly metastatic disease with nearly 80% incidence of brain metastasis (Chapter 2). These lines of evidence strongly support a role for AKT signaling in the pathogenesis of melanoma brain metastasis.

In mammals, AKT activation can occur through one of three isoforms: AKT1, AKT2, and AKT3. The AKT isoforms share ~80% amino acid sequence identity; however, *in vivo* studies indicate that they possess both redundant and nonoverlapping functions (Gonzalez and McGraw, 2009). Various human cancers hyper-activate a specific AKT isoform during tumorigenesis. In melanoma, activating mutations are observed in AKT1 and AKT3 but are yet to be found in AKT2 (Davies et al., 2008; Shi et al., 2014). Activating mutations in AKT1 confer a survival advantage for melanoma cells *in vitro* and are observed in the setting of drug-resistant, metastatic disease (Shi et al., 2014). AKT isoform specific knock-down in melanoma cell lines revealed that AKT3 is the predominately active isoform (Stahl et al., 2004). Aberrant AKT3 activity tempers MAPK signaling in mutant BRAF melanocytes and melanoma cells thus promoting oncogenic transformation rather than cellular senescence (Cheung et al., 2008). Collectively, these studies suggest that in melanoma, specific AKT isoforms may drive aberrant AKT signaling and subsequent pathology.

Previously we reported a highly penetrant, spontaneous model of melanoma brain metastasis driven by activated AKT1 in the context of mutant BRAF and *Ink4a/Arf* loss (Chapter 2). Interestingly, deletion of *Pten* alone did not result in brain metastases but combined with activated AKT1 expression cooperated to accelerate tumor formation and increase the incidence of brain metastasis. These findings led us to hypothesize that activation of specific AKT isoforms might be responsible for promoting brain metastasis in this context. In our current study, we tested this hypothesis by expressing both wild-type and activated AKT1, AKT2, or AKT3 in our established *in vivo* model of melanoma (VanBrocklin et al., 2010). We observed that expression of activated AKT1 and AKT3 promotes the development of brain metastases in 18% and 55% of tumor-bearing mice, respectively. In contrast, expression of activated AKT2 or any of the wild-type AKT isoforms failed to yield brain metastasis in this context. Our observation of brain metastases in nearly 20% of mice expressing activated human AKT1 is in agreement with our previous findings with mouse AKT1 in the same context (Chapter 2). Our results specifically highlight a role for aberrantly activated AKT3 in promoting melanoma brain metastasis. Furthermore, melanoma gene expression analysis from The Cancer Genome Atlas (TCGA) database provides corroborating evidence of increased AKT3 expression in melanomas that metastasize to the brain compared to non-metastatic melanomas (Zhu et al., 2014). Taken together, these data support a mechanism whereby aberrant AKT1 and AKT3 activation promotes melanoma metastasis to the brain. The results from our study demonstrate that the AKT isoforms differ in their ability to promote melanoma metastasis and provide a rationale for the development of therapies that specifically target AKT3 or its effectors to effectively combat melanoma brain metastasis.

3.2 Materials and Methods

3.2.1 Generation of DCT::TVA;Braf^{CA};Ink4a/Arf$^{lox/lox}$ mice. The melanoma model used in this study is based on the RCASBP(A)/TVA retroviral vector system and features *in vivo* melanocyte-specific infection via targeted expression of TVA, the viral receptor for the RCASBP(A) virus (VanBrocklin et al., 2010; von Werder et al., 2012). TVA expression under the control of the Dopachrome tautomerase (DCT) promoter (DCT::TVA) allows RCASBP(A) virus to specifically target melanocytes and facilitates somatic transfer of genetic information (Dunn et al., 2000; Steel et al., 1992). Transgenic DCT::TVA mice were bred with *Ink4a/Arf $^{lox/lox}$* mice (Aguirre et al., 2003a) and Cre-activated *Braf* (*Braf^{CA}*) mice (Dankort et al., 2007a) to yield DCT::TVA;*Braf^{CA}*;*Ink4a/Arf$^{lox/lox}$* mice. In the absence of Cre recombinase, DCT::TVA;*Braf^{CA}*;*Ink4a/Arf $^{lox/lox}$* mice express wild-type BRAF, p16^{INK4A} and p19^{ARF} (Aguirre et al., 2003b; Dankort et al., 2007b). Cre activity results in ablation of a functional *p16^{Ink4a}* and *p19^{Arf}* coding locus and recombination of the *Braf* allele to express mutant BRAF^{V600E}. PCR was conducted to confirm mouse genotyping for the *Dct::TVA* transgene, *Cdkn2a^{lox},* and *Braf^{CA}* and wild-type alleles as described (Dankort et al., 2007b; VanBrocklin et al., 2010)

3.2.2 Production of RCASBP(A) viruses. DF-1 chicken fibroblasts are an ideal host for RCASBP(A) viruses because of their proliferative capacity, their ease of growth in culture, and their endogenous expression of TVA. RCASBP(A) viral vectors containing FLAG tagged human *AKT1*, *AKT2*, or *AKT3* with or without a myristoylation (myr) sequence (designated myr*AKT1*, myr*AKT2*, and myr*AKT3* or wt*AKT1*, wt*AKT2*, and wt*AKT3*) (a kind gift from Wei Zhang) were transfected into DF-1 cells grown at

39°C in DMEM-high glucose media (Invitrogen, Waltham, MA USA) supplemented with 10% FBS (Invitrogen, Waltham, MA USA) using a calcium phosphate based method. Following reverse transcription, the viral DNA integrates into the host cell genome and produces infectious virus in transfected DF-1 cells. The produced infectious virus spreads within the media and eventually inoculates all the DF-1 cells in the culture plate. Expression of virally delivered genes was confirmed by Western blot using the following antibodies at the dilutions indicated: Akt1 (C73H10) Rabbit mAb #2938 (Cell Signaling, Danvers, MA USA) at 1:1000, Akt2 (D6G4) Rabbit mAb #3063 (Cell Signaling) at 1:1000, Akt3 (62A8) Rabbit mAb #3788 (Cell Signaling) at 1:1000, Monoclonal anti-FLAG M2 mAb F3165 (Sigma-Aldrich, St. Louis, MO USA) at 1:1000, Anti-beta Tubulin (HRP) pAb Ab21058 (Abcam, Cambridge, MA USA) at 1:1000, Anti-rabbit IgG, HRP-linked Ab #7074 (Cell Signaling) at 1:1000, and Anti-mouse IgG, HRP-linked Ab #7076 (Cell Signaling) at 1:2000.

3.2.3 Injection of DCT::TVA;Braf^{CA};Ink4a/Arf$^{lox/lox}$ neonatal mice with RCASBP(A) AKT isoform and Cre viruses. Confluent 10 cm plates of infected DF-1 cells were trypsinized, pelleted, and resuspended in 50 μL of Hank's balanced salt solution (HBSS; Invitrogen, Waltham, MA USA). Newborn DCT::TVA;*Braf*^{CA};*Ink4a/Arf*$^{lox/lox}$ mice were subcutaneously injected behind the ears with virus-producing DF-1 cells between postnatal day 1 and postnatal day 5. Mice were serially injected over two rounds with a total volume of 200 μL of the following suspended DF-1 cells: 100 μL of suspended RCASBP(A) *Cre* cells and 100 μL of either suspended RCASBP(A) myr*AKT1*, RCASBP(A) myr*AKT2*, RCASBP(A) myr*AKT3,* RCASBP(A) wt*AKT1*, RCASBP(A) wt*AKT2*, or RCASBP(A) wt*AKT3* cells. The health

status of the mice and tumor development were monitored daily.

3.2.4 Validation of AKT isoform expression in primary mouse melanomas. Expression of AKT isoforms was confirmed via Western blot by probing for the FLAG epitope on the virally-delivered AKTs. Tumors were isolated from DCT::TVA;*Braf*^{CA};*Ink4a/Arf* $^{lox/lox}$ mice injected with RCASBP(A) viruses containing *Cre* and myr*AKT1*, myr*AKT2*, myr*AKT3*, wt*AKT1*, wt*AKT2*, or wt*AKT3*. Samples of collected tumors were prepared for Western blot as previously described (See Chapter 2). The antibodies used for Western blot were monoclonal anti-FLAG M2 mAb F3165 (Sigma-Aldrich) at 1:1000 dilution, Anti-beta Tubulin (HRP) pAb Ab21058 (Abcam) at 1:1000 dilution, and Anti-mouse IgG, HRP-linked Ab #7076 (Cell Signaling) at 1:2000 dilution.

3.2.5 Hematoxylin and eosin staining of mouse melanomas, coronal brain sections and lungs. Mouse tissues were fixed overnight in 10% neutral buffered formalin, dehydrated in 70% ethyl alcohol, and paraffin-embedded. Tissues were cut at 4μm thickness and adhered to glass slides. Tissue sections were stained with hematoxylin and eosin (H&E) or left unstained for immunohistochemistry.

3.2.6 Immunohistochemistry (IHC) of primary mouse melanomas and brain metastases. Tissue sections were deparaffinized and rehydrated prior to antigen retrieval by boiling in 10 mM sodium citrate buffer at pH 6.0 for 20 minutes using a Decloaking Chamber (Biocare Medical, Concord, CA USA). Pre-treament with 3% hydrogen peroxide was employed to quench endogenous peroxidase activity and blocking was done with 5% normal goat serum #5425 (Cell Signaling) in 1× TBS/0.1% Tween-20 (TBS-T). Sections were incubated at 4 ^{o}C overnight with Phospho-Akt (S473) (D9E) XP® Rabbit

mAb #4060 (Cell Signaling) diluted 1:50 or Monoclonal anti-FLAG M2 mAb F3165 (Sigma-Aldrich) diluted at 1:200 in SignalStain® Antibody Diluent #8112 (Cell signaling). The antibody solution was removed and tissue sections were washed three times in 1× TBS-T. Sections were incubated for 1 hour at room temperature in SignalStain® Boost IHC Detection Reagent (HRP, Rabbit) #8114 (Cell Signaling), followed by staining with SignalStain® DAB Substrate Kit #8059 (Cell Signaling). All sections were counterstained with hematoxylin.

3.2.7 TCGA data analysis. Level 3 TCGA Skin Cutaneous Melanoma (SKCM) data was retrieved and processed using TCGA-Assembler software in the R statistical computing environment (Zhu et al., 2014). At the time of analysis, TCGA data was available from 437 individuals with melanoma. The patients were divided into two categories: patients with new tumor events (NTE) and patients without NTEs. Samples with missing NTE status or no information regarding the NTE were excluded (n = 117). The patients with NTE were stratified according to the type of NTE – distant metastasis, regional lymph node metastasis, locoregional recurrence, and new primary. Patients with distant metastasis as the NTE were further subdivided according to presence of brain metastases (hereafter referred to as "brain metastatic") or extracranial metastases. Patients without NTE were subdivided by submitted clinical samples - primary melanoma or metastatic tissue. The patient groups were as follows: 43 NTE patients with distant metastasis to the brain, 108 NTE patients with distant extracranial metastases, 18 NTE patients with lymph node metastases, 20 NTE patients with locoregional recurrence, 6 NTE patients with new primary melanomas, 125 patients without NTE. Of the 125 patients without NTE, 67 patients (hereafter referred to as "non-metastatic") submitted

primary melanoma tissue for analysis.

Taking a candidate approach, we investigated changes in copy number and gene expression for *AKT1*, *AKT2*, *AKT3*, *PTEN*, *PICK3CA*, *PHLPP1*, and *PH domain and leucine rich repeat protein phosphatase 2* (*PHLPP2*). Copy number data processed by the TCGA-Assembler program was initially expressed as an output value equaling the transformed base2log(copy number/2) centered on 0. The output values were re-transformed and centered to a normal copy number of 2. Patient-matched normal whole blood copy number data was used to normalize changes in melanoma tissue sample copy number. Gene expression data processed by the TCGA-Assembler was reported as normalized count values.

3.2.8 Statistical analysis. Censored survival data was analyzed using R software to calculate log-rank tests of the Kaplan-Meier estimate of survival. For all other statistical analyses performed in this study, two-tailed student t-tests were conducted assuming unequal variance.

3.2.9 Study approval. All animal experimentation was performed in AAALAC approved facilities at the University of Utah. All animal protocols were reviewed and approved prior to experimentation by the Institutional Animal Care and Use Committee at the University of Utah.

3.3 Results

3.3.1 AKT3 gene expression is significantly increased in melanomas that metastasize to the brain. Previous studies have reported an association between *AKT* gene loci amplification and melanoma (Bastian et al., 1998; Turner et al., 2015). We used

TCGA data to determine whether genomic amplification of *AKT* isoforms correlated with metastatic outcomes in melanoma. Significant differences in copy number were not observed between melanomas based on metastatic phenotype; however, in line with previous reports, *AKT3* gene amplification is a consistent feature of malignant melanoma with an average copy number of 2.37 (Figure 3.1 and Table 3.1). Interestingly, while *PTEN* exhibits decreased copy number with averages between 1.6-1.7 in melanomas, no significant copy number variations were found for *AKT1* or *AKT2* (Figure 3.1 and Table 3.1). We next sought to determine whether *AKT3* gene expression varies between non-metastatic melanomas and brain metastatic melanomas. Expression of AKT3 is significantly higher (P = 0.00076) in brain metastatic melanomas compared to non-metastatic melanomas (Figure 3.2 and Table 3.2). In contrast, *AKT1* expression is significantly decreased in melanomas that metastasize to the brain compared to non-metastatic melanomas (P = 0.009) while no differences in expression are observed with *AKT2* (Figure 3.2 and Table 3.2). Expression of *PTEN*, *PI3KCAI*, and *PHLPP2* is significantly increased in brain metastatic melanomas compared to non-metastatic melanomas (Table 3.2).

3.3.2 Expression of activated AKT3 increases melanoma incidence, decreases latency, and promotes brain metastasis. Given the TCGA data indicating that AKT3 gene expression is significantly increased in brain metastatic melanomas relative to non-metastatic melanomas, we tested whether *in vivo* expression of activated AKT3 in non-metastatic melanomas promotes tumor growth and metastasis. Newborn *Dct::TVA;Braf*^{CA};*Cdkn2a*$^{lox/lox}$ (*Pten*^{WT}) mice were co-injected with RCASBP(A) *Cre* viruses and RCASBP(A) viruses containing myr*AKT3* (Figure 3.3A). Of the *Pten*^{WT} mice

injected with RCASBP(A) myr*AKT3* and *Cre* viruses, 85% (11/13) developed tumors at the site of injection (Figure 3.3B, Figure 3.4 and Table 3.3). The mean survival of tumor-bearing mice was 53 ± 6.8 days (Table 3.3). Expression of AKT3 in mouse melanomas was confirmed by Western blot (Figure 3.3B) and activated AKT was confirmed by IHC staining for phosphorylated AKT (Ser473) (Figure 3.5). As a control, newborn *Pten*^{WT} mice were injected subcutaneously with RCASBP(A) *Cre* viruses alone. This cohort developed tumors at the site of injection in 47% (16/34) of the mice; mean survival of tumor-bearing mice in this cohort was 88.9 ± 8.6 days (Figure 3.4 and Table 3.3). A significant difference was observed in melanoma incidence and tumor latency between mice expressing activated AKT3 and control counterparts ($P = 6.02 \times 10^{-5}$; Figure 3.4). Upon euthanasia, all mice were examined for metastasis. Interestingly, 55% (6/11) of the mice whose melanomas expressed myr*AKT3* developed brain metastases while none of the *Pten*^{WT} mice injected with viruses containing Cre developed metastases to the brain (Figure 3.6 and Table 3.3).

3.3.3 Activated human AKT1 promotes brain metastases similar to activated mouse AKT1. Our previous work showed that *Pten*^{WT} mice injected with RCASBP(A) viruses containing *Cre* and activated mouse AKT1 developed melanomas in 88% (24/27) of mice and brain metastases were observed in 17% (3/18) of the mice whose tumors expressed myrAKT1 (Chapter 2). In this study, we tested whether expression of activated human AKT1 in the same context would promote melanoma metastasis. Newborn *Pten*^{WT} mice were injected with RCAS viruses containing myr*AKT1* and *Cre*. Tumors formed at the injection site in 79% (15/19) of the mice (Table 3.3). The mean survival of tumor-bearing mice in this cohort was 56 ± 5.7 days (Table 3.3). Expression of AKT1 was

confirmed by Western blot (Figure 3.3B) and activated AKT signaling in tumor tissue was demonstrated by immunohistochemical (IHC) staining for phospho-AKT Ser473 (Figure 3.7). A highly significant difference in tumor latency and incidence was observed between *Pten*^{WT} mice injected with myr*AKT1* and *Cre* viruses and *Pten*^{WT} mice injected with *Cre* virus alone ($P = 8.89 \times 10^{-5}$) (Figure 3.4). Similar to tumor-bearing *Pten*^{WT} mice injected with mouse myr*Akt1*and *Cre* viruses, *Pten*^{WT} mice expressing human myrAKT1 developed brain metastases in 13% (2/15) of the mice (Table 3.3).

3.3.4 Expression of activated AKT2 increases melanoma incidence and decreases latency but does not promote brain metastasis. Newborn *Pten*^{WT} mice were injected with RCASBP(A) viruses encoding myr*AKT2* and *Cre* and monitored for tumor development. All injected *Pten*^{WT} mice developed tumors at the site of injection (18/18; Figure 3.4 and Table 3.3). The mean survival of the mice in this cohort was 40 ± 1.6 days (Table 3.3). A highly significant difference in survival was observed compared to the *Pten*^{WT} cohort injected with RCASBP(A) *Cre* alone ($P < 1.00 \times 10^{-5}$) (Figure 3.4). Confirmation of AKT2 expression was made via Western blot (Figure 3.3B) and activated AKT signaling was confirmed by IHC for phospho-AKT Ser473 (Figure 3.8). No brain metastases were observed in any of the mice whose tumors expressed myr*AKT2*

3.3.5 Wild-type AKT isoforms increase melanoma incidence but do not promote brain metastasis. Following our results with activated AKT isoforms, we tested whether expression of AKT isoforms lacking the myristoylation sequence tag would promote melanoma development and metastasis in our *in vivo* melanoma model. Newborn *Pten*^{WT} mice co-injected with RCASBP(A) viruses encoding wt*AKT1* and *Cre* had a tumor incidence of 89% (8/9; Figure 3.9 and Table 3.3). The mean survival of the tumor-

bearing mice in this cohort was 74 ± 5.3 days (Table 3.3). *Pten*^{WT} mice injected with RCASBP(A) viruses encoding wt*AKT2* and *Cre* had a tumor incidence of 84% (17/20; Figure 3.9 and Table 3.3). The mean survival of the tumor-bearing mice in this cohort was 62.2 ± 4.0 days (Table 3.3). Injection of RCASBP(A) wt*AKT3* and *Cre* viruses into newborn *Pten*^{WT} mice resulted in tumor formation in 70% of the mice (7/10; Figure 3.9 and Table 3.3). The mean survival of the tumor-bearing mice in this cohort was 69 ± 5.3 days (Table 3.3). Although expression of the AKT isoforms in our melanoma model led to significant increases in melanoma incidence compared to control *Pten*^{WT} mice injected with RCASBP(A) *Cre* alone as demonstrated by the Kaplan-Meier survival curves (Figure 3.9), no observable brain metastases were observed in any of the mice whose tumors expressed wild-type AKT.

3.3.6 Expression of activated AKT2 promotes melanoma lung metastasis. We previously reported that *Pten*^{WT} mice injected with viruses containing mouse myrAKT1 and Cre develop highly metastatic melanomas with metastases to the lungs and brain (Chapter 2). Therefore, we examined all major organs of the tumor-bearing mice for melanoma metastases. Lung metastases were observed at a frequency of 18%, 29%, and 20% for melanomas expressing myrAKT1, myrAKT2, and myrAKT3, respectively, while no lung metastases were observed in tumor-bearing *Pten*^{WT} mice injected with RCASBP(A) *Cre* alone (Table 3.3). However, using a Fisher's exact test, we determined that only melanomas expressing myrAKT2 had a significant incidence of lung metastases when compared to mice with tumors only injected with *Cre* viruses ($P = 0.0445$).

3.4 Discussion

In this study, we investigated the metastatic potential of melanomas expressing different isoforms of AKT and observed that activation of AKT1 and AKT3 specifically promote brain metastases. We previously observed that PTEN silencing in melanoma does not mirror AKT1 activation in terms of promoting lung and brain metastases. This led us to hypothesize that activation of specific AKT-isoforms account for differences in metastatic potential. We observed that activated AKT3 expression in a non-metastatic mouse model of melanoma leads to lung and brain metastasis with 55% penetrance. In line with our previous findings, expression of activated AKT1 in non-metastatic melanomas results in lung and brain metastases with at incidence of 18%. Interestingly, expression of AKT2 or any of the wild-type AKT isoforms with Cre in this melanoma model leads to primary tumor growth and lung metastases but no observable brain metastases. Taken together, these findings suggest that the mechanisms driving melanoma to the brain are mediated through specific AKT isoforms.

We observed brain metastases in mice bearing tumors driven by activated AKT1 and AKT3. Mechanisms implicating AKT isoform-specific preferences in melanoma development and progression have previously been reported (Cheung et al., 2008; Stahl et al., 2004). Cheung et al. found that AKT3 cooperates with $BRAF^{V600E}$ by inhibitory phosphorylation, which tempers MAPK signaling to a level that promotes melanocyte proliferation and transformation (Cheung et al., 2008). Robertson and coworkers found clinical support for increased AKT3 activity in human melanomas compared with normal melanocytes and linked expression of AKT3 in melanomas with decreased apoptosis (Stahl et al., 2004). We previously demonstrated that expression of activated mouse

AKT1 is sufficient to elicit lung and brain metastasis in an *in vivo* non-metastatic model of melanoma (Chapter 2). In this study we observed similar patterns of metastasis when activated human AKT1 was expressed in the same context. Furthermore, we describe a novel finding that expression of activated AKT3 results in even higher incidence (55%) of brain metastasis than AKT1 in our *in vivo* model. While AKT3 has recently been associated with the pathogenesis of primary brain malignancies (Turner et al., 2015), this is to our knowledge the first report of AKT3 promoting melanoma metastasis to the brain.

Several lines of evidence point towards a neuro-developmental function of AKT3. The expression of AKT3 is predominately expressed in the brain and *Akt3*$^{-/-}$ mice exhibit a 20-25% decrease in brain size compared to than their wild-type littermates (Easton et al., 2005; Tschopp et al., 2005). Activating AKT3 mutations are associated with brain over-growth syndromes (Lee et al., 2012; Poduri et al., 2012; Riviere et al., 2012) and genetic duplications involving the *AKT3* locus are known to occur in patients with macrocephaly (Chung et al., 2014; Riviere et al., 2012; Wang et al., 2013). In contrast, patients with *AKT3* deletion or loss of the genomic region encoding *AKT3* (1q44) exhibit features such as microcephaly, seizure phenotype, and cognitive deficits (Ballif et al., 2012; Gai et al., 2015). Taken together, these studies suggest that AKT3 plays a prominent role in brain development and growth.

While we find that AKT1 and AKT3 activation promotes brain metastasis in melanoma, AKT2 activation does not promote this phenotype and instead is associated with lung metastases and rapid tumor growth. These phenomena may be related to the role of AKT2 in glucose metabolism. *Akt2* knock-out mice are impaired in glucose

metabolism and exhibit features of type II diabetes (Cho et al., 2001; Garofalo et al., 2003). Adipocytes derived from *Akt2*$^{-/-}$ fibroblasts display markedly reduced glucose uptake upon insulin stimulation compared to fibroblast from *Akt2* wild-type littermates (Bae et al., 2003; Hill et al., 1999). Insulin sensitivity is fully restored in AKT2-deficient adipocytes upon re-expression of AKT2 but not with overexpression of AKT1 (Bae et al., 2003). Mechanistically, AKT2 promotes translocation of Glucose transporter 4 (GLUT4) to the plasma membrane in an isoform-specific manner via regulation of several downstream effectors, the best characterized being the Rab GTPase activating protein (GAP), AS160, which negatively regulates GLUT4 exocytosis in adipocytes and muscle cells (Eguez et al., 2005; Gonzalez et al., 2009; Ishikura and Klip, 2008; Sano et al., 2007). Clinical evidence supports laboratory findings of AKT2-mediated glucose regulation. Inactivating mutations in *AKT2* have been linked with familial insulin resistance and diabetes mellitus (George et al., 2004). Alternatively, activating mutations in AKT2 are associated with severe hypoglycemia and accelerated growth (Hussain et al., 2011). The function of AKT2 in glucose homeostasis could explain the rapid tumor growth phenotype we observe in melanomas ectopically expressing activated AKT2 (Figures 3.4 and Figure 3.9).

Opposing or nonoverlapping roles of the AKT isoforms are well documented in the pathogenic processes of cancer, including metastasis. AKT1 and AKT2 are known to play opposing roles in mouse embryo fibroblast cell migration and regulation of the cytoskeleton. Using *in vitro* migration assays, Zhou *et al.* reported that *Akt2* knock-out cells migrate faster than wild-type cells while *Akt1*-null cells migrate slower than wild-type cells via a mechanism that involves differential isoform signaling through RAC and

PAK1 (Zhou et al., 2006). Distinct functional roles for the AKT isoforms are observed in disseminated tumor cells (DTC) found in the bone marrow of non-small cell lung cancer patients (Grabinski et al., 2011). While depletion of AKT3 and AKT1 reduces proliferation and survival of DTC cell lines in association with decreased levels of Cyclin D1 and impaired Epidermal growth factor (EGF)-dependent stimulation, knockdown of AKT2 in DTC cell lines does not reduce proliferation or survival (Grabinski et al., 2011). Irie *et al.* uncovered AKT isoform-specific differences in the regulation of cell migration and epithelial-mesenchymal transition using a 3D *in vitro* culture system to model breast cancer initiation and progression (Irie et al., 2005). AKT2 depletion in insulin-like growth factor-1 receptor (IGF-1R) stimulated breast epithelial cells (MCF-10A) abrogated hyper-proliferative and anti-apoptotic phenotypes while AKT1 down-regulation significantly enhances *in vitro* cell migration by a mechanism involving ERK activation (Irie et al., 2005). Using two different *in vivo* mouse models of breast cancer, Muller and coworkers demonstrated that AKT1 expression accelerates mammary tumor development but decreases the incidence of lung metastasis. On the other hand, AKT2 expression did not significantly affect tumor latency but dramatically increased the incidence of lung metastasis (Dillon et al., 2009). Similarly, we observed a significant incidence of lung metastases in mice with tumors expressing activated AKT2 but not with other isoforms. These examples of AKT isoform-specific mechanisms suggest that the functions of the different AKT isoforms are not uniform and vary greatly depending on the cellular context.

In this study, we found that expression of activated (myristolated), but not wild-type, AKT results in a metastatic melanoma phenotype. To become fully activated, AKT

is phosphorylated at two critical residues, Thr308 and Ser473, by PDK1 and mTORC2, respectively (Alessi et al., 1997; Sarbassov et al., 2005). Activation of AKT is limited by its access to the plasma membrane where phosphorylation occurs (Andjelkovic et al., 1997). Following phosphorylation, AKT becomes locked into a catalytically active conformation (Andjelkovic et al., 1997; Bellacosa et al., 1998; Yang et al., 2002) and disperses from the plasma membrane to a variety of cellular locations including the cytoplasm, nucleus, and mitochondria where it acts on downstream effectors (Toker, 2012). Compared to wild-type AKT, myristoylated AKT proteins display both increased and unregulated kinase activity *in vitro* (Mende, 2001). Expression of myristoylated AKT in chicken embryo fibroblasts exhibited stronger induction of oncogenic transformation by colony forming assay and promoted tumor formation *in vivo* while wild-type AKT isoforms lacked this ability (Mende, 2001). Our data supports these findings and suggests that expression of AKT1 or AKT3 in the context of melanomas driven by mutant $BRAF^{V600E}$ and silencing of INK4A and ARF, is not sufficient to elicit brain metastasis but that these proteins must also be aberrantly activated. This hypothesis could provide an explanation for our previous finding that PTEN loss cooperates with activated AKT1 to promote melanoma brain metastasis (Chapter 2). PTEN is a well-known negative regulator of AKT signaling and its loss could accentuate the dysregulated activation of myrAKT1 or myrAKT3 and thus further promote brain metastasis (Chalhoub and Baker, 2009). Whether this cooperative effect is due to enhanced AKT signaling or via an AKT-independent mechanism downstream of PTEN will need to be further studied by expressing other activated AKT isoforms in the context of PTEN silencing and assessing melanoma growth and metastasis.

We previously reported that PTEN silencing in melanomas driven by mutant $BRAF^{V600E}$ and loss of INK4A/ARF does not yield a significant metastatic phenotype like that observed in similar melanomas with expression of activated AKT1 (Chapter 2). A potential mechanism that could explain this phenomenon is that PTEN silencing preferentially activates a specific AKT isoform that does not promote melanoma metastasis. Indeed, one group reported preferential activation of AKT2 following PTEN inactivation in melanoma cells (Nogueira et al., 2010). Our current study demonstrates that while expression of activated AKT3 and to a lesser degree activated AKT1 in our melanoma model results in brain metastasis, the expression of activated AKT2 does not yield any brain metastases. It is tempting to speculate that our earlier observed lack of metastasis in PTEN silenced melanomas is due to predominant signaling through the AKT2 isoform. Our current study establishes that AKT signaling through specific AKT isoforms yields different metastatic potential for melanoma, yet it remains to be determined whether PTEN silencing preferentially allows activation of a specific AKT isoform during melanoma progression and metastasis.

Our findings that expression of aberrantly activated AKT3 results in a significant incidence (55%; 6/11) of melanoma brain metastasis and that AKT3 gene expression is significantly higher in human melanomas that metastasize to the brain compared to non-metastatic melanomas strongly implicate AKT3 signaling in promoting melanoma brain metastasis. Several previous studies have implicated AKT3 signaling in melanomagenesis, both clinically and experimentally (Cheung et al., 2008; Davies et al., 2008; Stahl et al., 2004). Characterized mechanisms of activated AKT3 include inhibition of apoptosis, regulation of angiogenesis, and activation of the DNA repair pathway

(Phung et al., 2015; Shao and Aplin, 2010; Turner et al., 2015). Whether or not theses mechanisms of activated AKT3 are responsible for the increase in brain metastasis will be determined in future studies.

In summary, we report that expression of activated AKT3 and AKT1 in a non-metastatic melanoma mouse model results in high incidence of lung and brain metastases. Notably, we find that in contrast to activated AKT2 expressing melanomas which significantly metastasize to the lungs, activation of AKT3 promotes melanoma brain metastasis and its expression is significantly upregulated in brain metastatic human melanomas. Future studies will focus on determining key downstream effectors and mechanisms of AKT3 signaling that promotes melanoma dissemination to the brain.

3.5 Acknowledgments

The work described in this chapter was completed in collaboration with James Robinson, Rowan Arave, Joyce Tross, Matthew VanBrocklin, and Sheri Holmen. J.R. contributed to the experimental design and execution. R.A. performed immunohistochemistry. J.T. assisted with mouse husbandry. M.V. and S.H. established the mouse model. S.H. advised on experimental design and guided the research.

3.6 References

Aguirre, A.J., Bardeesy, N., Sinha, M., Lopez, L., Tuveson, D.A., Horner, J., Redston, M.S., and DePinho, R.A. (2003a). Activated Kras and Ink4a/Arf deficiency cooperate to produce metastatic pancreatic ductal adenocarcinoma. Genes & Development *17*, 3112-3126.

Aguirre, A.J., Bardeesy, N., Sinha, M., Lopez, L., Tuveson, D.A., Horner, J., Redston, M.S., and DePinho, R.A. (2003b). Activated Kras and Ink4a/Arf deficiency cooperate to produce metastatic pancreatic ductal adenocarcinoma. Genes & Development *17*, 3112-

3126.

Alessi, D.R., James, S.R., Downes, C.P., Holmes, A.B., Gaffney, P.R.J., Reese, C.B., and Cohen, P. (1997). Characterization of a 3-phosphoinositide-dependent protein kinase which phosphorylates and activates protein kinase Bα. Current Biology *7*, 261-269.

Andjelkovic, M., Alessi, D.R., Meier, R., Fernandez, A., Lamb, N.J.C., Frech, M., Cron, P., Cohen, P., Lucocq, J.M., and Hemmings, B.A. (1997). Role of translocation in the activation and function of protein kinase B. Journal of Biological Chemistry *272*, 31515-31524.

Bae, S.S., Cho, H., Mu, J., and Birnbaum, M.J. (2003). Isoform-specific regulation of insulin-dependent glucose uptake by Akt/protein kinase B. Journal of Biological Chemistry *278*, 49530-49536.

Ballif, B., Rosenfeld, J., Traylor, R., Theisen, A., Bader, P., Ladda, R., Sell, S., Steinraths, M., Surti, U., McGuire, M.*, et al.* (2012). High-resolution array CGH defines critical regions and candidate genes for microcephaly, abnormalities of the corpus callosum, and seizure phenotypes in patients with microdeletions of 1q43q44. Human Genetics *131*, 145-156.

Bastian, B.C., LeBoit, P.E., Hamm, H., Bröcker, E.-B., and Pinkel, D. (1998). Chromosomal gains and losses in primary cutaneous melanomas detected by comparative genomic hybridization. Cancer Research *58*, 2170-2175.

Bellacosa, A., Chan, T.O., Ahmed, N.N., Datta, K., Malstrom, S., Stokoe, D., McCormick, F., Feng, J., and Tsichlis, P.N. (1998). Akt activation by growth factors is a multiple-step process: The role of the PH domain. Oncogene *17*, 313-325.

Bucheit, A.D., Chen, G., Siroy, A., Tetzlaff, M., Broaddus, R., Milton, D., Fox, P., Bassett, R., Hwu, P., Gershenwald, J.E.*, et al.* (2014). Complete loss of PTEN protein expression correlates with shorter time to brain metastasis and survival in stage IIIB/C melanoma patients with BRAFV600 mutations. Clinical Cancer Research *20*, 5527-5536.

Chaichana, K.K., and Chaichana, K.L. (2011). Diagnosis and treatment options for brain metastasis of melanoma. In treatment of metastatic melanoma, R. Morton, edition (Croatia: InTech), pp. 47-70.

Chalhoub, N., and Baker, S.J. (2009). PTEN and the PI3-Kinase pathway in cancer. Annual Review of Pathology: Mechanisms of Disease *4*, 127-150.

Cheung, M., Sharma, A., Madhunapantula, S.V., and Robertson, G.P. (2008). Akt3 and mutant V600EB-Raf cooperate to promote early melanoma development. Cancer Research *68*, 3429-3439.

Cho, H., Mu, J., Kim, J.K., Thorvaldsen, J.L., Chu, Q., Crenshaw, E.B., Kaestner, K.H.,

Bartolomei, M.S., Shulman, G.I., and Birnbaum, M.J. (2001). Insulin resistance and a diabetes mellitus-like syndrome in mice lacking the protein kinase Akt2 (PKBβ). Science *292*, 1728-1731.

Chung, B.K., Eydoux, P., ⁄an Karnebeek, C.D., and Gibson, W.T. (2014). Duplication of AKT3 is associated with macrocephaly and speech delay. American Journal of Medical Genetics Part A *164*, 1868-1869.

Dankort, D., Filenova, E., Collado, M., Serrano, M., Jones, K., and McMahon, M. (2007a). A new mouse model to explore the initiation, progression, and therapy of BRAFV600E-induced lung tumors. Genes & Development *21*, 379-384.

Dankort, D., Filenova, E., Collado, M., Serrano, M., Jones, K., and McMahon, M. (2007b). A new mouse model to explore the initiation, progression, and therapy of BRAFV600E-induced lung tumors. Genes & Development *21*, 000.

Davies, M.A., Liu, P., McIntyre, S., Kim, K.B., Papadopoulos, N., Hwu, W.J., Hwu, P., and Bedikian, A. (2011). Prognostic factors for survival in melanoma patients with brain metastases. Cancer *117*, 1687-1696.

Davies, M.A., Stemke-Hale, K., Tellez, C., Calderone, T.L., Deng, W., Prieto, V.G., Lazar, A.J.F., Gershenwald, J.E., and Mills, G.B. (2008). A novel AKT3 mutation in melanoma tumours and cell lines. British Journal of Cancer *99*, 1265-1268.

Dillon, R.L., Marcotte, R., Hennessy, B.T., Woodgett, J.R., Mills, G.B., and Muller, W.J. (2009). Akt1 and Akt2 play distinct roles in the initiation and metastatic phases of mammary tumor progression. Cancer Research *69*, 5057-5064.

Dunn, K.J., Williams, B.O., Li, Y., and Pavan, W.J. (2000). Neural crest-directed gene transfer demonstrates Wnt1 role in melanocyte expansion and differentiation during mouse development. Proceedings of the National Academy of Sciences *97*, 10050-10055.

Easton, R.M., Cho, H., Roovers, K., Shineman, D.W., Mizrahi, M., Forman, M.S., Lee, V.M.-Y., Szabolcs, M., de Jong, R., Oltersdorf, T.*, et al.* (2005). Role for Akt3/protein kinase Bγ in attainment of normal brain size. Molecular and Cellular Biology *25*, 1869-1878.

Eguez, L., Lee, A., Chavez, J.A., Miinea, C.P., Kane, S., Lienhard, G.E., and McGraw, T.E. (2005). Full intracellular retention of GLUT4 requires AS160 Rab GTPase activating protein. Cell Metabolism *2*, 263-272.

Flanigan, J.C., Jilaveanu, L.B., Faries, M., Sznol, M., Ariyan, S., Yu, J.B., Knisely, J.P.S., Chiang, V.L., and Kluger, H.M. (2011). Melanoma brain metastases: Is it time to reassess the bias? Current Problems in Cancer *35*, 200-210.

Gai, D., Haan, E., Scholar, M., Nicholl, J., and Yu, S. (2015). Phenotypes of AKT3

deletion: A case report and literature review. American Journal of Medical Genetics Part A *167*, 174-179.

Garofalo, R.S., Orena, S.J., Rafidi, K., Torchia, A.J., Stock, J.L., Hildebrandt, A.L., Coskran, T., Black, S.C., Brees, D.J., Wicks, J.R.*, et al.* (2003). Severe diabetes, age-dependent loss of adipose tissue, and mild growth deficiency in mice lacking Akt2/PKBβ. The Journal of Clinical Investigation *112*, 197-208.

George, S., Rochford, J.J., Wolfrum, C., Gray, S.L., Schinner, S., Wilson, J.C., Soos, M.A., Murgatroyd, P.R., Williams, R.M., Acerini, C.L.*, et al.* (2004). A family with severe insulin resistance and diabetes due to a mutation in AKT2. Science *304*, 1325-1328.

Girotti, M.R., Saturno, G., Lorigan, P., and Marais, R. (2014). No longer an untreatable disease: How targeted and immunotherapies have changed the management of melanoma patients. Molecular Oncology *8*, 1140-1158.

Gonzalez, E., and McGraw, T.E. (2009). The Akt kinases: Isoform specificity in metabolism and cancer. Cell Cycle *8*, 2502-2508.

Gonzalez, E., McGraw, T.E., and Sabatini, D.D. (2009). Insulin-modulated Akt subcellular localization determines Akt isoform-specific signaling. Proceedings of the National Academy of Sciences of the United States of America *106*, 7004-7009.

Hill, M.M., Clark, S.F., Tucker, D.F., Birnbaum, M.J., James, D.E., and Macaulay, S.L. (1999). A role for protein kinase Bβ/Akt2 in insulin-stimulated GLUT4 translocation in adipocytes. Molecular and Cellular Biology *19*, 7771-7781.

Hussain, K., Challis, B., Rocha, N., Payne, F., Minic, M., Thompson, A., Daly, A., Scott, C., Harris, J., Smillie, B.J.L.*, et al.* (2011). An activating mutation of AKT2 and human hypoglycemia. Science *334*, 474.

Irie, H.Y., Pearline, R.V., Grueneberg, D., Hsia, M., Ravichandran, P., Kothari, N., Natesan, S., and Brugge, J.S. (2005). Distinct roles of Akt1 and Akt2 in regulating cell migration and epithelial–mesenchymal transition. The Journal of Cell Biology *171*, 1023-1034.

Ishikura, S., and Klip, A. (2008). Muscle cells engage Rab8A and myosin Vb in insulin-dependent GLUT4 translocation. American Journal of Physiology - Cell Physiology *295*, C1016-C1025.

Lee, J.H., Huynh, M., Silhavy, J.L., Kim, S., Dixon-Salazar, T., Heiberg, A., Scott, E., Bafna, V., Hill, K.J., Collazo, A.*, et al.* (2012). De novo somatic mutations in components of the PI3K-AKT3-mTOR pathway cause hemimegalencephaly. Nature Genetics *44*, 941-945.

Mende, I.M., S.; Tsichlis, P.N.; Vogt, P.K.; Aoki, M. (2001). Oncogenic transformation induced by membrane-targeted Akt2 and Akt3. Oncogene *20*, 4419-4423.

Nogueira, C., Kim, K.H., Sung, H., Paraiso, K.H.T., Dannenberg, J.H., Bosenberg, M., Chin, L., and Kim, M. (2010). Cooperative interactions of PTEN deficiency and RAS activation in melanoma metastasis. Oncogene *29*, 6222-6232.

Phung, T.L., Du, W., Xue, Q., Ayyaswamy, S., Gerald, D., Antonello, Z., Nhek, S., Perruzzi, C.A., Acevedo, I., Ramanna-Valmiki, R.*, et al.* (2015). Akt1 and Akt3 exert opposing roles in the regulation of vascular tumor growth. Cancer Research *75*, 40-50.

Poduri, A., Evrony, Gilad D., Cai, X., Elhosary, Princess C., Beroukhim, R., Lehtinen, Maria K., Hills, L.B., Heinzen, Erin L., Hill, A., Hill, R.S.*, et al.* (2012). Somatic activation of AKT3 causes hemispheric developmental brain malformations. Neuron *74*, 41-48.

Riviere, J.-B., Mirzaa, G.M., O'Roak, B.J., Beddaoui, M., Alcantara, D., Conway, R.L., St-Onge, J., Schwartzentruber, J.A., Gripp, K.W., Nikkel, S.M.*, et al.* (2012). De novo germline and postzygotic mutations in AKT3, PIK3R2 and PIK3CA cause a spectrum of related megalencephaly syndromes. Nature Genetics *44*, 934-940.

Sano, H., Eguez, L., Teruel, M.N., Fukuda, M., Chuang, T.D., Chavez, J.A., Lienhard, G.E., and McGraw, T.E. (2007). Rab10, a target of the AS160 Rab GAP, is required for insulin-stimulated translocation of GLUT4 to the adipocyte plasma membrane. Cell Metabolism *5*, 293-303.

Sarbassov, D.D., Guertin, D.A., Ali, S.M., and Sabatini, D.M. (2005). Phosphorylation and regulation of Akt/PKB by the Rictor-mTOR complex. Science *307*, 1098-1101.

Shao, Y., and Aplin, A.E. (2010). Akt3-mediated resistance to apoptosis in B-RAF-targeted melanoma cells. Cancer Research *70*, 6670-6681.

Shi, H., Hong, A., Kong, X., Koya, R.C., Song, C., Moriceau, G., Hugo, W., Yu, C.C., Ng, C., Chodon, T.*, et al.* (2014). A novel AKT1 mutant amplifies an adaptive Melanoma response to BRAF inhibition. Cancer Discovery *4*, 69-79.

Stahl, J.M., Sharma, A., Cheung, M., Zimmerman, M., Cheng, J.Q., Bosenberg, M.W., Kester, M., Sandirasegarane, L., and Robertson, G.P. (2004). Deregulated Akt3 activity promotes development of malignant melanoma. Cancer Research *64*, 7002-7010.

Steel, K.P., Davidson, D.R., and Jackson, I.J. (1992). TRP-2/DT, a new early melanoblast marker, shows that steel growth factor (c-kit ligand) is a survival factor. Development *115*, 1111-1119.

Toker, A. (2012). Achieving specificity in Akt signaling in cancer. Advances in Biological Regulation *52*, 78-87.

Tschopp, O., Yang, Z.-Z., Brodbeck, D., Dummler, B.A., Hemmings-Mieszczak, M., Watanabe, T., Michaelis, T., Frahm, J., and Hemmings, B.A. (2005). Essential role of protein kinase Bγ (PKBγ/Akt3) in postnatal brain development but not in glucose homeostasis. Development *132*, 2943-2954.

Turner, K.M., Sun, Y., Ji, P., Granberg, K.J., Bernard, B., Hu, L., Cogdell, D.E., Zhou, X., Yli-Harja, O., Nykter, M.*, et al.* (2015). Genomically amplified Akt3 activates DNA repair pathway and promotes glioma progression. Proceedings of the National Academy of Sciences *112*, 3421-3426.

VanBrocklin, M.W., Robinson, J.P., Lastwika, K.J., Khoury, J.D., and Holmen, S.L. (2010). Targeted delivery of NRASQ61R and Cre-recombinase to post-natal melanocytes induces melanoma in Ink4a/Arflox/lox mice. Pigment Cell & Melanoma Research *23*, 531-541.

Von Werder, A., Seidler, B., Schmid, R.M., Schneider, G., and Saur, D. (2012). Production of avian retroviruses and tissue-specific somatic retroviral gene transfer in vivo using the RCAS/TVA system. Nature Protocols *7*, 1167-1183.

Wang, D., Zeesman, S., Tarnopolsky, M.A., and Nowaczyk, M.J.M. (2013). Duplication of AKT3 as a cause of macrocephaly in duplication 1q43q44. American Journal of Medical Genetics Part A *161*, 2016-2019.

Yang, J., Cron, P., Thompson, V., Good, V.M., Hess, D., Hemmings, B.A., and Barford, D. (2002). Molecular mechanism for the regulation of protein kinase B/Akt by hydrophobic motif phosphorylation. Molecular Cell *9*, 1227-1240.

Zhou, G.-L., Tucker, D.F., Bae, S.S., Bhatheja, K., Birnbaum, M.J., and Field, J. (2006). Opposing roles for Akt1 and Akt2 in Rac/Pak signaling and cell migration. Journal of Biological Chemistry *281*, 36443-36453.

Zhu, Y., Qiu, P., and Ji, Y. (2014). TCGA-Assembler: Open-source software for retrieving and processing TCGA data. Nature Methods *11*, 599-600.

Table 3.1 Average copy number (CN) of selected genes reveals *AKT3* gene amplification in brain metastatic and non-metastatic melanomas. The average CN with standard deviations are listed for several genes associated with AKT signaling in non-metastatic melanomas and brain metastasic melanomas. In both melanoma groups, average CN increase and decrease was observed for *AKT3* and *PTEN*, respectively. The *P* values from comparison statistics between the two groups are listed. Copy number data for melanomas were acquired from The Cancer Genome Atlas (TCGA) database.

	Non-metastaic (n = 67)		Brain metastatic (n =43)		Statistics
	average CN	stdev	Average CN	stdev	p value, T-test
PTEN	1.603	0.354	1.695	0.306	0.150
AKT1	1.945	0.340	1.928	0.293	0.779
AKT2	2.034	0.256	2.039	0.140	0.895
AKT3	2.362	0.494	2.383	0.420	0.819
PIK3CA	2.022	0.280	2.050	0.231	0.568
PHLPP1	2.070	0.313	2.023	0.388	0.501
PHLPP2	1.867	0.374	2.030	0.726	0.179

Table 3.2 Significant increase in *AKT3* gene expression in brain metastatic melanomas relative to non-metastatic melanomas. The normalized gene expression with standard deviations are listed for several genes associated with AKT signaling in non-metastatic melanomas (n=66) and brain metastatic melanomas (n=43). The *P* values from comparison statistics between the two groups are listed. Significant differences in expression are noted for several genes, including *AKT3* ($P = 0.00076$). Normalized gene expression data for melanomas were acquired from The Cancer Genome Atlas (TCGA) database.

	Non-metastatic (n=66)*		Brain metastatic (n=43)		Statistics
	Normalized Gene Expression	stdev	Normalized Gene Expression	stdev	p value, T-test
PTEN	1171.46	758.36	1561.13	868.37	0.01844
AKT1	6652.39	2844.78	5245.54	2564.87	0.00867
AKT2	3538.69	1303.62	3213.38	1153.78	0.17507
AKT3	1638.51	902.20	2299.37	1002.28	0.00076
PIK3CA	288.05	172.52	409.41	191.18	0.00116
PHLPP1	2051.17	1285.63	1678.07	970.01	0.08796
PHLPP2	168.55	88.05	226.31	135.40	0.01586

*TCGA-GN-A269 has no gene expression data.

Table 3.3 Summary of tumor formation. Tumor incidence, mean survival ± standard error of the mean (SEM) and percent of tumor-bearing mice with lung and brain metastasis are listed according to tumor genotype after viral delivery of genes.

Comparison of mouse melanomas				
Tumor Genotype	**Incidence**	**Mean survival ± SEM (days) of tumor mice**	**Lung Mets (%)**	**Brain Mets (%)**
Braf^{V600E}*;Cdkn2a*$^{-/-}$	47% (16/34)	88.9 ± 8.6	0	0
Braf^{V600E}*;Cdkn2a*$^{-/-}$ + myrAKT1	79% (15/19)	56 ± 5.7	18	13
Braf^{V600E}*;Cdkn2a*$^{-/-}$ + myrAKT2	100% (18/18)	40 ± 1.6	29	0
Braf^{V600E}*;Cdkn2a*$^{-/-}$ + myrAKT3	85% (11/13)	53 ± 6.8	20	55
Braf^{V600E}*;Cdkn2a*$^{-/-}$ + wtAKT1	89% (8/9)	74 ± 5.3	29	0
Braf^{V600E}*;Cdkn2a*$^{-/-}$ + wtAKT2	85% (17/20)	59 ± 3.8	0	0
Braf^{V600E}*;Cdkn2a*$^{-/-}$ + wtAKT3	70% (7/10)	69 ± 5.3	0	0

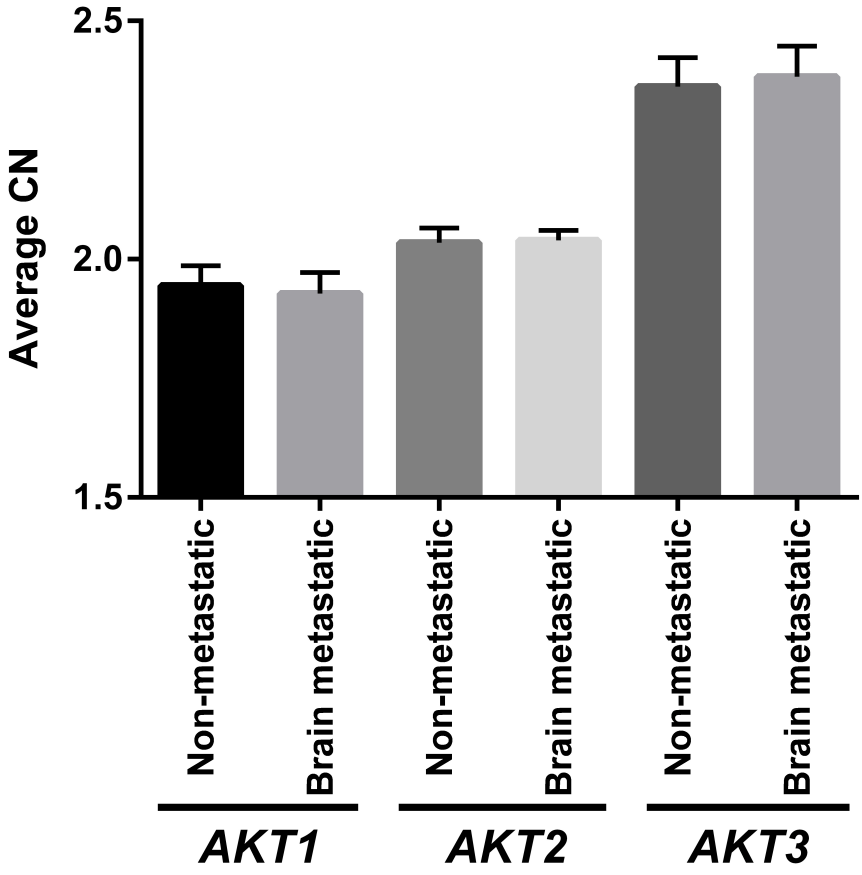

Figure 3.1 Increased average copy number (CN) for AKT3 in melanoma but no significant difference in average CN for AKT isoforms between non-metastatic and brain metastatic melanomas. Average CN for non-metastatic melanomas (No NTE; n=67) are compared side-by-side with average CN for brain metastatic melanomas (Brain met; n=43). Error bars represent the standard error of the mean (SEM). Copy number data for melanomas were acquired from The Cancer Genome Atlas (TCGA) database.

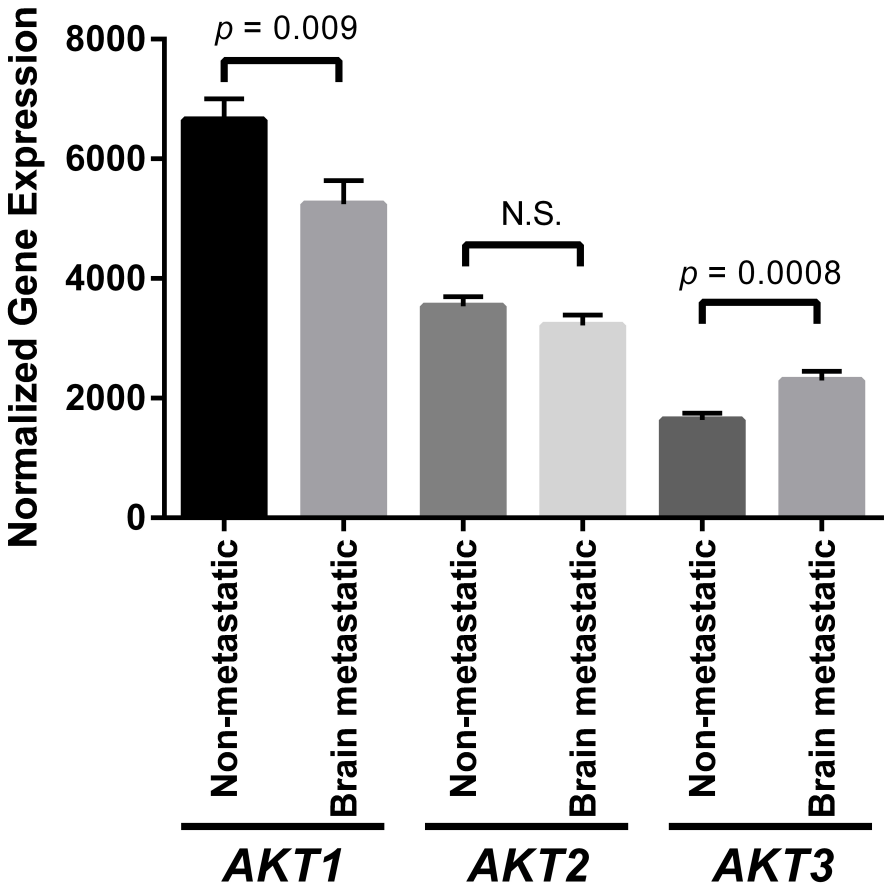

Figure 3.2 Significant increase in *AKT3* gene expression between non-metastatic and brain metastatic melanomas. Normalized gene expression for non-metastatic melanomas (No NTE; n=66) are compared side-by-side with normalized gene expression for brain metastatic melanomas (Brain met; n=43). *AKT3* gene expression is significantly higher (P = 0.0008) in brain metastatic melanomas compared to non-metastatic melanomas. \Brain metastatic melanomas have significantly decreased (P = 0.009) *AKT1* gene expression compared to non-metastatic melanomas. The difference in *AKT2* gene expression between the two melanoma groups was not significant (N.S.). Error bars represent the standard error of the mean (SEM). Copy number data for melanomas were acquired from The Cancer Genome Atlas (TCGA) database.

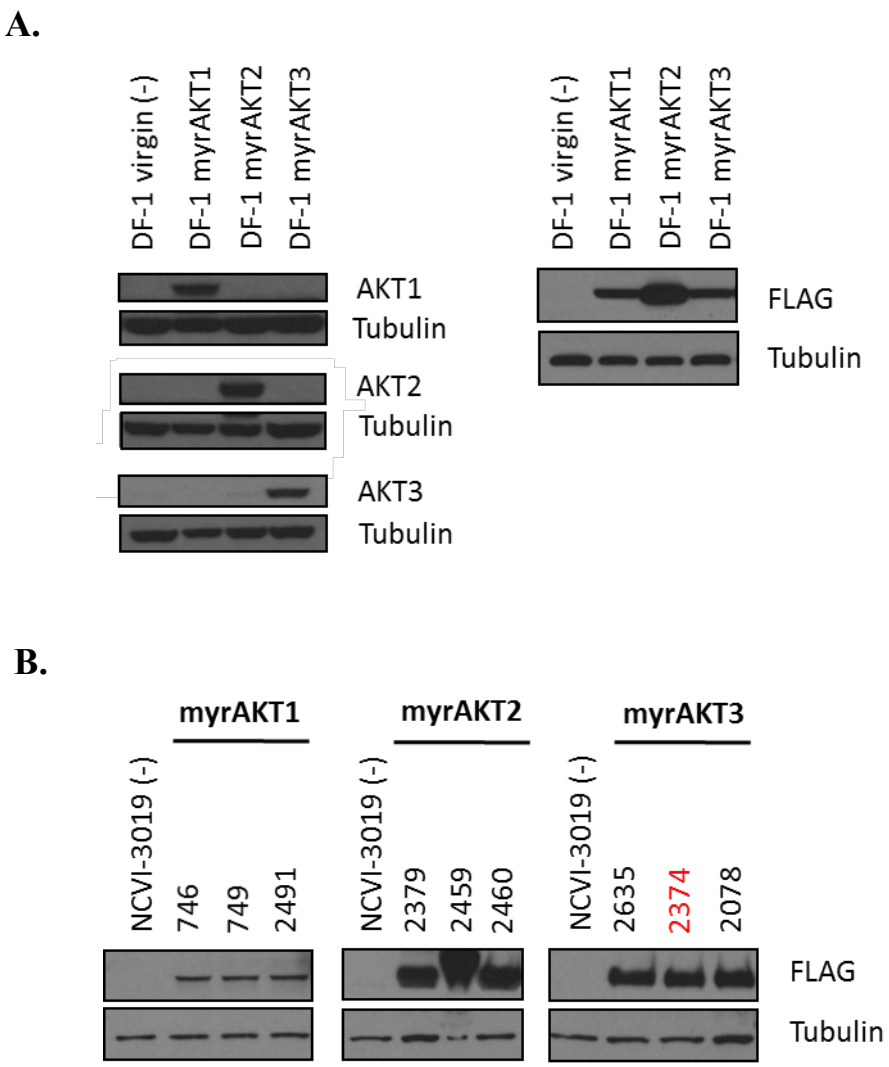

Figure 3.3 Expression of activated AKT isoforms in DF-1 cells and melanomas. A: Expression of myrAKT1, myrAKT2 and myrAKT3 was assessed in respectively infected DF-1 cells using AKT isoform-specific and FLAG antibodies. B: Expression of myrAKT1, myrAKT2 and myrAKT3 was assessed in tumors induced by injection of RCASBP(A) *Cre* and respective myr*AKT* isoform viruses. Virally delivered myrAKT1, myrAKT2 and myrAKT3 expression was detected with an antibody to the FLAG epitope tag on the myrAKT isoforms. Tubulin expression was used as a loading control. *Note: Sample 2374 was mistakenly classified as a myrAKT3 melanoma instead of a myrAKT2 melanoma.*

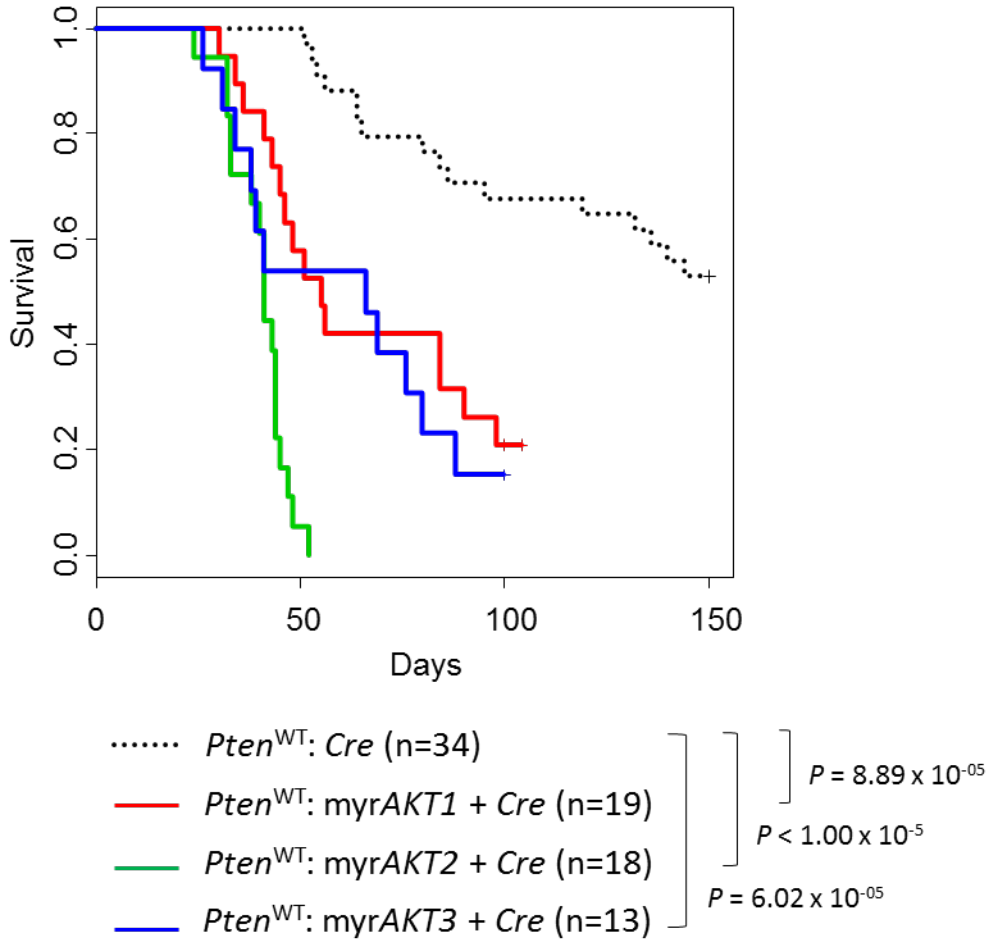

Figure 3.4 Kaplan-Meier percent survival curves demonstrate that expression of activated AKT isoforms significantly increases tumor incidence and reduces tumor latency. *Dct::TVA;Braf* ^{CA};*Cdkn2a*$^{lox/lox}$ mice (*Pten*^{WT}) were injected at birth with either *Cre* (small dashed line n = 34), myr*AKT1* and *Cre* (red line n = 19), myr*AKT2* and *Cre* (green line n = 18), or myr*AKT3* and *Cre* (blue line n = 13) containing viruses as indicated. Significant differences were observed between the survival of *Pten*^{WT} mice injected with *Cre* containing viruses and the following: *Pten*^{WT} mice injected with myr*AKT1* and *Cre* containing viruses (P = 8.89 x 10^{-5}), *Pten*^{WT} mice injected with myr*AKT2* and *Cre* containing viruses (P < 1 x 10^{-5}), and *Pten*^{WT} mice injected with myr*AKT3* and *Cre* containing viruses (P = 6.02 x 10^{-5}).

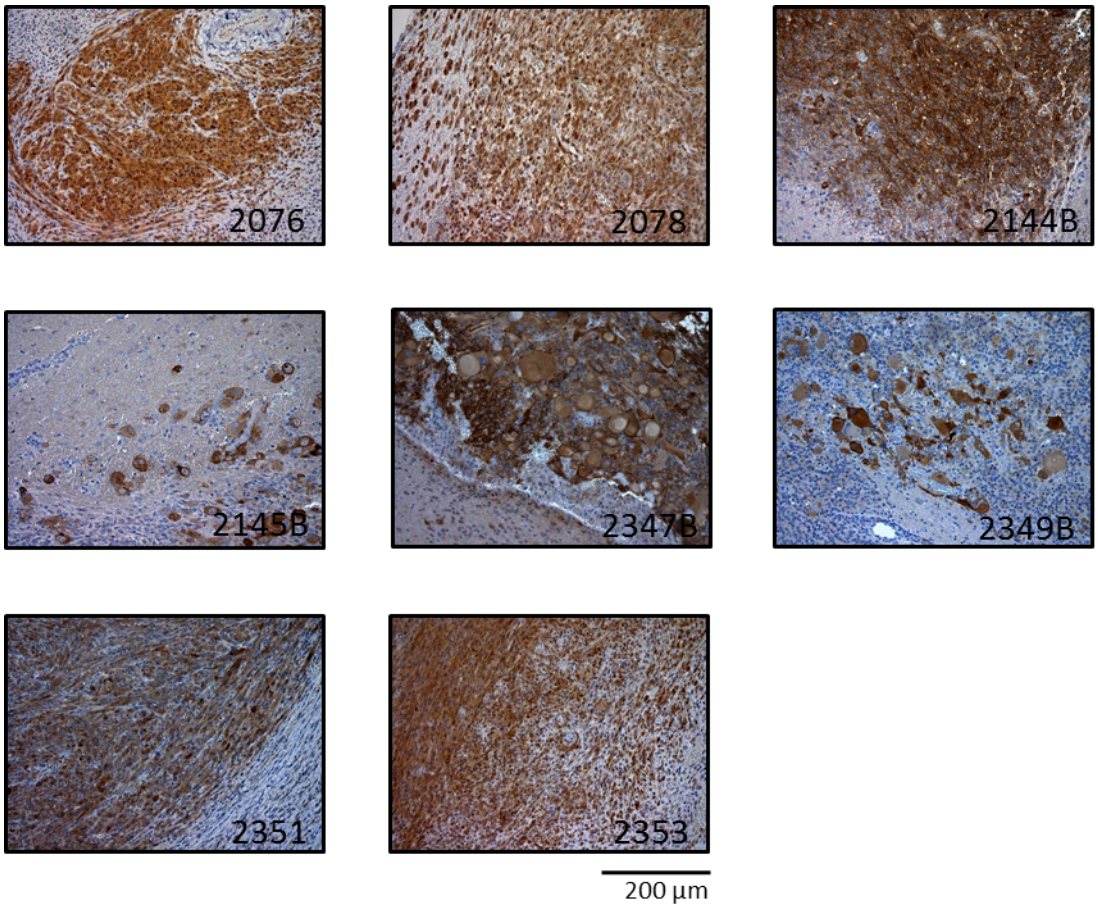

Figure 3.5 Robust activation of AKT in melanomas of *Dct::TVA;Braf*$^{CA/CA}$*;Cdkn2a*$^{lox/lox}$ mice (*Pten*^{WT}) injected with myr*AKT3* and *Cre* containing viruses. Representative P-AKT (pS473) IHC staining is shown from melanomas induced by injecting *Pten*^{WT} with myr*AKT3* and *Cre* containing viruses. Tumors are shown by mouse ID number. The letter B next to the mouse ID indicates the image is a brain metastasis. Tumor tissues were unavailable from the following experimental mice: 2141, 2348, and 2635. Scale bar represents 200 μm.

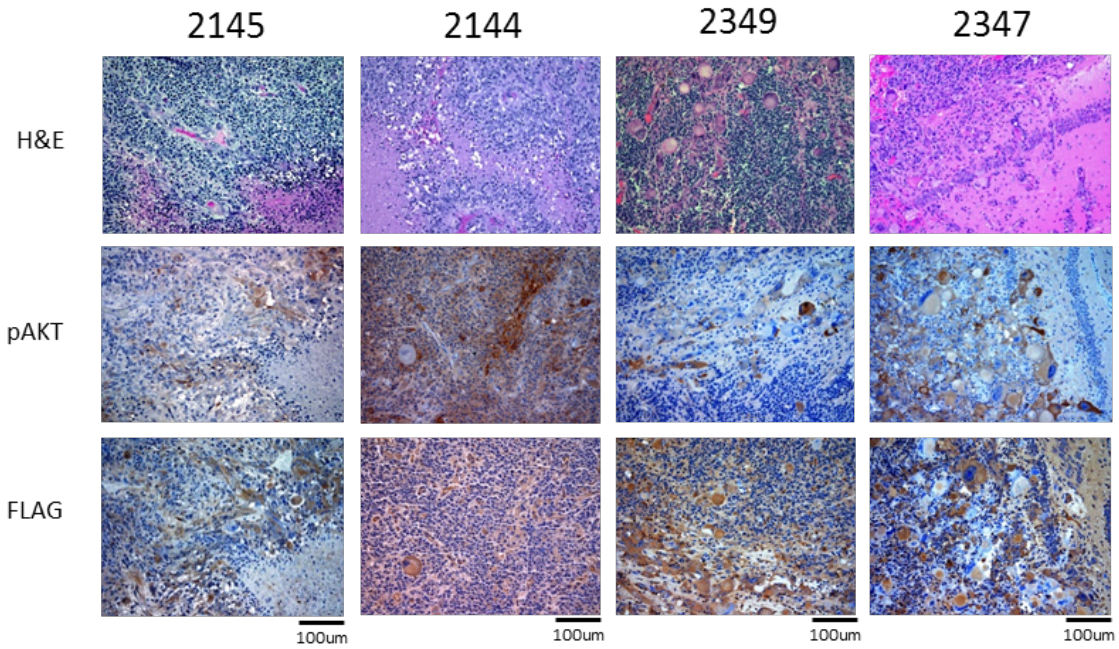

Figure 3.6 AKT activity in myrAKT3 driven melanoma brain metastases. The row of images representative H&E of the melanoma brain metastases. Mouse ID numbers are written above the images. The middle row of images show P-AKT (pS473) IHC staining of an adjacent section. The bottom row are adjacent sections probed for FLAG by IHC staining to confirm the presence of myrAKT3. Scale bar represents 200 μm.

Figure 3.7 AKT activity in melanomas of *Dct::TVA;Braf*$^{CA/CA}$*;Cdkn2a*$^{lox/lox}$ mice (*Pten*^{WT}) injected with myr*AKT1* and *Cre* containing viruses. Representative P-AKT (pS473) IHC staining is shown from melanomas induced by injecting *Pten*^{WT} with myr*AKT1* and *Cre* containing viruses. Tumors are shown by mouse ID number. Scale bar represents 200 μm. *Note: Mouse 2492 developed a tumor after 100 days (experimental endpoint) and was thus considered negative when calculating tumor incidence. P-AKT IHC for tumor mouse 2942 is shown.*

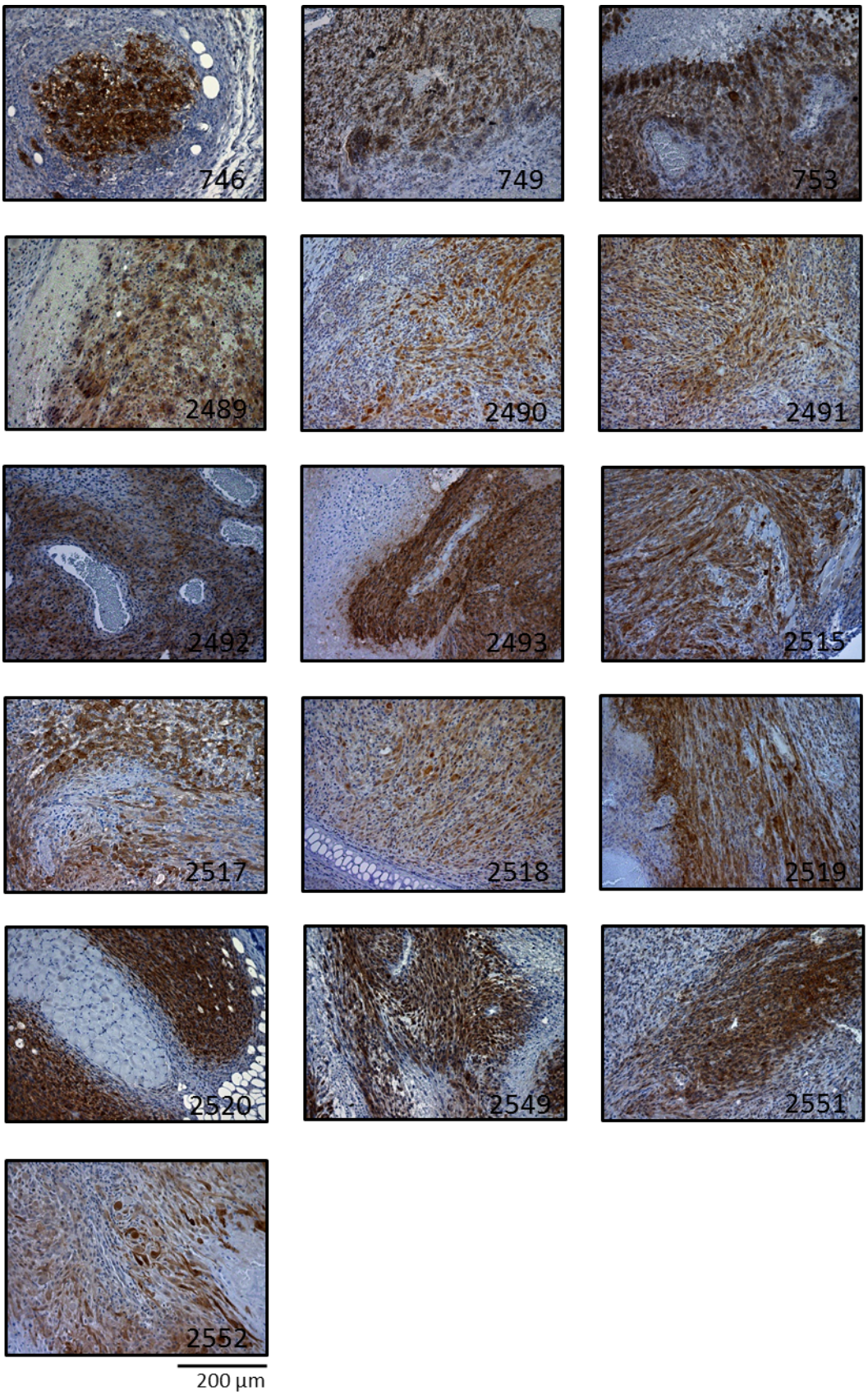
746
749
753
2489
2490
2491
2492
2493
2515
2517
2518
2519
2520
2549
2551
2552
200 µm

Figure 3.8 AKT activity in melanomas of *Dct::TVA;Braf*$^{CA/CA}$*;Cdkn2a*$^{lox/lox}$ mice (*Pten*^{WT}) injected with myr*AK2* and *Cre* containing viruses. Representative P-AKT (pS473) IHC staining is shown from melanomas induced by injecting *Pten*^{WT} with myr*AKT2* and *Cre* containing viruses. Tumors are shown by mouse ID number. Tumor tissues were unavailable from the following experimental mice: 2375, 2462, and 2471. Scale bar represents 200 μm.

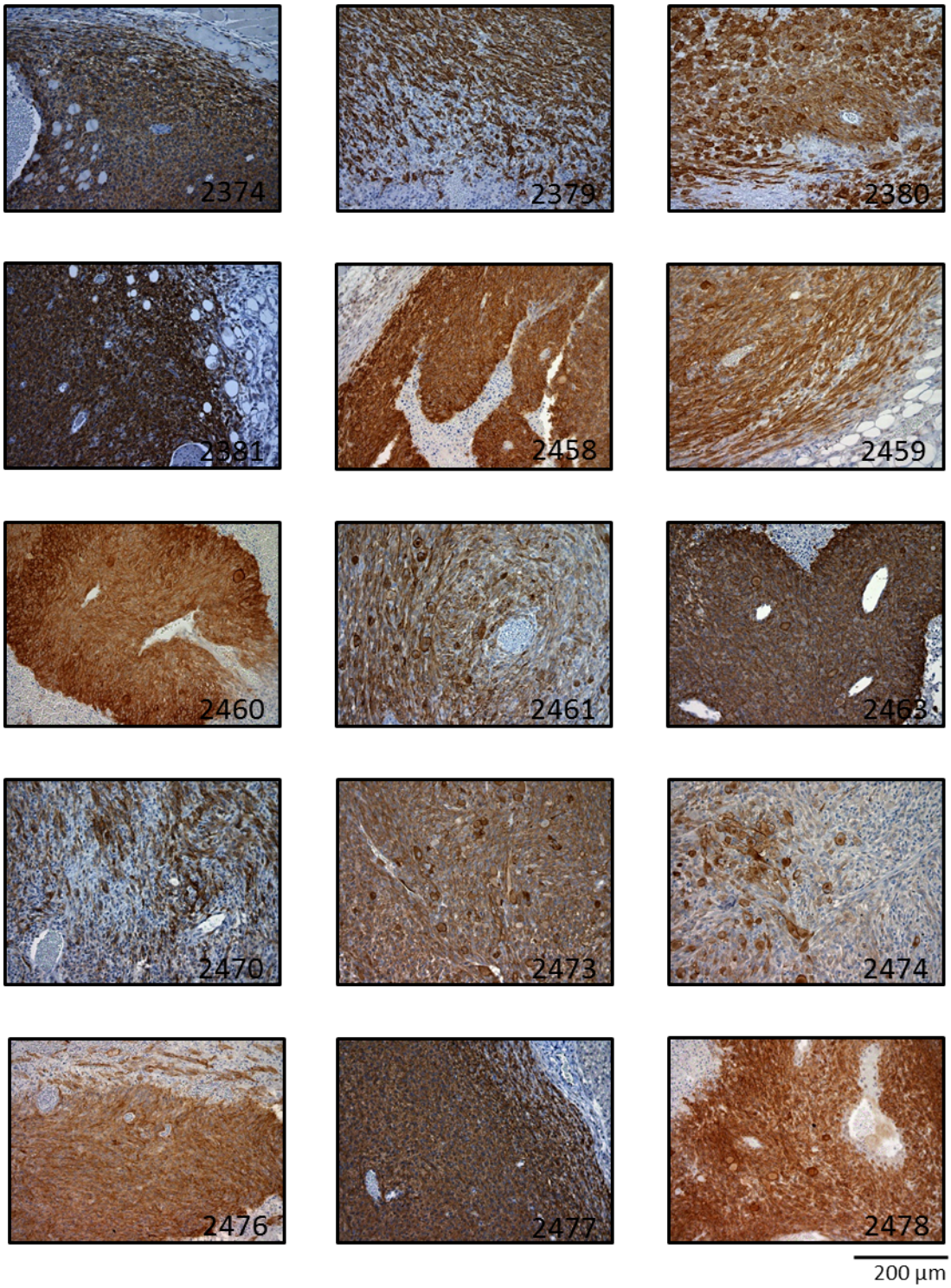
2374
2379
2380
2381
2458
2459
2460
2461
2463
2470
2473
2474
2476
2477
2478
200 µm

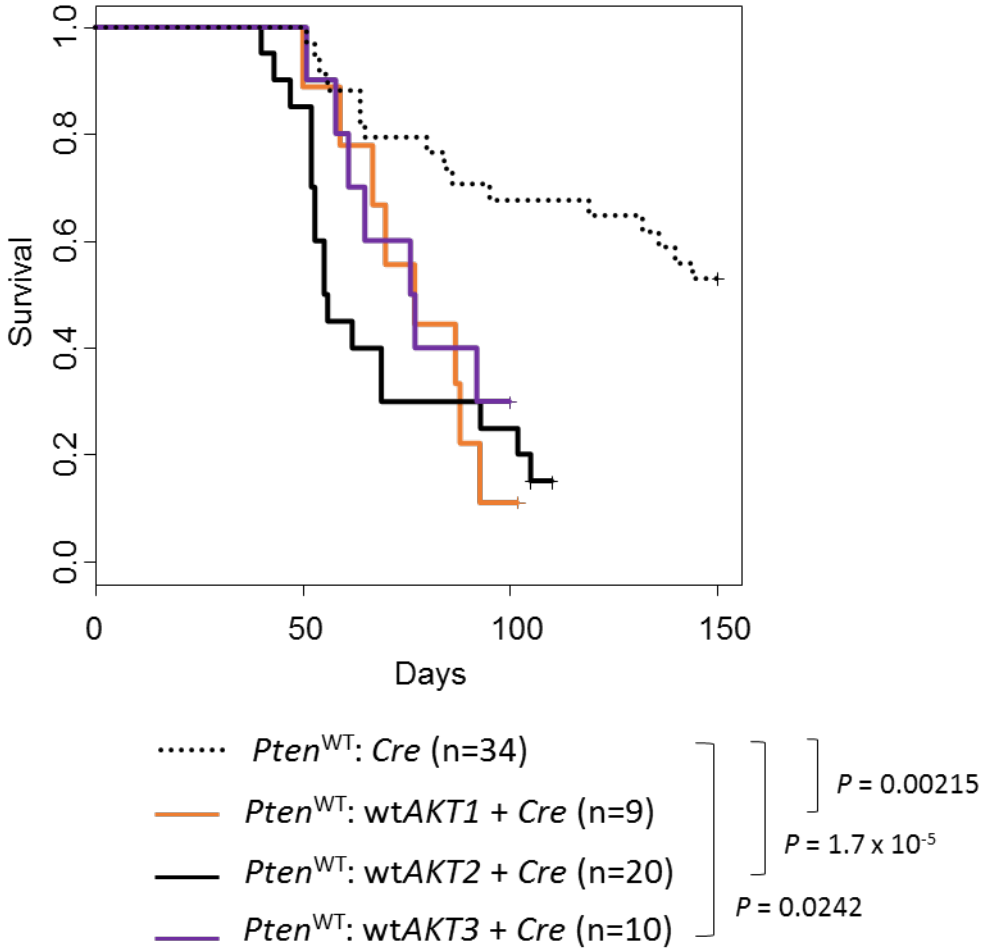

Figure 3.9 Kaplan-Meier percent survival curves demonstrate that expression of wild-type AKT isoforms significantly increases tumor incidence. *Dct::TVA;Braf*^{CA};*Cdkn2a*$^{lox/lox}$ mice (*Pten*^{WT}) were injected at birth with either *Cre* (small dashed line n = 34), wt*AKT1* and *Cre* (orange line n = 9), wt*AKT2* and *Cre* (solid black line n = 20), or wt*AKT3* and *Cre* (blue line n = 10) containing viruses as indicated. Significant differences were observed between the survival of *Pten*^{WT} mice injected with *Cre* containing viruses and the following: *Pten*^{WT} mice injected with wt*AKT1* and *Cre* containing viruses ($P = 0.00215$), *Pten*^{WT} mice injected with wt*AKT2* and *Cre* containing viruses ($P = 1.7 \times 10^{-5}$), and *Pten*^{WT} mice injected with wt*AKT3* and *Cre* containing viruses ($P = 0.0242$).

CHAPTER 4

AKT3^{E17K} PROMOTES MELANOMA LUNG METASTASES

4.1 Introduction

Melanoma is not only the most aggressive form of skin cancer, it also boasts one of the highest average mutation burdens amongst all cancer types (Alexandrov et al., 2013). Large-scale sequencing studies reveal that genetic alterations in melanoma are not entirely random and instead implicate specific cellular pathways in the initiation and progression of this malignancy (Hodis et al., 2012; Krauthammer et al., 2012). Recent breakthroughs in melanoma therapy with targeted inhibitors have defined driver mutations in this disease (Chapman et al., 2011; Flaherty et al., 2012; Hodis et al., 2012). Thus, melanoma's genomic mutational landscape shapes our current understanding of the disease and continues to hold mechanistic secrets.

The AKT pathway is aberrantly activated in up to 70% of melanomas (Davies et al., 2009a; Smalley, 2009). Genomic alterations that contribute to increased AKT signaling in melanoma range from activating mutations and gene copy number amplification in AKT itself to gene deletions, inactivating mutations and DNA hypermethylation in other genes involved in the pathway. Melanomas acquire activating mutations in *NRAS* and *PIK3CA,* two positive AKT regulators, in 15-25% and 1-2% of

cases, respectively (Davies and Samuels, 2010). The negative AKT regulator, Phosphatase and tensin homolog (PTEN), is silenced by gene deletion, truncating mutations or inactivating mutations in 10-30% of melanomas. PHLPP1, a phosphatase that selectively deactivates AKT2 and AKT3, is suppressed at the gene expression level in melanoma by a mechanism that involves DNA methylation and promoter-specific inhibition (Dong et al., 2014). Finally, isoforms of AKT are known to acquire activating mutations (1-2%) as well as increased copy number in melanoma (Bastian et al., 1998; Davies et al., 2008). These genomic changes contributing to AKT activation highlight the significance of activated AKT in melanoma.

Aberrant AKT activation is strongly implicated in driving melanoma progression and brain-specific metastasis (Dai et al., 2005; Davies et al., 2009b). The overexpression of AKT in a radially growing melanoma cell line confers an invasive, vertical growth phenotype when implanted in mice (Govindarajan et al., 2007). Clinical biopsies reveal that melanoma brain metastases have significantly higher levels of activated AKT compared with melanoma lung and liver metastases (Davies et al., 2009b; Niessner et al., 2013). Follow-up studies comparing patient-matched brain versus extra-cranial melanoma metastases confirmed increased AKT activity as a specific feature of brain metastasis (Chen et al., 2014). We recently demonstrated that expression of activated AKT1 in a non-metastatic *in vivo* model of PTEN-null melanoma is sufficient to promote brain metastases at an incidence of 79% (Chapter 2). Furthermore, activated AKT3 expression in a non-metastatic *in vivo* model of PTEN wild-type melanoma yields brain metastases in 55% of animals (Chapter 3). These data firmly establish the importance of activated AKT in melanoma metastasis; however, the question remains as to what is "activated AKT" and what level of

activation is required?

Phosphorylation of AKT at key residues is required for full activation of this kinase (Datta et al., 1999; Toker, 2012). These residues, known as threonine 308 and serine 473, are phosphorylated by PDK-1 and mTORC2, respectively (Alessi et al., 1997; Sarbassov et al., 2005). Phosphorylation at these two sites locks AKT into a catalytically active conformation and is rate limited by the recruitment of AKT to the cellular membrane (Andjelkovic et al., 1997; Bellacosa et al., 1998; Yang et al., 2002). The affinity of the pleckstrin homology (PH) domain of AKT for phosphatidylinositol-3,4,5-triphosphate (PIP3) on the inner leaflet of the cellular membrane promotes AKT recruitment to the membrane and induces a conformational change in AKT that facilitates the activating phosphorylation events (Toker, 2012). PIP3 levels are regulated by two key enzymes, Phosphatidylinositol-4,5-bisphosphate 3-kinase (PI3K) and PTEN (Chalhoub and Baker, 2009). PI3K converts phosphatidylinositol-4,5-bisphosphate (PIP_2) to PIP3 while PTEN is a phosphatase that drives the reverse reaction and decreases the levels of PIP3. In this way, PI3K and PTEN act in an antagonistic fashion in terms of regulating AKT signaling. Once AKT is activated by phosphorylation, it disperses to a variety of cellular locations including the cytoplasm, nucleus, and mitochondria where it acts on downstream effectors (Toker, 2012).

The PH domain of AKT is critical for AKT membrane recruitment and activation (Andjelkovic et al., 1997; Bellacosa et al., 1998). The binding of PIP3 to the PH domain of AKT is driven by ionic interactions between the negatively charged PIP3 phosphate groups and the positively charged residues found in the PH domain (Thomas et al., 2002). Deletion of the PH domain abolishes binding to PIP3, results in loss of membrane

targeting and reduced AKT activation (Andjelkovic et al., 1997; Thomas et al., 2002). Conversely, replacing the PH domain with a myristoylation sequence is sufficient to rescue AKT membrane recruitment and subsequent activation (Aoki et al., 1998; Kohn et al., 1996). Furthermore, certain mutations in the PH domain of AKT are associated with constitutive AKT activation (Carpten et al., 2007; Parikh et al., 2012; Shi et al., 2014).

The most notable AKT PH domain mutation is a substitution of glutamate to lysine at the 17th amino acid residue (E17K), which changes the PH domain conformation, induces aberrant subcellular localization, and increases AKT activity in an oncogenic, transformative manner (Carpten et al., 2007). The E17K mutation is found in all three AKT isoforms and is associated with a variety of clinical pathologies, including melanoma (Davies et al., 2008; Hussain et al., 2011; Lindhurst et al., 2011; Shi et al., 2014). Given the prominent role of AKT hyper-activation in melanomagenesis, it is not surprising that E17K mutations in AKT1 and AKT3 are found in 1-2% of melanomas (Davies et al., 2008). These AKT mutations are anecdotally associated with melanoma brain metastasis and drug-resistance mechanisms; however, *in vivo* functional studies have yet to be conducted (Davies et al., 2009a; Shi et al., 2014).

Our previous work demonstrated that activated AKT3 is sufficient to promote metastases to the brain and lung in an established non-metastatic, mouse model of melanoma (Chapter 3). We expressed human myristoylation sequence tagged (myr)AKT3 in *Braf*^{V600E}*;Ink4a/Arf*-null melanomas and observed brain metastasis in 55% (6/11) of the mice. In the current study, we set out to determine the role of AKT3^{E17K} in melanoma formation and metastasis. Using our established non-metastatic mouse models of melanoma driven by BRAF^{V600E}; INK4A/ARF loss, we tested tumor incidence,

growth, organ-specific metastasis, and overall survival of mice with melanomas expressing $AKT3^{E17K}$.

4.2 Materials and Methods

4.2.1 Generation of DCT::TVA;$Braf^{CA}$;$Ink4a/Arf^{lox/lox}$ mice. Previously, we described a murine model of melanoma based on the RCAS/TVA retroviral vector system, which allows for tissue- and cell-specific infection of mammalian cells through ectopic expression of the viral receptor (VanBrocklin et al., 2010; von Werder et al., 2012). This system utilizes a viral vector, RCASBP(A), derived from the avian leukosis virus (ALV). The receptor for RCASBP(A) is encoded by the TVA gene and is normally expressed in avian cells. Transgenic mice expressing TVA under the control of the Dopachrome tautomerase (DCT) promoter, which allow specific targeting of melanocytes (Dunn et al., 2000; Steel et al., 1992), were crossed with *Ink4a/Arf* $^{lox/lox}$ mice (Aguirre et al., 2003) and mice carrying a Cre-activated allele of *Braf* (*$Braf^{CA}$*) (Dankort et al., 2007b) to generate DCT::TVA;*$Braf^{CA}$*;*Ink4a/Arf* $^{lox/lox}$ mice. In the absence of Cre, the *$BRaf^{CA}$* allele expresses wild-type BRAF. Following Cre-mediated recombination, $BRAF^{V600E}$ is expressed at physiological levels and undergoes normal differential exon usage and alternative splicing (Dankort et al., 2007b). Exons 2 and 3 of the *Ink4a/Arf* locus are flanked by *LoxP* sites such that in the absence of Cre, these mice express normal levels of $p16^{INK4A}$ and $p19^{ARF}$. Cre-mediated excision eliminates functional *$p16^{Ink4a}$* and *$p19^{Arf}$* (Aguirre et al., 2003). DNA from tail biopsies were genotyped by PCR for the *Dct::TVA* transgene, *$Cdkn2a^{lox}$,* and BrafCA and wild-type alleles as previously described (Dankort et al., 2007a; VanBrocklin et al., 2010).

4.2.2 Construction of RCASBP(A) viral vector containing AKT3^{E17K}. The retroviral vectors in this study are replication-competent ALV, Bryan polymerase-containing vectors of envelope subgroup A [designated RCASBP(A)]. The RCASBP(A) vector is Gateway compatible allowing for efficient transfer of DNA into the retroviral vector (Loftus et al., 2001). To construct RCASBP(A) HA-*AKT3*^{E17K}, we employed PCR-based site-directed mutagenesis to create a transition at the 49th base of *AKT3* cDNA (a gift from Wei Zhang) from guanine to alanine. A hemagglutinin (HA) epitope encoding sequence was placed at the N-terminus of *AKT3*. The HA-*AKT3*^{E17K} cDNA was cloned into a pCR8 entry vector and verified for correct sequence and orientation. The *att*L sites flanking the 5′ and 3′ ends of the HA-*AKT3*^{E17K} cDNA in the pCR8 vector allowed efficient transfer of the transgene into the RCASBP(A) vector containing *att*R sites upon incubation with a cocktail of bacteriophage lambda and *E. coli* enzymes (LR Clonase II; Invitrogen, Waltham, MA USA) yielding RCASBP(A) HA-*AKT3*^{E17K}.

4.2.3 Production of infectious RCASBP(A) HA-AKT3^{E17K} virus. DF-1 chicken fibroblasts were grown at 39°C in DMEM-high glucose media (Invitrogen) supplemented with 10% FBS. Viral infection of RCASBP(A) HA-*AKT3*^{E17K} was initiated by calcium phosphate transfection of plasmid DNA into DF-1 cells. Viral spread was monitored by GFP positive control transfection and viral expression of AKT3^{E17K} was validated by Western blot. Viral infectivity was confirmed by inoculating TVA-expressing C3 murine melanocytes with filtered (0.45 μm filter) supernatant from RCASBP(A) HA-*AKT3*^{E17K} infected DF-1 cells in the presence of 8 μg/mL polybrene.

4.2.4 Injection of DCT::TVA;Braf^{CA};Ink4a/Arf$^{lox/lox}$ neonatal mice with RCASBP(A) AKT3^{E17K} and Cre viruses. Infected DF-1 cells were trypsinized, pelleted,

and resuspended in 50 μL Hank's balanced salt solution (HBSS; Invitrogen). The viral-producing cells were subcutaneously injected behind the ears of newborn mice between postnatal day 1 and postnatal day 5. Mice received a total of 100 μL of suspended RCASBP(A) *AKT3*^{E17K} cells and 100 μL of suspended RCASBP(A) *Cre* cells over two rounds of injection. Mice were then monitored daily for tumor development.

4.2.5 RT-PCR validation of AKT3^{E17K} expression in primary mouse tumors. To assess gene expression of *AKT3*^{E17K} in primary mouse tumors, total RNA was extracted from mouse primary tumors using TRIzol reagent (Invitrogen, Waltham, MA USA) and chloroform. Precipitated nucleic acid was column purified using RNEasy Mini Kit (Qiagen, Hilden, Germany). SuperScript III First-Strand Synthesis System (Invitrogen, Waltham, MA USA) was employed to synthesize cDNA from total RNA. PCR reactions were set up using EconoTaq Plus Green 2x Master Mix (Lucigen, Middleton, WI USA). The forward PCR primer was as follows: 5′-GGTGGAGGACCAGATGATGCAAAAG-3′ and designed to anneal within the *AKT3*^{E17K} cDNA. The reverse PCR primer was as follows: 5′-GAAAGCTGGGTCTAGATTATTCTCGTCCAC-3′ and specifically complemented the 3′ end of the *AKT3*^{E17K} transgene and the *att*B2 site from the RCASBP(A) vector. The expected PCR amplicon from this reaction was 289bp.

4.2.6 Hematoxylin and eosin staining of mouse melanomas, coronal brain sections, and lungs. Mouse tissues were fixed in 10% neutral buffered formalin overnight, cut into three sections, and then dehydrated in 70% ethyl alcohol. Tissues were paraffin-embedded, sectioned at a thickness of 4μm, and placed on glass slides. Sections were stained with Hematoxylin and Eosin (H&E) or left unstained for immunohistochemistry.

4.2.7 Expression of AKT3^{E17K} by Immunohistochemistry (IHC) staining for HA in primary mouse tumors. Tissue sections were hydrated and deparaffinized. Antigen retrieval was performed by boiling sections in 1× Rodent Decloaker buffer (Biocare Medical, Concord, CA USA) for 20 minutes in a Decloaking Chamber (Biocare Medical). Endogenous peroxidase activity was quenched by incubating sections in 3% hydrogen peroxide for 10 minutes. Sections were then blocked in Rodent Block (Biocare Medical) for 30 minutes. The HA-tagged, exogenous AKT3^{E17K} was detected using a primary antibody to the HA epitope (HA.11, Covance, Princeton, NJ USA), diluted 1:1000 in Renaissance Background Reducing Diluent (Biocare Medical). Sections were incubated overnight at 4°C and probed with Mouse on Mouse HRP polymer reagent (Biocare Medical). Visualization was carried out with DAB (Biocare Medical). All sections were counterstained with hematoxylin.

4.2.8 Statistical analysis. Censored survival data was analyzed using R software to calculate a log-rank test of the Kaplan-Meier estimate of survival.

4.2.9 Study approval. All animal experimentation was performed in AAALAC approved facilities at the University of Utah. All animal protocols were reviewed and approved prior to experimentation by the Institutional Animal Care and Use Committee at the University of Utah.

4.3 Results

4.3.1 Expression of AKT3^{E17K} promotes BRAF^{V600E}/INK4A-ARF^{Null} melanoma growth. We previously observed metastatic melanomas in 85% (11/13) of DCT::TVA;*Braf*^{CA};*Ink4a/Arf* $^{lox/lox}$ (*Pten*^{WT}) mice co-injected with RCASBP(A) *Cre* and

myr*AKT3* viruses (Chapter 3; Figure 4.1). In addition to primary tumors at the site of injection, these mice also developed brain and lung metastases in 55% and 20% of the tumor-bearing mice, respectively (Chapter 3). We chose to extend our study of aberrant AKT3 signaling in melanomagenesis by testing whether expression of mutant $AKT3^{E17K}$ enhances $BRAF^{V600E}$/INK4A-ARF^{Null} melanoma initiation, growth, or metastasis similarly to our observations with myrAKT3 expression. Neonatal $Pten^{WT}$ mice were co-injected with infectious RCASBP(A) *Cre* and RCASBP(A) $AKT3^{E17K}$ viruses (Figure 4.2A, B). Tumors developed at the injection site in 69% (9/13) of injected $Pten^{WT}$ mice. It is important to note that $AKT3^{E17K}$ expression is not required for tumor formation in the context of $BRAF^{V600E}$/INK4A-ARF silencing as tumors develop in nearly half of *Dct::TVA; Braf* ^{CA}; $Cdkn2a^{lox/lox}$ mice infected with viruses encoding *Cre* alone (Chapter 2; Figure 4.1). Of the nine tumor-bearing mice, eight had tumors with confirmed expression of $AKT3^{E17K}$ (Figure 4.3A, B). The mean survival for the confirmed $AKT3^{E17K}$ cohort was 73.6 ± 7.2 days (Table 4.1). Compared to $Pten^{WT}$ mice injected with *Cre* virus alone, the $AKT3^{E17K}$ melanoma mice had significantly increased tumor incidence and decreased survival (P=0.007; Figure 4.1). Statistically significant differences in survival were not observed between $AKT3^{E17K}$ melanoma mice and myrAKT3 or wtAKT3 melanoma mice (Figure 4.1).

4.3.2 Expression of $AKT3^{E17K}$ in $BRAF^{V600E}$/$INK4A\text{-}ARF^{Null}$ melanomas yields highly metastatic lung disease. Upon euthanasia all major organs of the tumor-bearing mice were examined for melanoma metastases. Interestingly, metastatic melanoma cells were detected in the lungs of 100% (8/8) of the mice harboring melanomas with confirmed expression of $AKT3^{E17K}$ (Figure 4.4). In contrast, no lung lesions were

observed in the one *Cre* and *AKT3*^{E17K} injected tumor-bearing *Pten*^{WT} mouse without confirmed expression of AKT3^{E17K} (5168; not shown).

4.3.3 Brain metastases are not observed in Pten^{WT} mice with BRAF^{V600E}/INK4A-ARF^{Null} melanoma expressing AKT3^{E17K}. In contrast to BRAF^{V600E}/INK4A-ARF^{Null} melanomas expressing myrAKT3 that spontaneously metastasize to the brain in 55% of tumor-bearing mice, no brain metastases were observed in *Pten*^{WT} mice with BRAF^{V600E}/INK4A-ARF^{Null} melanoma expressing AKT3^{E17K} (0/8; Figure 4.5).

4.4 Discussion

The present study was conducted to determine the role of AKT3^{E17K} in melanoma growth and metastasis. The AKT signaling pathway plays a key role in cellular processes such as cell growth, metabolism, proliferation, and survival (Bellacosa et al., 2003; Gonzalez and McGraw, 2009; Xu et al., 2012). Melanoma is known to aberrantly activate this pathway to promote disease progression (Davies et al., 2009a; Smalley, 2009). E17K mutations in *AKT1* and *AKT3* occur in 1-2% of melanomas and represent one mechanism by which AKT activation occurs in this disease (Davies et al., 2008). We found that *in vivo* expression of AKT3^{E17K} in BRAF^{V600E}/INK4A-ARF^{Null} melanomas results in aggressive lung metastases in 100% of tumor-bearing mice. We initially hypothesized that AKT3^{E17K} would act similarly to myrAKT3 in BRAF^{V600E}/INK4A-ARF^{Null} melanomas; however, unlike the myr*AKT3* mice that frequently succumb to brain metastasis, no cranial lesions were observed in any of the tumor-bearing *AKT3*^{E17K} mice (0/8). This study, while still in progress, contributes to our current understanding of

mutant AKT3^{E17K} in melanomagenesis and promises to reveal more about the role of aberrant AKT signaling in melanoma metastasis.

Substitution of lysine in place of glutamate at the 17th amino acid position (E17K) creates a bona fide AKT activating mutation. In addition to melanomas, *AKT1*^{E17K} mutations are associated with ovarian, breast, colorectal, and lung cancers (Carpten et al., 2007; Malanga et al., 2008). Proteus syndrome is characterized by epithelial tissue over-growth of skin, connective tissue, brain, and other tissues (Lindhurst et al., 2011). Somatic mosaicism for *AKT1*^{E17K} mutation was detected in 26 out of 29 Proteus syndrome patients, suggesting this mutation and AKT activation plays a prominent role in driving the overgrowth phenotype. *AKT2*^{E17K} mutation has been reported in association with severe hypoglycemia and an asymmetrical left-sided overgrowth (Hussain et al., 2011). The hypoglycemia phenotype is consistent with AKT2 activation, given AKT2's established role in glucose metabolism (Cho et al., 2001; Garofalo et al., 2003). To date, melanoma is the only malignancy associated with *AKT3*^{E17K} mutations (Davies et al., 2008). *In vitro* studies demonstrate that the E17K mutation promotes AKT recruitment to the cell membrane where it is activated (Carpten et al., 2007). AKT1^{E17K} mutant protein shows much greater localization to the membrane over the wild-type protein. In addition, the E17K mutation also confers gain of function to AKT1. While AKT1^{E17K} is sufficient to rescue glucose metabolism in AKT2-null cells, wild-type AKT1 and AKT3 are incapable of this function (Gonzalez et al., 2009). Furthermore, AKT1^{E17K} expression in hematopoietic stem cells induces oncogenic transformation and leukemia when transduced into mice (Carpten et al., 2007).

Two mechanisms might explain how E17K mutations promote activation of AKT.

The 17th amino acid is located within PH domain of AKT, a domain that physically interacts via intermolecular forces with PIP3 on the cell membrane. One mechanism suggests that lysine substitution at the 17th position increases the electrostatic attraction between the PH domain and PIP3, thus facilitating AKT membrane localization and subsequent activation. Indeed, x-ray crystallography of mutant AKT1^{E17K} confirms enhanced binding of the PH domain with PIP3 and *in vitro* cell culture assays with E17K mutations in all three AKT isoforms demonstrate increased membrane localization and activation (Carpten et al., 2007; Davies et al., 2008; Hussain et al., 2011). An alternative mechanism suggests that the E17K mutation facilitates the opening up or unmasking of the catalytic domain of AKT. Prior to AKT activation, the PH domain interacts with the kinase domain of AKT and the 17th amino acid is located at the contacting interface of the two domains (Parikh et al., 2012). Mutations perturbing the PH domain–kinase domain interaction lead to increased AKT activation as measured by phosphorylation of threonine 308 and serine 473. In their landmark study, Carpten *et al.* interestingly noted that the activity of AKT1^{E17K} was unaffected by treatment with an AKT inhibitor that blocks membrane association and with PI3K inhibition, implying a mechanism of activation independent of PH domain-PIP3 interaction (Carpten et al., 2007). This phenomenon could be explained by the alternative mechanism where E17K mutations disrupt PH domain-kinase domain interactions and thereby enhance AKT activation. Given the evidence supporting both mechanisms and the nonmutual exclusivity of the two mechanisms, it is likely that both PH domain-PIP3 interactions are enhanced and PH domain-kinase domain interactions are disrupted in E17K mutations of AKT.

The *in vivo* functional consequence of AKT E17K mutant proteins in melanoma

development and progression is not well understood. We embarked on a study to test the role of AKT3^{E17K} in a BRAF^{V600E}/INK4A-ARF^{Null} mouse model of melanoma. Previously, we showed that AKT activation, specifically AKT1 and AKT3, promotes melanoma metastasis to the brain (Chapter 2, 3). Based on our previous results, we hypothesized that AKT3^{E17K} expressing BRAF^{V600E}/INK4A-ARF^{Null} melanomas would metastasize to the brain; however, this outcome was not observed and instead we observed highly aggressive lung tumors. The lung tumors appear to be metastatic lesions from the primary melanomas, but additional confirmatory evidence is required.

Clinically, *AKT1*^{E17K} mutations are also observed in melanomas. We are currently generating RCASBP(A) *Akt1*^{E17K} virus for injection along with RCASBP(A) *Cre* into DCT::TVA;*Braf*^{CA};*Ink4a/Arf*$^{lox/lox}$ to test the role of AKT1^{E17K} in the context of BRAF^{V600E}/INK4A-ARF^{Null} melanoma development and metastasis. We also observed in previous studies that *Pten* silencing cooperates with AKT activation in promoting melanoma brain metastasis (Chapter 2). We are currently testing the role of AKT3^{E17K} in BRAF^{V600E}/INK4A-ARF^{Null}/PTEN^{Null} melanoma development and metastasis. Future experiments will also test AKT1^{E17K} in this context.

The research presented in this chapter is a work in progress and should be considered in that context. Many control and follow-up experiments are required before any conclusions are drawn. A critical experiment yet to be conducted is determining whether the E17K mutation in AKT3 results in increased *in vivo* AKT activation in our melanoma model. Also of interest is a comparison of the differences in molecular targets between myrAKT3 and AKT^{E17K} expressing BRAF^{V600E}/INK4A-ARF^{Null} melanomas to determine why one leads to brain metastasis in 55% of mice while the other yields no

observable brain metastases. The highly aggressive lung lesions are of interest and will be followed-up, especially given that the lungs are one of the most frequent sites of melanoma metastasis (de la Monte et al., 1983). Overall, the research described in this chapter increases our understanding of mutant $AKT3^{E17K}$ in $BRAF^{V600E}$/INK4A-ARF^{Null} melanomas and reveals an unexpected aggressive phenotype which we will continue to investigate with on-going research.

4.5 Acknowledgments

The work described in this chapter was done with the help of James Robinson, Rowan Arave, Joyce Tross, Adam Welker, Sean Strain, Matthew VanBrocklin, and Sheri Holmen. J.P., M.V. and S.H. assisted with the experimental design. R.A. performed the immunohistochemistry. J.T. assisted with mouse husbandry. A.W and S.S. helped with acquiring lung and brain images.

4.6 References

Aguirre, A.J., Bardeesy, N., Sinha, M., Lopez, L., Tuveson, D.A., Horner, J., Redston, M.S., and DePinho, R.A. (2003). Activated Kras and Ink4a/Arf deficiency cooperate to produce metastatic pancreatic ductal adenocarcinoma. Genes & Development *17*, 3112-3126.

Alessi, D.R., James, S.R., Downes, C.P., Holmes, A.B., Gaffney, P.R.J., Reese, C.B., and Cohen, P. (1997). Characterization of a 3-phosphoinositide-dependent protein kinase which phosphorylates and activates protein kinase Bα. Current Biology *7*, 261-269.

Alexandrov, L.B., Nik-Zainal, S., Wedge, D.C., Aparicio, S.A.J.R., Behjati, S., Biankin, A.V., Bignell, G.R., Bolli, N., Borg, A., Borresen-Dale, A.-L.*, et al.* (2013). Signatures of mutational processes in human cancer. Nature *500*, 415-421.

Andjelkovic, M., Alessi, D.R., Meier, R., Fernandez, A., Lamb, N.J.C., Frech, M., Cron, P., Cohen, P., Lucocq, J.M., and Hemmings, B.A. (1997). Role of translocation in the activation and function of protein kinase B. Journal of Biological Chemistry *272*, 31515-

31524.

Aoki, M., Batista, O., Bellacosa, A., Tsichlis, P., and Vogt, P.K. (1998). The Akt kinase: Molecular determinants of oncogenicity. Proceedings of the National Academy of Sciences *95*, 14950-14955.

Bastian, B.C., LeBoit, P.E., Hamm, H., Bröcker, E.-B., and Pinkel, D. (1998). Chromosomal gains and losses in primary cutaneous melanomas detected by comparative genomic hybridization. Cancer Research *58*, 2170-2175.

Bellacosa, A., Chan, T.O., Ahmed, N.N., Datta, K., Malstrom, S., Stokoe, D., McCormick, F., Feng, J., and Tsichlis, P.N. (1998). Akt activation by growth factors is a multiple-step process: The role of the PH domain. Oncogene *17*, 313-325.

Bellacosa, A., Testa, J.R., moore, r., and Larue, L. (2003). A portrait of AKT kinases: human cancer and animal models depict a family with strong individualities. Cancer Biology & Therapy *3*, 268-275.

Carpten, J.D., Faber, A.L., Horn, C., Donoho, G.P., Briggs, S.L., Robbins, C.M., Hostetter, G., Boguslawski, S., Moses, T.Y., Savage, S.*, et al.* (2007). A transforming mutation in the pleckstrin homology domain of AKT1 in cancer. Nature *448*, 439-444.

Chalhoub, N., and Baker, S.J. (2009). PTEN and the PI3-Kinase pathway in cancer. Annual Review of Pathology: Mechanisms of Disease *4*, 127-150.

Chapman, P.B., Hauschild, A., Robert, C., Haanen, J.B., Ascierto, P., Larkin, J., Dummer, R., Garbe, C., Testori, A., Maio, M.*, et al.* (2011). Improved survival with vemurafenib in melanoma with BRAF V600E mutation. New England Journal of Medicine *364*, 2507 - 2516.

Chen, G., Chakravarti, N., Aardalen, K., Lazar, A.J., Tetzlaff, M., Wubberhorst, B., Kim, S.B., Kopetz, S., Ledoux, A., Vashisht Gopal, Y.N.*, et al.* (2014). Molecular profiling of patient-matched brain and extracranial melanoma metastases implicates the PI3K pathway as a therapeutic target. Clinical Cancer Research *20*, 5537-5546.

Cho, H., Mu, J., Kim, J.K., Thorvaldsen, J.L., Chu, Q., Crenshaw, E.B., Kaestner, K.H., Bartolomei, M.S., Shulman, G.I., and Birnbaum, M.J. (2001). Insulin resistance and a diabetes mellitus-like syndrome in mice lacking the protein kinase Akt2 (PKBβ). Science *292*, 1728-1731.

Dai, D.L., Martinka, M., and Li, G. (2005). Prognostic significance of activated Akt expression in melanoma: A clinicopathologic study of 292 cases. Journal of Clinical Oncology *23*, 1473-1482.

Dankort, D., Filenova, E., Collado, M., Serrano, M., Jones, K., and McMahon, M. (2007a). A new mouse model to explore the initiation, progression, and therapy of

BRAFV600E-induced lung tumors. Genes & Development *21*, 000.

Dankort, D., Filenova, E., Collado, M., Serrano, M., Jones, K., and McMahon, M. (2007b). A new mouse model to explore the initiation, progression, and therapy of BRAFV600E-induced lung tumors. Genes & Development *21*, 379-384.

Datta, S.R., Brunet, A., and Greenberg, M.E. (1999). Cellular survival: A play in three Akts. Genes & Development *13*, 2905-2927.

Davies, M.A., and Samuels, Y. (2010). Analysis of the genome to personalize therapy for melanoma. Oncogene *29*, 5545-5555.

Davies, M.A., Stemke-Hale, K., Lin, E., Tellez, C., Deng, W., Gopal, Y.N., Woodman, S.E., Calderone, T.C., Ju, Z., Lazar, A.J.*, et al.* (2009a). Integrated molecular and clinical analysis of AKT activation in metastatic melanoma. Clinical Cancer Research *15*, 7538-7546.

Davies, M.A., Stemke-Hale, K., Lin, E., Tellez, C., Deng, W., Gopal, Y.N., Woodman, S.E., Calderone, T.C., Ju, Z., Lazar, A.J.*, et al.* (2009b). Integrated Molecular and Clinical Analysis of AKT Activation in Metastatic Melanoma. Clinical Cancer Research *15*, 7538-7546.

Davies, M.A., Stemke-Hale, K., Tellez, C., Calderone, T.L., Deng, W., Prieto, V.G., Lazar, A.J.F., Gershenwald, J.E., and Mills, G.B. (2008). A novel AKT3 mutation in melanoma tumours and cell lines. British Journal of Cancer *99*, 1265-1268.

de la Monte, S.M., Moore, G.W., and Hutchins, G.M. (1983). Patterned distribution of metastases from malignant melanoma in humans. Cancer Research *43*, 3427-3433.

Dong, L., Jin, L., Tseng, H.Y., Wang, C.Y., Wilmott, J.S., Yosufi, B., Yan, X.G., Jiang, C.C., Scolyer, R.A., Zhang, X.D.*, et al.* (2014). Oncogenic suppression of PHLPP1 in human melanoma. Oncogene *33*, 4756-4766.

Dunn, K.J., Williams, B.O., Li, Y., and Pavan, W.J. (2000). Neural crest-directed gene transfer demonstrates Wnt1 role in melanocyte expansion and differentiation during mouse development. Proceedings of the National Academy of Sciences *97*, 10050-10055.

Flaherty, K.T., Infante, J.R., Daud, A., Gonzalez, R., Kefford, R.F., Sosman, J., Hamid, O., Schuchter, L., Cebon, J., Ibrahim, N.*, et al.* (2012). Combined BRAF and MEK inhibition in melanoma with BRAF V600 mutations. New England Journal of Medicine *367*, 1694-1703.

Garofalo, R.S., Orena, S.J., Rafidi, K., Torchia, A.J., Stock, J.L., Hildebrandt, A.L., Coskran, T., Black, S.C., Brees, D.J., Wicks, J.R.*, et al.* (2003). Severe diabetes, age-dependent loss of adipose tissue, and mild growth deficiency in mice lacking Akt2/PKBβ. The Journal of Clinical Investigation *112*, 197-208.

Gonzalez, E., and McGraw, T.E. (2009). The Akt kinases: Isoform specificity in metabolism and cancer. Cell Cycle *8*, 2502-2508.

Gonzalez, E., McGraw, T.E., and Sabatini, D.D. (2009). Insulin-modulated Akt subcellular localization determines akt isoform-specific signaling. Proceedings of the National Academy of Sciences of the United States of America *106*, 7004-7009.

Govindarajan, B., Sligh, J.E., Vincent, B.J., Li, M., Canter, J.A., Nickoloff, B.J., Rodenburg, R.J., Smeitink, J.A., Oberley, L., Zhang, Y.*, et al.* (2007). Overexpression of Akt converts radial growth melanoma to vertical growth melanoma. The Journal of Clinical Investigation *117*, 719-729.

Hodis, E., Watson, I.R., Kryukov, G.V., Arold, S.T., Imielinski, M., Theurillat, J.-P., Nickerson, E., Auclair, D., Li, L., Place, C.*, et al.* (2012). A landscape of driver mutations in melanoma. Cell *150*, 251-263.

Hussain, K., Challis, B., Rocha, N., Payne, F., Minic, M., Thompson, A., Daly, A., Scott, C., Harris, J., Smillie, B.J.L.*, et al.* (2011). An activating mutation of AKT2 and human hypoglycemia. Science *334*, 474.

Kohn, A.D., Takeuchi, F., and Roth, R.A. (1996). Akt, a Pleckstrin homology domain containing kinase, is activated primarily by phosphorylation. Journal of Biological Chemistry *271*, 21920-21926.

Krauthammer, M., Kong, Y., Ha, B.H., Evans, P., Bacchiocchi, A., McCusker, J.P., Cheng, E., Davis, M.J., Goh, G., Choi, M.*, et al.* (2012). Exome sequencing identifies recurrent somatic RAC1 mutations in melanoma. Nature Genetics *44*, 1006-1014.

Lindhurst, M.J., Sapp, J.C., Teer, J.K., Johnston, J.J., Finn, E.M., Peters, K., Turner, J., Cannons, J.L., Bick, D., Blakemore, L.*, et al.* (2011). A mosaic activating mutation in AKT1 associated with the Proteus syndrome. New England Journal of Medicine *365*, 611-619.

Loftus, S.K., Larson, D.M., Watkins-Chow, D., Church, D.M., and Pavan, W.J. (2001). Generation of RCAS vectors useful for functional genomic analyses. DNA Research *8*, 221-226.

Malanga, D., Scrima, M., De Marco, C., Fabiani, F., De Rosa, N., de Gisi, S., Malara, N., Savino, R., Rocco, G., Chiappetta, G.*, et al.* (2008). Activating E17K mutation in the gene encoding the protein kinase AKT in a subset of squamous cell carcinoma of the lung. Cell Cycle *7*, 665-669.

Niessner, H., Forschner, A., Klumpp, B., Honegger, J.B., Witte, M., Bornemann, A., Dummer, R., Adam, A., Bauer, J., Tabatabai, G.*, et al.* (2013). Targeting hyperactivation of the AKT survival pathway to overcome therapy resistance of melanoma brain

metastases. Cancer Medicine *2*, 76-85.

Parikh, C., Janakiraman, V., Wu, W.-I., Foo, C.K., Kljavin, N.M., Chaudhuri, S., Stawiski, E., Lee, B., Lin, J., Li, H.*, et al.* (2012). Disruption of PH-kinase domain interactions leads to oncogenic activation of AKT in human cancers. Proceedings of the National Academy of Sciences *109*, 19368-19373.

Sarbassov, D.D., Guertin, D.A., Ali, S.M., and Sabatini, D.M. (2005). Phosphorylation and regulation of Akt/PKB by the Rictor-mTOR complex. Science *307*, 1098-1101.

Shi, H., Hong, A., Kong, X., Koya, R.C., Song, C., Moriceau, G., Hugo, W., Yu, C.C., Ng, C., Chodon, T.*, et al.* (2014). A novel AKT1 mutant amplifies an adaptive melanoma response to BRAF inhibition. Cancer Discovery *4*, 69-79.

Smalley, K.S.M. (2009). Understanding melanoma signaling networks as the basis for molecular targeted therapy. Journal of Investigative Dermatology *130*, 28-37.

Steel, K.P., Davidson, D.R., and Jackson, I.J. (1992). TRP-2/DT, a new early melanoblast marker, shows that steel growth factor (c-kit ligand) is a survival factor. Development *115*, 1111-1119.

Thomas, C.C., Deak, M., Alessi, D.R., and van Aalten, D.M.F. (2002). High-resolution structure of the Pleckstrin homology domain of protein kinase B/Akt bound to phosphatidylinositol (3,4,5)-trisphosphate. Current Biology *12*, 1256-1262.
Toker, A. (2012). Achieving specificity in Akt signaling in cancer. Advances in Biological Regulation *52*, 78-87.

VanBrocklin, M.W., Robinson, J.P., Lastwika, K.J., Khoury, J.D., and Holmen, S.L. (2010). Targeted delivery of NRASQ61R and Cre-recombinase to post-natal melanocytes induces melanoma in Ink4a/Arflox/lox mice. Pigment Cell & Melanoma Research *23*, 531-541.

von Werder, A., Seidler, B., Schmid, R.M., Schneider, G., and Saur, D. (2012). Production of avian retroviruses and tissue-specific somatic retroviral gene transfer in vivo using the RCAS/TVA system. Nature Protocols *7*, 1167-1183.

Xu, N., Lao, Y., Zhang, Y., and Gillespie, D.A. (2012). Akt: A double-edged sword in cell proliferation and genome stability. Journal of Oncology *2012*, 15.

Yang, J., Cron, P., Thompson, V., Good, V.M., Hess, D., Hemmings, B.A., and Barford, D. (2002). Molecular mechanism for the regulation of protein kinase B/Akt by hydrophobic motif phosphorylation. Molecular Cell *9*, 1227-1240.

Table 4.1 Summary of tumor formation. The mean survival (days) and tumor incidence (fraction of tumor-bearing mice per cohort) are listed for each mouse cohort according to genetic background and virally delivered genes.

Strain	Gene(s) delivered	Tumor Incidence	Mean survival (days)
Dct::TVA;Braf ^{CA}***;Cdkn2a*** $^{lox/lox}$	*Cre*	16/34	88.9 ± 8.6
Dct::TVA;Braf ^{CA}***;Cdkn2a*** $^{lox/lox}$	*AKT3* ^{E17K}*; Cre*	9/13	71.3 ± 6.7
	AKT3 ^{E17K} positive*	8/9	73.6 ± 7.2
Dct::TVA;Braf ^{CA}***;Cdkn2a*** $^{lox/lox}$	myr*AKT3; Cre*	11/13	53.5 ± 6.8
Dct::TVA;Braf ^{CA}***;Cdkn2a*** $^{lox/lox}$	wt*AKT3; Cre*	7/10	68.6 ± 5.3

*HA positive by IHC and/or positive by RT-PCR

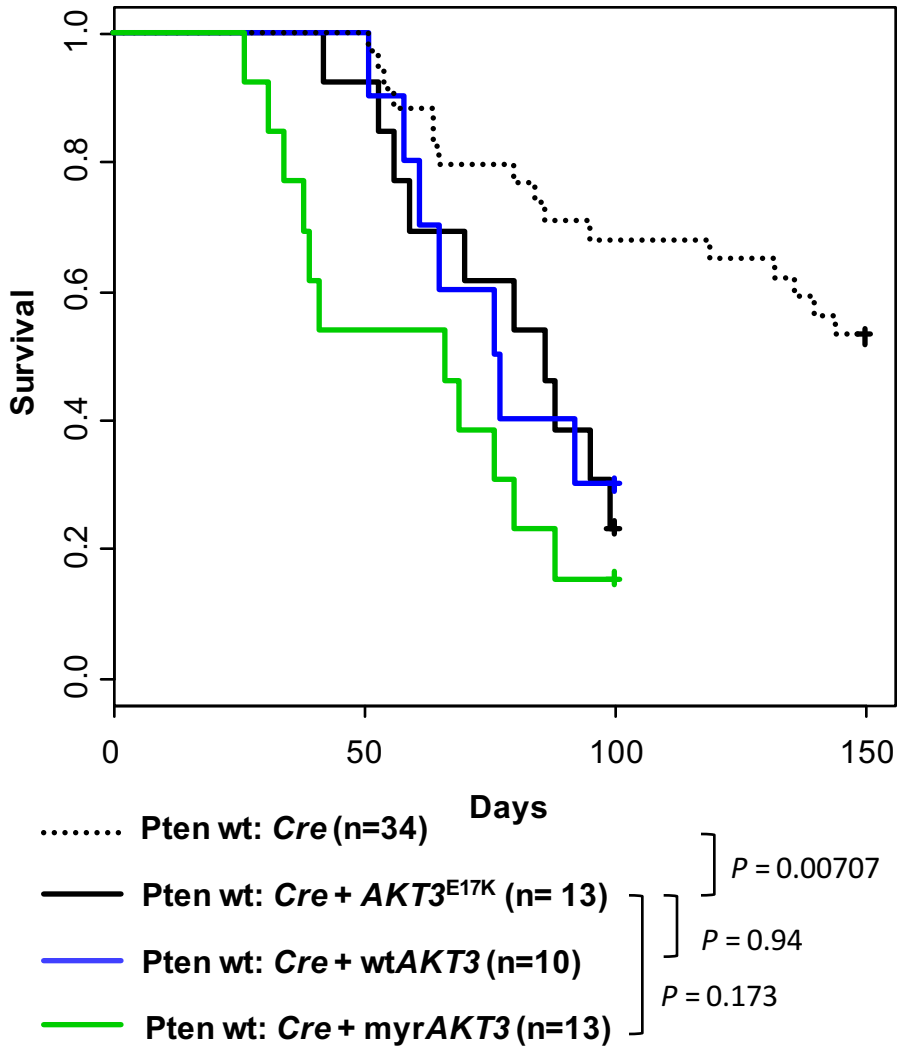

Figure 4.1 Kaplan-Meier percent survival curves demonstrate that expression of AKT3^{E17K} significantly increases tumor incidence and reduces tumor latency. *Dct::TVA;Braf*^{CA};*Cdkn2a*$^{lox/lox}$ mice (*Pten*^{WT}) were injected at birth with either *Cre* (small dashed line n = 34), *AKT3*^{E17K} and *Cre* (black line n = 13), myr*AKT3* and *Cre* (green line n = 13), or wt*AKT3* and *Cre* (blue line n = 10) containing viruses as indicated. A significant difference was observed between the survival of *Pten*^{WT} mice injected with *Cre* containing viruses and *Pten*^{WT} mice injected with *AKT3*^{E17K} and *Cre* containing viruses ($P = 0.00707$).

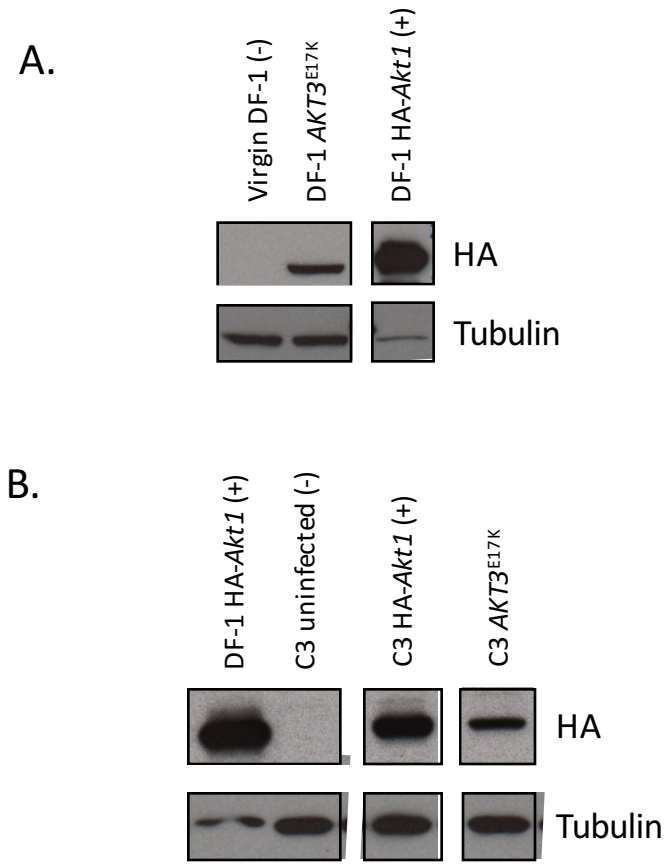

Figure 4.2 Expression of AKT3^{E17K} in DF-1 cells and primary melanocytes. A: Expression of AKT3^{E17K} was detected in infected DF-1 with an antibody to the HA epitope tag on AKT3^{E17K}. DF-1 cells expressing HA tagged mouse AKT1 was used as a positive control. B: C3 primary melanocytes that ectopically express the TVA receptor were inoculated with RCASBP(A) *AKT3*^{E17K} virus produced from infected DF-1 cells. Virally delivered *AKT3*^{E17K} expression was detected with an antibody to the HA epitope tag on AKT3^{E17K}. Tubulin expression was used as a loading control.

Figure 4.3 Expression of AKT3^{E17K} in BRAF^{V600E}/INK4A-ARF-null mouse melanomas. A: Expression of AKT3^{E17K} was assessed by RT-PCR using primers specific for the transgene product. B: Expression of AKT3^{E17K} was assessed in tumors induced by injection of RCASBP(A) *Cre* and *AKT3*^{E17K} viruses by IHC using an antibody to the HA epitope tag on AKT3^{E17K}. Scale bar represents 200 μm. *Note: Tumor from Mouse ID 5198 is negative by HA IHC but positive by RT-PCR.*

A.

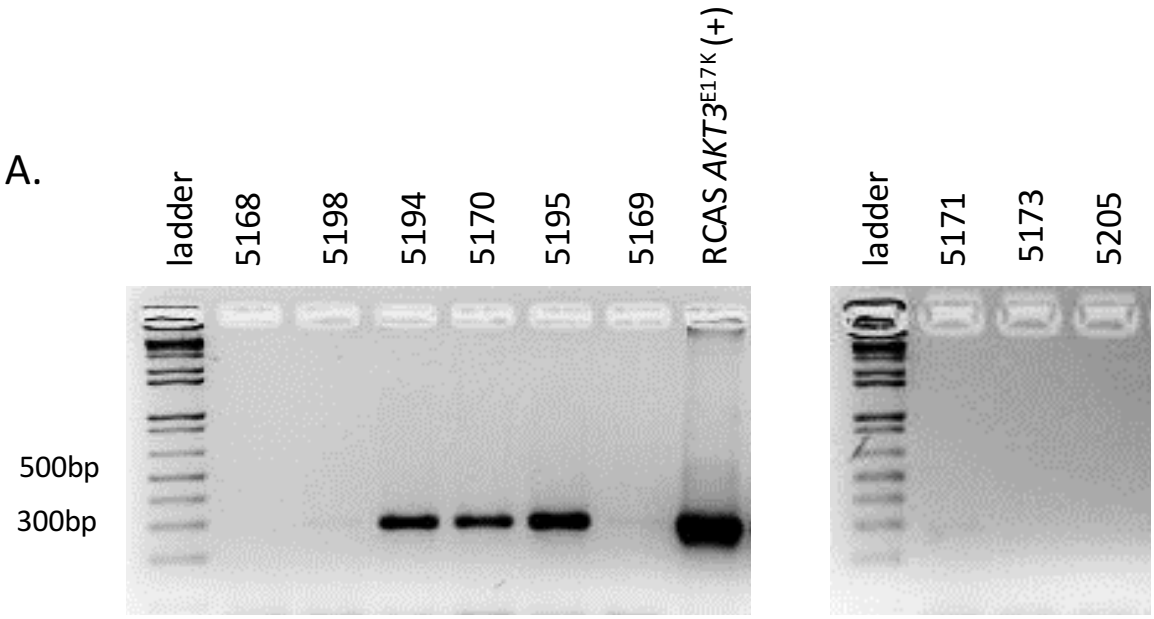
ladder
5168
5198
5194
5170
5195
5169
RCAS AKT3E17K (+)
ladder
5171
5173
5205
500bp
300bp

B.

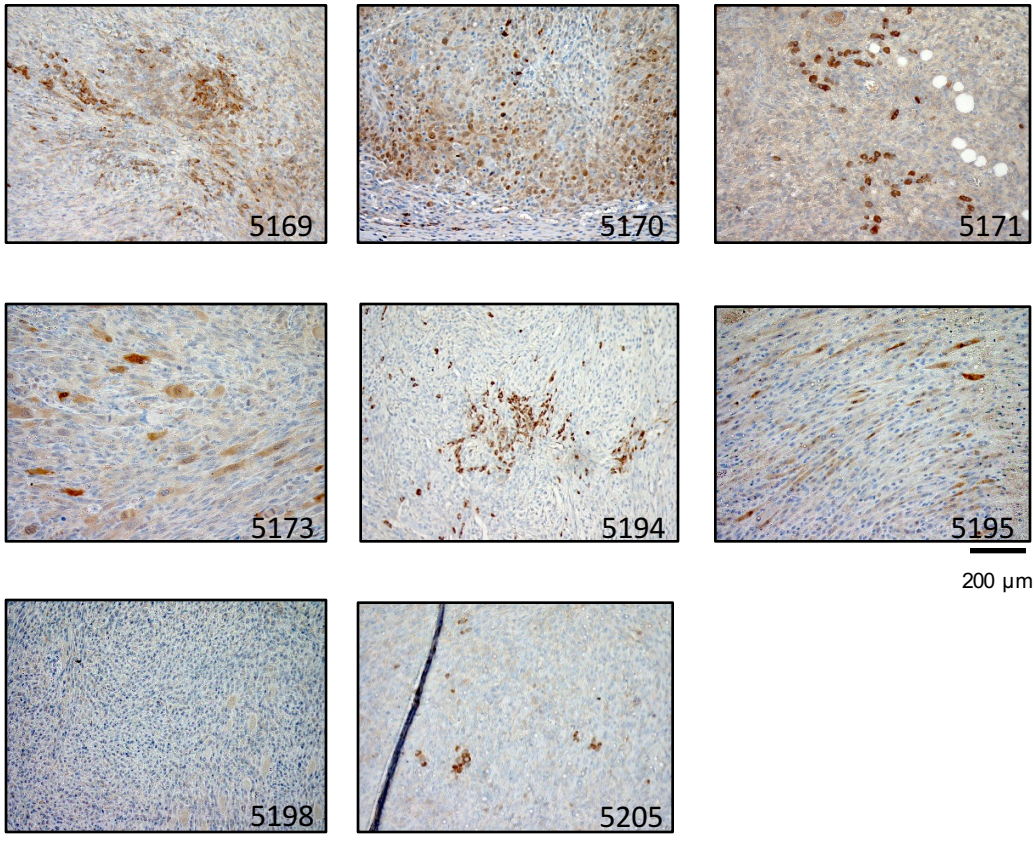
5169
5170
5171
5173
5194
5195
200 µm
5198
5205

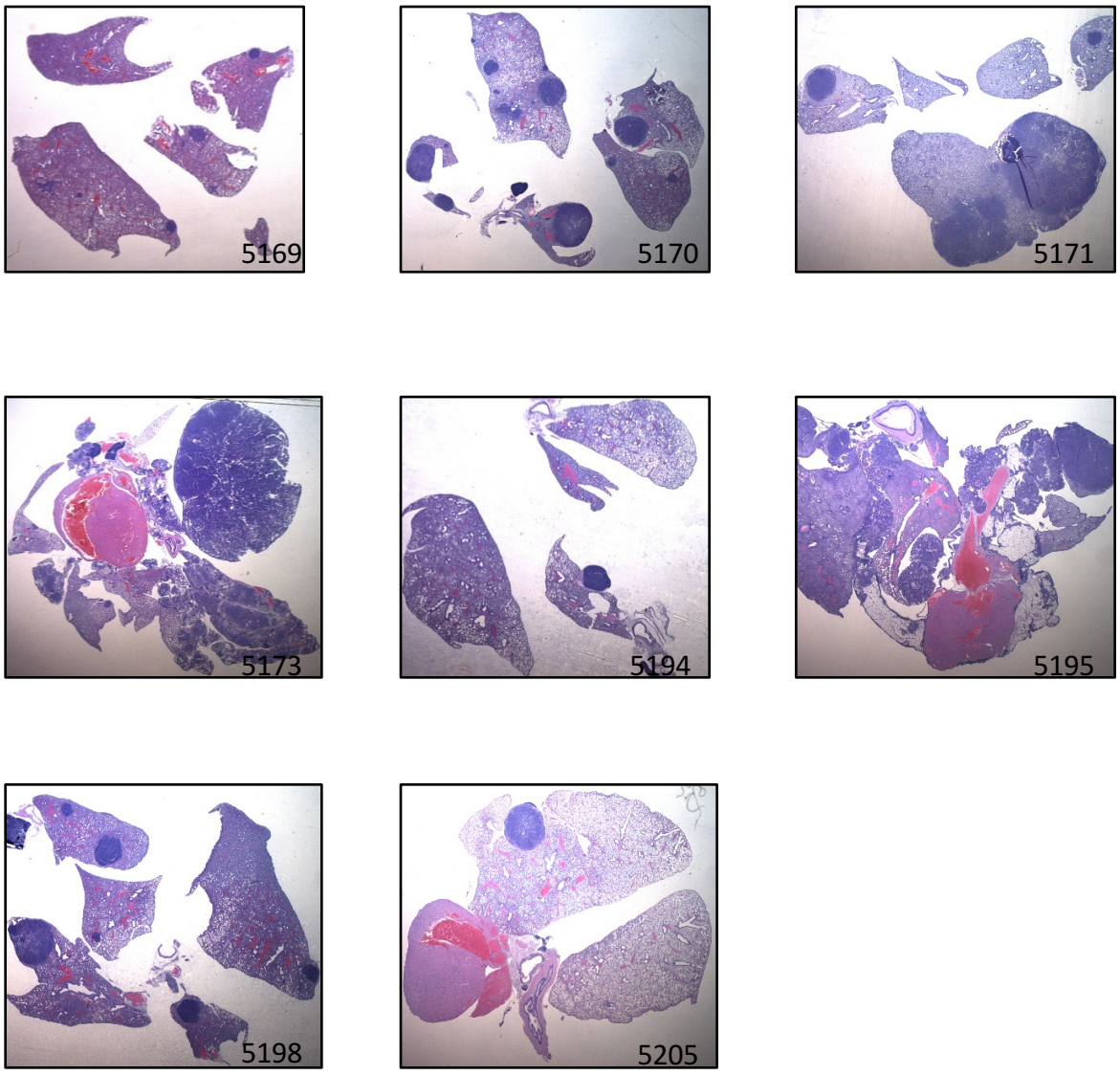

Figure 4.4 Histological examination reveals aggressive lung lesions in *Pten*^{WT} mice injected with RCASBP(A) *Cre* and *AKT3*^{E17K} viruses. Lung lesions were observed in 100% (8/8) of tumor-bearing mice with confirmed expression of AKT3^{E17K}. Shown above are hematoxylin and eosin (H&E) stained lung sections by mouse ID number.

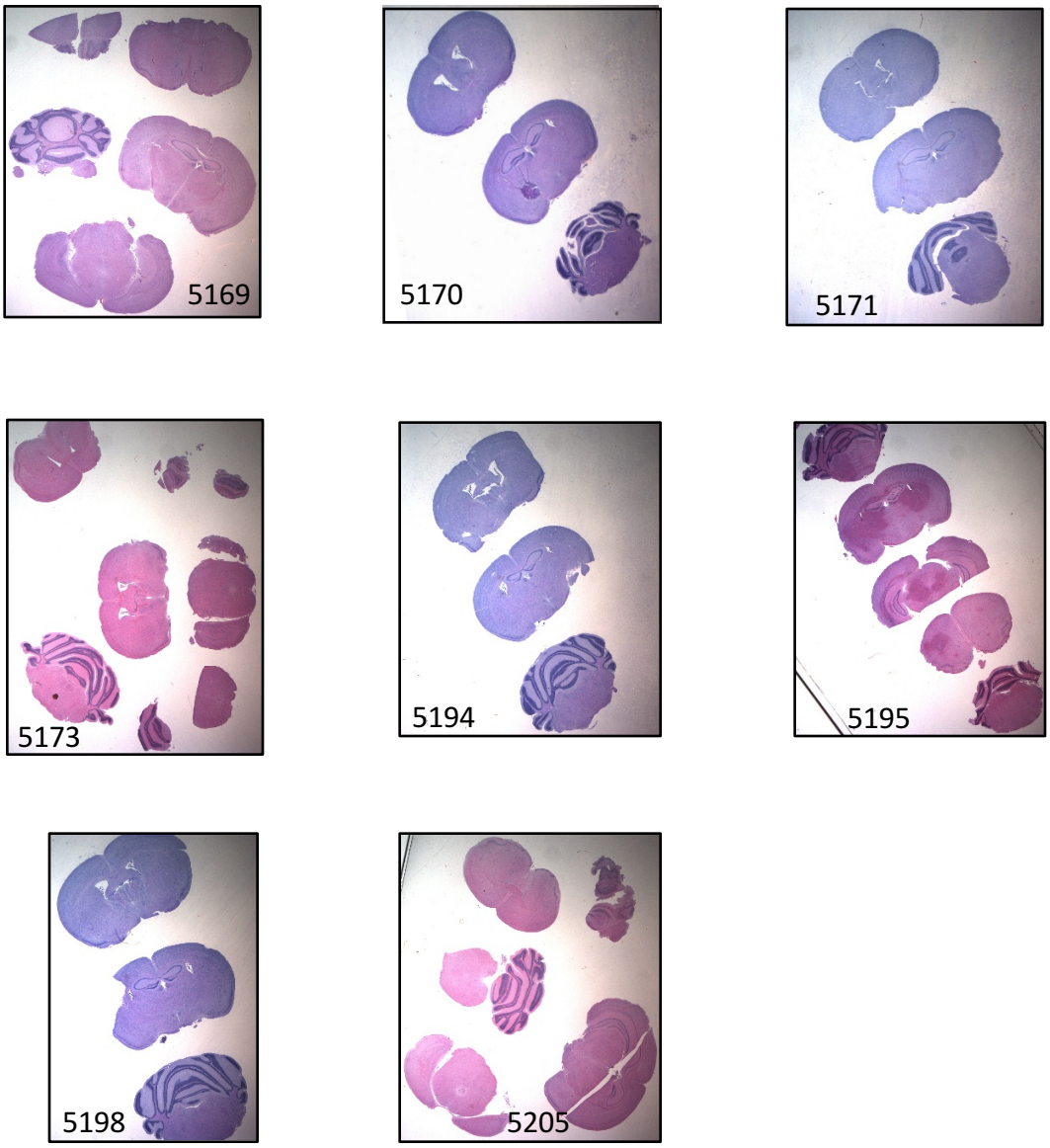

Figure 4.5 Absence of observable brain metastasis in *Pten*^{WT} mice injected with RCASBP(A) *Cre* and *AKT3*^{E17K} viruses. Brain sections from tumor-bearing mice with confirmed expression of AKT3^{E17K} were negative for observable metastasis. H&E stained sections are shown by mouse ID number.

CHAPTER 5

SUMMARY AND PERSPECTIVES

5.1 Introduction

The work presented in this dissertation examines the role of AKT signaling in melanoma metastasis. Although previous clinical studies and *in vitro* work have implicated aberrant AKT activation as a mechanism driving melanoma metastasis, studies addressing the *in vivo* role of activated AKT in melanoma progression and metastasis were lacking (Dai et al., 2005; Davies et al., 2009; Stahl et al., 2004). Loss of *PTEN* is often considered a surrogate marker of AKT activation and in combination with mutant BRAF results in melanomas that metastasize to the lungs and lymph nodes in less than 10% of mice (Dankort et al., 2009). Interestingly, our data demonstrates that aberrant AKT activation differs from *Pten* loss in terms of promoting melanoma metastasis and that AKT signaling in melanoma metastasis is mediated via activation of specific AKT isoforms. This chapter summarizes the work presented in prior chapters and concludes with perspectives for future work.

5.2 Chapter Summaries

Chapter 2 of this dissertation describes our finding that expression of activated AKT1 in the context of mutant $BRAF^{V600E}$ and *Cdkn2a* loss results in highly aggressive

melanomas that metastasize to the brain and lungs. We report that while PTEN silencing does not result in significant metastasis in this context, loss of PTEN cooperates with activated AKT1 in promoting brain metastasis at an incidence of nearly 80% in tumor-bearing mice. In this chapter, we show that targets of the mTOR pathway are upregulated and implicated in eliciting melanoma lung and brain metastasis. To our knowledge, the mouse model of metastatic melanoma described in this chapter is the first *in vivo* autochthonous model of melanoma lung and brain metastasis in an immunocompetent animal. This model system provides a powerful platform to further study the mechanisms of melanoma metastasis and sheds light on the involvement of AKT signaling in this process.

Chapter 3 builds on our findings in Chapter 2 and investigates the role of AKT isoform-specific signaling in melanoma progression and metastasis. Our previous finding that PTEN silencing and expression of activated AKT1 does not yield similar metastatic phenotypes led us to hypothesize that AKT isoform-specific signaling facilitates the metastatic potential of melanoma cells. Using our non-metastatic *in vivo* model of melanoma, we identified AKT3 as the dominant isoform promoting AKT-mediated metastasis to the brain. We also found that in human melanomas that metastasize to the brain, AKT3 gene expression is significantly increased compare to non-metastatic melanomas. Expression of activated AKT1 elicits the formation of melanoma brain metastases at a lower incidence compared with activated AKT3 in $Pten^{WT}$ mice; however, expression of activated AKT2 in this context does not result in brain metastases. Furthermore, we found that the expression of wild-type AKT isoforms in $Pten^{WT}$ mice also does not promote brain metastases. Taken together, these findings indicate that aberrant activation of AKT3 and to a lesser extent AKT1 but not AKT2 is critical in

promoting melanoma metastasis to the brain in the context of $BRAF^{V600E}$ and INK4A/ARF loss.

Chapter 4 describes our studies investigating the role of $AKT3^{E17K}$ in melanoma development and progression. The E17K mutation has been found in all three isoforms and is thought to result in aberrant AKT signaling. The E17K mutations of AKT1 and AKT3 have been described in metastatic melanoma and are found in 1-2% of melanomas. Using our previously described non-metastatic mouse model of melanoma, we expressed $AKT3^{E17K}$ in the context of $BRAF^{V600E}$ and INK4A/ARF loss. Interestingly, brain metastases were not observed in our study however very aggressive lung lesions were noted. While it remains too early to draw conclusions, our work suggests that $AKT3^{E17K}$ is not functionally equivalent to activated (myristoylated) AKT3 in promoting melanoma metastasis and instead possess alternative neomorphic functions.

5.3 Perspectives for Future Work

The current understanding of metastasis holds that in order for melanoma to colonize the brain, several steps must occur. These steps include local infiltration of tumor cells into adjacent tissue of the primary melanoma, intravasation of melanoma cells into a blood vessel, survival in the circulatory system, arrest at a branch point in the cerebral vasculature, extravasation through the blood-brain barrier, persistent close contact to microvessels, and perivascular growth by vessel co-option (Kienast et al., 2010; Zbytek et al., 2008). How melanoma cells acquire the ability to fulfill these steps of metastasis is an active area of research. The previous chapters of this dissertation describe experiments that clearly demonstrate the critical role of aberrant AKT signaling in the

development of melanoma brain metastasis. Both experimental and clinical data strongly implicate aberrantly activated AKT3 in promoting melanoma spread to the brain. Moving forward, we aim to elucidate the specific step(s) of melanoma brain metastasis that aberrant AKT3 signaling facilitates.

Theories regarding melanoma's tropism for the brain can be categorized mechanistically as either intrinsic or extrinsic. An example of a theory based on an intrinsic mechanism would be linking melanoma's predilection for the brain with the neural crest origin of melanoma cells. A theory based on extrinsic mechanisms would consider factors of the brain that are specifically favorable for melanoma colonization such as being an immune-privileged site. While it is very plausible that both intrinsic and extrinsic views are valid and play a role in melanoma's spread to the brain, the work presented in this dissertation favors the theory of an intrinsic mechanism. Using a non-metastatic mouse model of melanoma, we observed that expression of either activated AKT3 or AKT1 in melanoma cells is sufficient to elicit lung and brain metastasis in the context of $BRAF^{V600E}$ and INK4A/ARF loss. Furthermore, our findings – that aberrant AKT3 and/or AKT1 activity in melanoma cells promotes metastasis to the brain – are supported by human data, which indicates that AKT signaling is a signature feature of brain metastases (Chen et al., 2014; Improta et al., 2011; Niessner et al., 2013).

The regulation of angiogenesis during early colonization of the brain parenchyma is a distinguishing feature between melanoma cells and other cancer cells that metastasize to the brain. *In vivo* studies by Kienast *et al.* showed that melanoma cells differs from lung cancer cells during the establishment of brain metastases by promoting perivascular growth by vessel co-option rather than early angiogenesis (Kienast et al., 2010).

Interestingly, a different study on vascular tumor growth found that aberrant AKT3 activation inhibits angiogenesis by a mechanism involving mTOR signaling. Given our findings that expression of activated AKT3 is sufficient to elicit brain metastasis, it is tempting to speculate that activated AKT3 in melanoma cells might oppose early angiogenesis and thereby facilitate the perivascular growth and vessel co-option of brain micro-metastases. Whether this is the case will need to be determined in future studies.

The predominant expression of AKT3 in the brain along with changes in brain growth depending on its presence, absence or function, demonstrate that AKT3 plays a critical role in brain development (Easton et al., 2005; Gai et al., 2015; Lee et al., 2012; Tschopp et al., 2005). It is known that melanoma cells colonizing the brain adopt neuron-like characteristics, especially during the early metastatic growth phase in the brain (Nygaard et al., 2014). The mechanisms driving plasticity of melanoma cells during brain colonization are not well understood. The exact role of AKT3 signaling during brain development is also unknown. It is reasonable to hypothesize that AKT3 activation promotes a brain-adaptive phenotype in melanoma cells and thus confers an advantage for growing in the brain. As of yet, brain-specific molecular targets of AKT3 have not been identified in melanoma.

Aberrant AKT signaling is associated with increased brain-specific invasiveness of melanoma cells (Niessner et al., 2013). Using a trans-well invasion assay with astrocyte-conditioned media as an attractant, Niessner *et al*. found that both AKT activation and an invasive phenotype increased in melanoma cells relative to control conditions using fibroblast conditioned media as an attractant. These findings are in line with general increased invasiveness in melanoma conferred by AKT overexpression

(Govindarajan et al., 2007). Whether aberrant AKT3 or AKT1 activation promotes brain-specific invasion of melanoma cells crossing the blood-brain barrier or whether increased invasiveness is a general phenomenon from AKT signaling remains to be determined.

Genomic amplification of *AKT3* in glioma was recently linked to tumor progression via activation of the DNA repair pathway (Turner et al., 2015). DNA repair proteins are frequently overexpressed in breast cancer cells that metastasize to the brain (Woditschka et al., 2014). While ectopic expression of DNA repair proteins BARD1 or RAD51 in MDA-MB-231-BR cells increased brain metastasis formation by 3 to 4-fold in mice, siRNA mediated knockdown of RAD51 decreased brain metastasis formation nearly 3-fold (Woditschka et al., 2014). In our study, we found that in addition to *AKT3* copy number amplification, AKT3 gene expression is significantly upregulated in brain metastatic melanomas relative to non-metastatic melanomas. Whether aberrant AKT3 activation induces DNA repair machinery in melanomas will be determined by future studies.

The implications of this dissertation extend into the clinical management of melanoma. There is an acute need for more sophisticated tools to prognosticate a melanoma patient's risk for metastasis. Our findings that aberrant AKT1/3 activation in the context of $BRAF^{V600E}$ and INK4A/ARF null melanomas leads to significant lung and brain metastases while myrAKT2 and $AKT3^{E17K}$ expression in the same context results in lung but not brain metastases indicates that aberrant AKT signaling drives melanoma metastasis via isoform or mutant-specific mechanisms. The TCGA database reveals that melanomas metastasizing to the brain have significantly higher expression of AKT3 compared to non-metastatic melanomas. Collectively, these data suggest that aberrant

AKT isoform/mutant signaling not only plays a role in driving melanoma metastasis but that increased expression of specific AKT isoforms or mutants may predict the risk of melanoma metastasis to specific organs such as the brain.

The therapeutic implications of our study argue that targeting the PI3K/AKT/mTOR pathway may impede melanoma metastasis. Our findings are corroborated by other *in vivo* studies also implicating the role of unregulated mTOR signaling in melanoma progression and metastasis (Damsky et al., 2015; Liu et al., 2012). Several melanoma preclinical studies have demonstrated that PI3K/AKT inhibition retards cell growth, promotes tumor regression and delays the emergence of drug resistance to MAPK inhibitors (Bedogni et al., 2006; Lassen et al., 2014; Marsh Durban et al., 2013). Preliminary data from our lab reveals that dual inhibition of PI3K and mTOR using NVP-BEZ235 robustly inhibits *in vitro* migration of BRAF mutant melanoma cells (unpublished) and implies that increased migration downstream of aberrant AKT activation may contribute to the metastatic phenotypes observed in our *in vivo* studies. Currently, several clinical trials are underway testing the efficacy of PI3K/AKT/mTOR inhibitors in combination with other therapies for the treatment of metastatic melanoma (Fedorenko et al., 2015). However, early inhibition of the PI3K/AKT/mTOR pathway in melanoma at Stage 3 (regional lymph node involvement) or lower, where there is a dearth of therapeutic options, may prove more efficacious than after melanoma has disseminated to distant organs. Our study and *in vivo* model provides the optimal platform to test whether early intervention with PI3K/AKT/mTOR blockade is an effective strategy against the metastatic spread of melanoma.

As a part of on-going research, we plan to continue investigating aberrant AKT

isoform specific signaling and E17K mutant AKT proteins in melanoma development and progression. We are specifically interested in continuing the work pertaining to melanoma brain metastasis and aberrant AKT activation. The work presented in this dissertation establishes the role of aberrantly activated AKT1 and AKT3 in eliciting melanoma brain metastasis in a non-metastatic mouse model of melanoma featuring mutant $BRAF^{V600E}$ and *Cdkn2a* loss. We demonstrate that PTEN silencing is not equivalent to AKT1 activation in terms of metastatic potential in melanoma and that expression of activated AKT1 in melanoma results in significantly increased mTOR signaling compared to melanomas with *Pten* loss. We considered AKT isoform-specific signaling in melanoma and found that AKT3, and to a lesser extent AKT1, promotes melanoma brain metastasis while AKT2 activation does not. We are currently exploring the role of $AKT3^{E17K}$ in melanoma and have noted phenotypic differences from melanomas expressing activated AKT3.

Brain metastases are a major cause of death in melanoma (Budman et al., 1978; Davies et al., 2011; Yashin et al., 2013). The AKT pathway is aberrantly activated in up to 70% of melanomas and is clinically correlated with melanoma brain metastasis (Chen et al., 2014; Davies et al., 2009; Niessner et al., 2013; Smalley, 2009). Our work provides the first *in vivo* evidence that aberrant AKT3 and AKT1 activity are sufficient to elicit brain metastases in melanomas harboring $BRAF^{V600E}$ mutation and loss of *Cdkn2a* locus. Furthermore, our work demonstrates that PTEN silencing is not equivalent to AKT1 activation in terms of promoting melanoma metastasis. We also developed the first autochthonous *in vivo* model of melanoma brain metastasis. Our work continues with investigating AKT isoform specific signaling and melanoma metastasis as well as the

E17K mutation of AKT in melanoma. Finally, work presented in this dissertation provides insights into the mechanism of melanoma brain metastasis that may prove useful in the future management of this disease complication.

5.4 References

Bedogni, B., Welford, S.M., Kwan, A.C., Ranger-Moore, J., Saboda, K., and Powell, M.B. (2006). Inhibition of phosphatidylinositol-3-kinase and mitogen-activated protein kinase kinase 1/2 prevents melanoma development and promotes melanoma regression in the transgenic TPRas mouse model. Molecular Cancer Therapeutics *5*, 3071-3077.

Budman, D.R., Camacho, E., and Wittes, R.E. (1978). The current causes of death in patients with malignant melanoma. European Journal of Cancer (1965) *14*, 327-330.

Chen, G., Chakravarti, N., Aardalen, K., Lazar, A.J., Tetzlaff, M.T., Wubbenhorst, B., Kim, S.-B., Kopetz, S., Ledoux, A.A., Gopal, Y.N.V.*, et al.* (2014). Molecular profiling of patient-matched brain and extracranial melanoma metastases implicates the PI3K pathway as a therapeutic target. Clinical Cancer Research *20*, 5537-5546.

Dai, D.L., Martinka, M., and Li, G. (2005). Prognostic significance of activated Akt expression in melanoma: A clinicopathologic study of 292 cases. Journal of Clinical Oncology *23*, 1473-1482.

Damsky, W., Micevic, G., Meeth, K., Muthusamy, V., Curley, D.P., Santhanakrishnan, M., Erdelyi, I., Platt, J.T., Huang, L., Theodosakis, N.*, et al.* (2015). mTORC1 activation blocks BrafV600E-induced growth arrest but is insufficient for melanoma formation. Cancer cell *27*, 41-56.

Dankort, D., Curley, D.P., Cartlidge, R.A., Nelson, B., Karnezis, A.N., Damsky Jr, W.E., You, M.J., DePinho, R.A., McMahon, M., and Bosenberg, M. (2009). BrafV600E cooperates with Pten loss to induce metastatic melanoma. Nature Genetics *41*, 544-552.

Davies, M.A., Liu, P., McIntyre, S., Kim, K.B., Papadopoulos, N., Hwu, W.-J., Hwu, P., and Bedikian, A. (2011). Prognostic factors for survival in melanoma patients with brain metastases. Cancer *117*, 1687-1696.

Davies, M.A., Stemke-Hale, K., Lin, E., Tellez, C., Deng, W., Gopal, Y.N., Woodman, S.E., Calderone, T.C., Ju, Z., Lazar, A.J.*, et al.* (2009). Integrated molecular and clinical analysis of AKT activation in metastatic melanoma. Clinical Cancer Research *15*, 7538-7546.

Easton, R.M., Cho, H., Roovers, K., Shineman, D.W., Mizrahi, M., Forman, M.S., Lee,

V.M.-Y., Szabolcs, M., de Jong, R., Oltersdorf, T.*, et al.* (2005). Role for Akt3/protein kinase Bγ in attainment of normal brain size. Molecular and Cellular Biology *25*, 1869-1878.

Fedorenko, I.V., Gibney, G.T., Sondak, V.K., and Smalley, K.S.M. (2015). Beyond BRAF: where next for melanoma therapy[quest]. British Journal of Cancer *112*, 217-226.

Gai, D., Haan, E., Scholar, M., Nicholl, J., and Yu, S. (2015). Phenotypes of AKT3 deletion: A case report and literature review. American Journal of Medical Genetics Part A *167*, 174-179.

Govindarajan, B., Sligh, J.E., Vincent, B.J., Li, M., Canter, J.A., Nickoloff, B.J., Rodenburg, R.J., Smeitink, J.A., Oberley, L., Zhang, Y.*, et al.* (2007). Overexpression of Akt converts radial growth melanoma to vertical growth melanoma. The Journal of Clinical Investigation *117*, 719-729.

Improta, G., Zupa, A., Fillmore, H., Deng, J., Aieta, M., Musto, P., Liotta, L.A., Broaddus, W., Petricoin, E.F., and Wulfkuhle, J.D. (2011). Protein pathway activation mapping of brain metastasis from lung and breast cancers reveals organ type specific drug target activation. Journal of Proteome Research *10*, 3089-3097.

Kienast, Y., von Baumgarten, L., Fuhrmann, M., Klinkert, W.E.F., Goldbrunner, R., Herms, J., and Winkler, F. (2010). Real-time imaging reveals the single steps of brain metastasis formation. Nature Medicine *16*, 116.

Lassen, A., Atefi, M., Robert, L., Wong, D., Cerniglia, M., Comin-Anduix, B., and Ribas, A. (2014). Effects of AKT inhibitor therapy in response and resistance to BRAF inhibition in melanoma. Molecular Cancer *13*, 83.

Lee, J.H., Huynh, M., Silhavy, J.L., Kim, S., Dixon-Salazar, T., Heiberg, A., Scott, E., Bafna, V., Hill, K.J., Collazo, A.*, et al.* (2012). De novo somatic mutations in components of the PI3K-AKT3-mTOR pathway cause hemimegalencephaly. Nature Genetics *44*, 941-945.

Liu, W., Monahan, K.B., Pfefferle, A.D., Shimamura, T., Sorrentino, J., Chan, K.T., Roadcap, D.W., Ollila, D.W., Thomas, N.E., Castrillon, D.H.*, et al.* (2012). LKB1/STK11 inactivation leads to expansion of a prometastatic tumor subpopulation in melanoma. Cancer Cell *21*, 751-764.

Marsh Durban, V., Deuker, M.M., Bosenberg, M.W., Phillips, W., and McMahon, M. (2013). Differential AKT dependency displayed by mouse models of BRAFV600E-initiated melanoma. The Journal of Clinical Investigation *123*, 5104-5118.

Niessner, H., Forschner, A., Klumpp, B., Honegger, J.B., Witte, M., Bornemann, A., Dummer, R., Adam, A., Bauer, J., Tabatabai, G.*, et al.* (2013). Targeting hyperactivation of the AKT survival pathway to overcome therapy resistance of melanoma brain

metastases. Cancer Medicine *2*, 76-85.

Nygaard, V., Prasmickaite, L., Vasiliauskaite, K., Clancy, T., and Hovig, E. (2014). Melanoma brain colonization involves the emergence of a brain-adaptive phenotype. Oncoscience *1*, 82-94.

Smalley, K.S.M. (2009). Understanding Melanoma Signaling Networks as the Basis for Molecular Targeted Therapy. Journal of Investigative Dermatology *130*, 28-37.

Stahl, J.M., Sharma, A., Cheung, M., Zimmerman, M., Cheng, J.Q., Bosenberg, M.W., Kester, M., Sandirasegarane, L., and Robertson, G.P. (2004). Deregulated Akt3 activity promotes development of malignant melanoma. Cancer Research *64*, 7002-7010.

Tschopp, O., Yang, Z.-Z., Brodbeck, D., Dummler, B.A., Hemmings-Mieszczak, M., Watanabe, T., Michaelis, T., Frahm, J., and Hemmings, B.A. (2005). Essential role of protein kinase B-gamma (PKB-gamma/Akt3) in postnatal brain development but not in glucose homeostasis. Development *132*, 2943-2954.

Turner, K.M., Sun, Y., Ji, P., Granberg, K.J., Bernard, B., Hu, L., Cogdell, D.E., Zhou, X., Yli-Harja, O., Nykter, M.*, et al.* (2015). Genomically amplified Akt3 activates DNA repair pathway and promotes glioma progression. Proceedings of the National Academy of Sciences *112*, 3421-3426.

Woditschka, S., Evans, L., Duchnowska, R., Reed, L.T., Palmieri, D., Qian, Y., Badve, S., Sledge, G., Gril, B., Aladjem, M.I.*, et al.* (2014). DNA double-strand break repair genes and oxidative damage in brain metastasis of breast cancer. Journal of the National Cancer Institute *106*.

Yashin, A.I., Wu, D., Arbeev, K.G., Kulminski, A.M., Stallard, E., and Ukraintseva, S.V. (2013). Why does melanoma metastasize into the brain? Genes with pleiotropic effects might be the key. Frontiers in Genetics *4*, 75.

Zbytek, B., Carlson, J.A., Granese, J., Ross, J., Mihm, M., and Slominski, A. (2008). Current concepts of metastasis in melanoma. Expert Review of Dermatology *3*, 569-585.